Mémoires de Géologie (Lausanne) No. 35, 2001

Metamorphism and tectonics of the transition between non metamorphic Tethayan Himalaya sediments and the North Himalayan Crystalline Zone (Rupshu area, Ladakh, NW India).

by Matthieu Girard

IMPRIMERIE CHABLOZ S.A., TOLOCHENAZ

ISSN 1015-3578

Mémoires de Géologie (Lausanne)

Section des Sciences de la Terre
Université de Lausanne
BFSH-2, 1015 Lausanne, Suisse

35

Mémoires de Géologie (Lausanne)

Mémoires de Géologie (Lausanne)
Section des Sciences de la Terre
Institut de Géologie et Paléontologie
Université de Lausanne
BFSH-2, CH-1015 Lausanne

GIRARD Matthieu
Titre : Metamorphism and tectonics of the transition between non metamorphic Tethyan Himalaya sediments and the North Himalayan Crystalline Zone (Rupshu area, Ladakh, NW India).
Mém. Géol. (Lausanne), n°35, 2001, 99 pp., 7 pl.

Imprimeur : Chabloz SA, Lausanne

Metamorphism and tectonics of the transition between non metamorphic Tethyan Himalaya sediments and the North Himalayan Crystalline Zone

(Rupshu area, Ladakh, NW India).

Matthieu Girard

Imprimé grâce à une subvention de la Fondation Dr. Joachim de Giacomi de l'ASSN.

Mémoires de Géologie (Lausanne), No 35, 2001

"Le monde n'est beau que si nous le regardons."

Albert Jacquard

Table of contents

Résumé

Le territoire du Rupshu, au NO de l'Inde, permet d'étudier la transition entre l'Himalaya Téthysien, formé de sédiments très faiblement métamorphiques, et la Zone Cristalline du Nord Himalaya (ZCNH). L'Himalaya Téthysien comprend une série sédimentaire allant du Précambrien au Crétacé, avec une grande lacune entre l'Ordovicien et le Permien. Les formations du Trias Inférieur et Moyen sont très monotones et reflètent un environnement distal le long de la marge nord-indienne. A partir du Trias supérieur les formations commencent à ressembler à celles du bassin sédimentaire Spiti-Zanskar. Toutefois, en raisons de la situation plus distal du Rupshu, la composant détritique y est généralement moins abondante. Le chevauchement du Kum Tso, à vergence SW, superpose des séries typiquement distales du Trias Moyen, sur des sédiments plus proximaux du Trias Supérieur à Lias. Le très faible métamorphisme de l'Himalaya Téthysien a été étudié à l'aide de la "cristallinité de l'illite". Ceci permit d'estimer à environ 16 km le rejet d'une zone d'extension observée le long de deux profils parallèles, distants d'environ 70 km. Cette zone d'extension est interprétée comme étant un équivalent superficiel de la Zone de Cisaillement du Zanskar.

La ZCNH est quant à elle formée d'équivalents métamorphiques de sédiments paléozoïques. Une analyse des lithologies probablement permiennes de la formation de Karzok, montre d'importantes variations latérales de facies. La transition entre l'Himalaya Téthysien et la ZCNH est parfaitement graduelle et se marque par une augmentation progressive du métamorphisme, de la diagenèse à la zone à sillimanite. Ce métamorphisme barrovien, engendré par la mise en place de la nappe du Tso Morari et de celle du Mata, toutes deux à vergence SW, oblitère un métamorphisme éclogitique de haute pression - basse température, lié à la subduction de l'Inde sous la plaque asiatique. Seule la nappe du Tso Morari possède des reliques de ce premier événement métamorphique himalayen. Le métamorphisme barrovien, présent dans les deux nappes, a été étudié à l'aide de plusieurs méthodes de thermobarométrie quantitatives. Les bases de données thermodynamiques de Holland et Powell (1998) et de Berman (1988), les géothermomètres isotopiques quartz-grenat et quartz-disthène, ainsi que le géothermomètre basé sur la teneur en Ti de l'amphibole, on permit de quantifier les différences de métamorphisme observées le long du profil entre Pang et le Tso Kar. Ces méthodes ont notamment montré qu'il n'y a pas de saut métamorphique entre l'Himalaya Téthysien et la ZCNH, ainsi qu'entre la nappe du Tso Morari et celle du Mata.

Dans la partie SE du terrain, au Spiti, une tectonique à vergence NE crée un équivalent latéral de la nappe de Shikar Beh, définie plus à l'ouest par Steck et al. (1993). Au Spiti celle-ci engendre la formation du chevauchement du Lagudarsi La. Des structures d'interférences avec la front de la nappe du Mata montrent que les mouvements à vergence NE précédent ceux à vergence SW.

Un événement tectono-métamorphique Cambro-Ordovicien est fortement suspecté en Himalaya. Le granite peralumineux du Tso Morari et le granite alcalin du Rupshu, datés respectivement à 479 ± 2 Ma et 482.5 ± 1 Ma par U/Pb sur zircons, semblent s'être mis en place dans un contexte d'extension post-orogénique. Bien que ces deux granites soient généralement fortement déformés, ils ont gardés des signatures bien différentiées notamment concernant la typologie des zircons.

Les observations de terrain, ainsi que de nombreux résultats analytiques, ont montré que le granite du Polokongka La n'est en fait que le protolite non déformé du gneiss du Tso Morari. Par contre le granite du Rupshu est lui fortement différent non seulement du gneiss du Tso Morari, mais aussi de son équivalent latéral, le granite de Nyimaling, situé plus au NW.

Abstract

The Rupshu area, in NW India, illustrates the transition between the Tethyan Himalaya, made of very low grade metasediments, and the North Himalayan Crystalline Zone (NHCZ). The Tethyan Himalaya contains a sedimentary series that spans from Precambrian to Cretaceous, with an important gap between Ordovician and Permian. The Lower and Middle Triassic formations are very monotonous and reflect a distal environment along the north Indian margin. From Upper Triassic, the formations begin to look like those of the Spiti-Zanskar sedimentary basin. However, because of the more distal situation of Rupshu, the detritic component is generally less important. The SW-vergent Kum Tso Thrust overthrusts distal Middle Triassic series over more proximal Upper Triassic to Liassic sediments. The very low grade metamorphism of the Tethyan Himalaya has been studied with "illite crystallinity". This allows us to estimate to about 16 km, the offset of an extensional shear zone observed along two parallel profiles, distant by about 70 km. This extensional shear zone is interpreted as a superficial equivalent of the Zanskar Shear Zone.

The NHCZ is formed by metamorphic equivalents of Paleozoic sediments. A description of the probably Permian lithologies of the Karzok Formation shows important lateral variations. The transition between the Tethyan Himalaya and the NHCZ is perfectly gradual and is marked by an increase of the metamorphic grade from diagenesis to the sillimanite zone. This Barrovian metamorphism, triggered by the SW-vergent emplacement of the Tso Morari and Mata nappes, overprints a High Pressure - Low Temperature eclogitic metamorphism, linked to the subduction of the Indian plate below Asia. Only the Tso Morari nappe has been affected by this first Himalayan metamorphic event. The Barrovian metamorphism, present in both of the nappes, has been studied with several quantitative thermobarometric methods. The thermodynamic data set of Holland and Powell (1998) and of Berman (1988), the isotopic quartz-garnet or quartz-kyanite geothermometers, and the geothermometers based on the Ti content of amphibole, quantified the metamorphic grade differences observed along the profile between Pang and the Tso kar. These methods showed

that there are no metamorphic jumps between either the Tethyan Himalaya and the NHCZ or between the Tso Morari and Mata nappes.

In the SE area, in Spiti, a NE-vergent tectonic creates a lateral equivalent of the Shikar Beh nappe, defined westward by Steck et al. (1993). In Spiti this nappe creates the Lagudarsi La Thrust. Interference structures with the frontal part of the Mata nappe show that the NE-vergent movements precede the SW-vergent ones.

A Cambro-Ordovician tectono-metamorphic event is highly suspected in Himalaya. The peraluminous Tso Morari granite and the alkaline Rupshu granite, dated respectively at 479 ± 2 Ma and 482.5 ± 1 Ma by U/Pb on zircons, seem to have set up in a post-orogenic extensional setting. Even so both of them are generally highly deformed, they preserved well differentiated signatures, particularly concerning their zircon typologies.

Field observations, as well as several analytical results, have shown that the Polokongka La granite is nothing other than the undeformed protolith of the Tso Morari gneiss. On the other hand, the Rupshu granite is very different not only from the Tso Morari gneiss, but also from its lateral equivalent, the Nyimaling granite, situated north-westward.

Acknowledgements

Completing this study would not have been possible without the support and the enthusiasm of my thesis director, Prof. Albrecht Steck. He not only taught me geology, but he also showed me a way of working, based on observations. I have always been impressed by the way in which he literally scans nature. Nothing, from a small mosquito that bites you in Manali, to the gigantic bearded vulture of the Tso Morari, escaped his attention. His incredible knowledge in all domains of natural science brought a touch of diversity during the field seasons. To this true naturalist, I would like to express my sincere gratitude.

Of course, the next persons to whom I am most indebted are all the geologists who accompanied me in the field. François Baillifard, normally a social guy, experienced a two-month trip in this isolated area. Then, I had the support of the enthusiastic Maria Laetizia Fillipi, who would merit to receive the title of *Master in Himalayan Field Assistance* in light of time she has spent with students in Himalaya. And at last Thierry Bussard, who underwent the last field seasons, when everything has to be checked, of course at every field extremities. I will not forget my other colleagues who accompanied me during part of the 1996 season. Jean Claude Vannay, Jean Luc Epard, Johannes Hunziker, Martin Robyr and Alain Morard shared the first discovery of this field, when you still don't understand what's going on, and when you begin to doubt. In 1997, Hugo Bucher, accompanied by Alex Vogel, helped me with the stratigraphy, which finally fell into place for me.

Back in the office, in Switzerland, the support of my colleagues was absolutely necessary to finish this thesis. First of all I would like to thank the co-writer of my papers. Apart A. Steck who followed the whole process of this thesis, François Bussy shared with me

his strong background in the granites. His excellent age determinations are the pillars of my work on the granites. Philippe Thélin guided me during the realisation and the interpretation of the X Ray diffractometry. In the same domain, I would like to thank Lilianne Dufresne and O. Lokosha for their help during the X-Ray analyses. I cannot forget the help of Jorge Spangenberg, who tried to fix the isotope line several times for me. His patient work did not help me, but the next student will benefit from his efforts. In Albuquerque, USA, Zack Sharp permitted me to use his isotopic extraction line, and his Game Boy (the computer assisted laser). I thank him for his enthusiasm and for the trust he accorded me. Viorel Atudorei welcomed me warmly and helped me with the isotope analyses, when I arrived in this land of deserts and Mc Donalds. Jean Guex and Hugo Bucher determined the ammonoids, even when I felt ashamed to show them something that hardly reflected a fossil.

There are people who can make incredibly precise work with huge mechanical machines and their hands. I am not that kind of person, but L. Niccod certainly is, based on the quality of the thin sections he gave me. I also want to thank all my other colleagues and friends at the University of Lausanne, particularly Micha Schlup, with whom I shared my passion for mountaineering ... during week ends! Tatjana Brombach, who wins the race concerning who will finish first. Sabrina Pastorelli, the only Italian girl who does not eat tomatoes, Sebastien Pillet the biker, Pierre Dezes the game player, Jean Claude Vannay the *Calvin & Hobbes* reader, and several others who contributed to this thesis, even if it is only by sharing coffee at the cafeteria.

None of the analytical work would have been possible without the support of Georges Mascles and the French Embassy in New Delhi, who kindly and safely sent all my heavy samples to Europe. I am also grateful to all those people in India, and particularly to Norboo, my faithful guide, who accompanied me during those unusually long treks in areas where grass is rare, the wind is always blowing and the nights are cold.

This study was financed by the Université de Lausanne, by the Swiss National Science Fund (FNRS grants n° 20-45063.95/1 and 20-52165.7) and by the Herbette Fund.

This publication has been sponsored by *Fondation Dr. J. de Giacomi*, *Fonds de subsides pour l'Impression des Thèse* and the *Fondation du 450^{ième} de l'Université de Lausanne.*

I am also grateful to my parents, who permitted me to study geology and who welcomed me home when I missed the last train to Sion. In the same category of people also come Stéphane Cuchet and Sabina Schmidt, with whom I shared several dinners in their home or in mountain huts. Last but not least, I would like to thank Romaine, for having endured the long months when I was in the field, and also the long months when I was always at home writing this thesis. I'll let her choose which was the worst.

1/ Introduction

"What is incomprehensible is that the world is comprehensible"

A. Einstein

Himalayan geology is a fascinating world that pioneers began to explore at the end of the XIXth century. Since then, numerous authors have made numerous observations, numerous analyses and numerous hypotheses. All these works led the Himalayan geologists to some certitudes. Himalayan mountains are (too?) high, Himalayan buses are not made like ordinary buses (neither are bus drivers!) and Himalayan highways only exist on maps. But Himalayan gods must exist as we are still here to tell you what we observed over there! Starting from these truths we can try to go forward in the understanding of the Himalayan belt.

When a geologist formed in an alpine country arrives in Himalaya, he is first surprised by the scale. The belt reach 8846 m, is about 2500 km long and 300 km large, rivers are bigger, gorges are deeper, valleys are longer and rains are heavier; no wonder that geological phenomena are also at another scale. In fact, all these morphological features derive from the particular geological history of the belt.

During these four years of PhD thesis work, I tried to immerse myself in this history to better understand things that might well be incomprehensible. This PhD thesis leads to the publication of three papers in international revues and to the redaction of this "Mémoire de Géologie".

1.1/ Geography

Geographically the Himalayan range is an important feature of the Asian continent. It has great historical, cultural, economical and ecological influence. From west to east, the belt stretches over five countries: Pakistan, India, Tibet, Nepal, Bhutan and China. The main rivers, namely the Yarlung Tsangpo, Indus and Sutlej rivers, spring up near the sacred Mt Kailash in Tibet. Indus and Yarlung Tsangpo follow the range towards northwest and southeast respectively, while the Sutlej cross cuts the Himalayan belt almost perpendicularly to the structures.

The area studied is located in NW India, not far from the Tibetan border and north of the Main Himalayan Range, represented here by the high mountains of Lahul and Spiti (e.g. Mulkila, 6517m; Shilla, 7026m). As the monsoon is stopped by the main range, climate is very dry on the northern slope of the Himalaya. The northern part of this field, composed mainly of quartz-schists and gneisses, shows a rounded morphology with numerous hills and soft slops, while the southern part is the land of massive limestone with steep gorges and sharp summits. The almost complete absence of vegetation, except some shrubs and some grass in the bottom of the valleys, makes for good outcropping quality, diminished only by the large amount of quaternary deposits.

The area investigated is mainly in the Rupshu district, which belongs to the state of Jammu and Kashmir of India (Fig 1.1). It covers about 5000 km^2 and stretches from 3600m in the Spiti valley up to 6200m at the Mata Peak. Villages are mainly located along the Zara

river, which delimits the western border of the area. These are the villages of Zara, Pangjin, Jakang, Sangtha, Pogmar and Lun (Plate 1.1). Karzok Gompa, situated on the shore of the Tso Morari, is probably the biggest village and one or the rare ones which are inhabited the whole year. Nuruchan, in the center of Rupshu, is the administrative village, but is uninhabited during summer. Tudje Gompa has a few houses around a nice Buddhist monastery that dominates the Tso Kar plain. The inhabitants of the Rupshu district form semi-nomad communities, and live in tents the whole summer. Their only goods are huge pashmina-goat herds, their tent, jewels, religious artifacts and their smiles. Each year they follow the same itinerary, and have reserved places to build their camps. Since China invaded Tibet, many refugees have come to northern India. In Rupshu, modern villages (e.g. Pogmar) have been built. They stay here in winter and spend the rest of the year in their tent. Due to the desert landscape, cultivation is only possible along the main rivers, but in fact there are very few fields in Rupshu. Most of them are found in Karzok, Lun and along the valleys that go down to the Indus River. Access to the rest of the world passes via the Indus valley, which is easily reached from Karzok, while from the Zara valley or from the Tso Kar area one has to get over the Taglang La at more than 5000 m. Towards the south, a long and vertiginous road reaches Manali in Himachal Pradesh.

One can not describe the Rupshu geography without mentioning its lakes (Tso in Ladakhi and Tibetan languages). The 25 km long Tso Morari is dammed in the south by the huge Phirse alluvial fan. As it is a closed basin, it is slightly salty. Karzok is the only village along its banks. This lake is an important migration stop for many birds, like barred head gooses and wild spotted bill ducks. Since its opening to foreigners, this area has become more and more popular. The project of creating a protected area would help avoid anarchic tourist development.

The Tso Kar and the Starstapuk Tso are other lakes located in a closed basin. The Tso Kar is very salty, and is probably destined to disappear. The old water level is clearly visible and testifies that the lake was much larger and probably extended into the nearby More Plain towards the west. The last lake of Rupshu is the small Kum Tso located in the large Phirse Phu alluvial plain. Once more it is a closed lake, but surprisingly it is not very salty. Rivers in Rupshu belong to three hydrographic basins. Most of them are parts of the Indus basin and reach the Indus either via the Zara, Tsarap and Zanskar rivers, or directly in the NE area. The other basins are the closed basins of Tso Morari and Tso Kar. In the SE, all rivers join the Spiti river, and finally the Sutlej river.

Fig 1.1: Geographical map of NW India, based on Landsat imagery. In grey is the location of the area studied.

1.2/ The geological history of India and the forming of the Himalaya

The study of the Himalayan belt allows us to reconstruct the evolution of the northern passive margin of India from Late Precambrian to Cenozoic. During the Paleozoic, the Indian continent was part of Gondwana (Smith et al., 1981; Dalziel, 1991; Sacks et al., 1997) and connected in the north with the Cimmerian Superterranes. The Gondwana supercontinent was separated from Eurasia by the Paleotethys ocean. Many Gondwanien terranes recorded a thermo-tectonic event, responsible for the assembly of Gondwana, known as the Pan-African event (Kennedy, 1964). The northern margin of India is no exception to this rule and the Pan African event is principally marked by the widespread Cambro-Ordovician plutonism and by a few signs of pre-Himalayan metamorphism (Frank et al., 1977; Ferrara et al., 1983; Le Fort et al., 1986; Pognante and Lombardo, 1989; Argles et al., 1999; Wyss, 1999).

During Early Permian, the Cimmerian Superterranes separate from India and begin to migrate towards north, to collide with Eurasia. They form large part of the nowadays Iran, Afghanistan and Tibet. The beginning of rifting between India and the Cimmerians Superterranes is marked by the Panjal Traps volcanics and will lead to the opening of the Neotethys ocean.

In Early Cretaceous East Gondwana, previously separated from West Gondwana, begins to break up with the separation of the Indian plate from Australia and Antarctica. The Indian plate will then move northwards at a speed of 16 cm/year until its collision with Eurasia and the accreted Cimmerians Superterranes. The collision begins west and propagates towards the east. A significant drop in the drift rate to less than 5 cm/year at 55-50 Ma is usually interpreted as the onset of the collision of the Indian plate with Eurasia (Patriat and Achache, 1984; Besse and Courtillot, 1988). A vertebrate fauna, with distinct Eurasian affinities, has been found in sediments of the Cretaceous-Tertiary boundary, interbedded in the Deccan traps of the Indian peninsula. This suggests that India was probably in contact with Eurasia at 65 Ma. However, as suggested by Treolar and Izatt (1993), this fauna could have taken advantage of an early collision between the Kabul block and India.

Ever since that collision, India has been indenting Eurasia. The Indian continental crust has been partly subducted below Tibet, but the system rapidly got stuck and other mechanisms have gotten started. The deformation is probably partly absorbed by lateral shearing and an eastern escape of the Indochina blocks, in front of the Indian indenter (Molnar and Tapponier, 1975; Burchfiel et al., 1989). However a large amount of shortening is also probably absorbed by the important folding and thrusting that created the greatness and the complexity of the Himalayan range.

1.3/ Main subdivisions of the Himalaya

At first glance, since the main tectonic structures can be followed all along the belt, Himalayan geology seems quite simple. Things become more complicated at both syntaxis (Nanga Parbat and Namche Barwa). Along most profiles a similar succession can be found, with several small local particularities (Gansser, 1964; Hodges, 2000). From south to north the Himalayan belt is classically divided into several domains (Fig. 1.2). Some of them are real tectonic units, but some are only zones without clear boundaries.

The Subhimalaya

Lying in front of the Himalayan range, it is made principally of Miocene to Pleistocene molasse sediments known as the Muree and Siwaliks Groups. As the Himalaya is still an active belt (Patriat and Achache, 1984) these molasses are folded and thrust along the Main Frontal Thrust (MFT), over the quaternary alluvium of the Indo-Gangetic plain.

The Lesser Himalaya (LH)

This unit, mainly composed of Upper Proterozoic to Lower Paleozoic sediments, is thrust over the subhimalaya, along the Main Boundary Thrust (MBT). This important thrust formed prior 10 Ma along the whole belt (Andrew et al., 1995). Proterozoic granite-gneiss are intercalated within the metasediments.

The Lower Himalayan Crystalline Zone (LHCZ)

Along some cross sections (e.g. Sutlej, Nepal...), the Lower Himalayan Crystalline Zone comes in-between the Lesser Himalaya and the High Himalayan Crystalline Zone (HHCZ). The LHCZ is similar to the HHCZ but it is separated from the latter by an important thrust (e.g. the Vaikrita Thrust or MCT 2). Actually this zone results from the imbrication of the Main Central Thrust which spread over a thick Schuppenzone (Gansser, 1991).

The High Himalayan Crystalline Zone (HHCZ)

Or High Himalayan Crystalline Sequence, Tibetan Slab, Greater Himalaya, Crystalline Nappe Zone, Central Crystalline Zone.

This 10-15-km-thick zone is defined by its medium to high grade metamorphism. It is principally made of Precambrian and Lower Cambrian metasediments, but can also locally include younger formations. The HHCZ is frequently intruded by Cambro-Ordovician

granites and by Tertiary leucogranites. A steep topography with deep gorges and high summits characterizes the morphology of this zone, essentially made of massive rocks.

In the south, the HHCZ overthrusts the Lesser Himalaya along the Main Central Thrust (MCT, (Heim and Gansser, 1939)), which began to be active at ~21 Ma (Hubbard and Harrison, 1989). The youngest ages obtained on the MCT are Late Miocene to Pliocene (Catlos et al., 1999).

Contrary to the southern limit, its northern one is less clearly defined. A normal fault zone (the South Tibetan Detachment System) usually separates the HHCZ from the overlying lower grade zone. However in some places (e.g. Lahul (Vannay and Steck, 1995; Wyss et al., 1999; 2000) or Central Himalaya (Gansser, 1991), no detachment marks a precise boundary between both units, showing that the transition can be gradual.

The Tethyan Himalaya (TH)

Or Tibetan Himalaya, Tethyan Himalaya domain

Introduced by Auden (1937), this domain comprises the very low grade to non-metamorphic sediments of the northern margin of India. An almost complete stratigraphic series, ranging from Precambrian to Eocene, documents the whole history of the northern margin of India. The Permian basic intrusions of the Panjal Traps are intercalated in this sedimentary record. Several kilometer thick formations can be followed all along the belt. Although the formations names are usually different, correlation can be made between Bhutan and western India. The sediments of the TH are highly deformed and folded and several nappes have been described within this domain (e.g. the North Himalayan Nappes of Steck et al. 1993).

The North Himalayan Crystalline Zone (NHCZ)

Or North Himalaya

Along some profiles, metamorphic rocks can be found at the northern border of the Tethyan Himalaya. This is the case in the area presented here. The NHCZ represents large domes (Tso Morari, Gurla Mandhata…) of medium to high grade metamorphic rocks. Like in the HHCZ, these rocks are either the metamorphic equivalent of the Precambrian to Paleozoic Tethyan sediments, or gneisses derived from Cambro-Ordovician granitic intrusions.

The occurrence of eclogites within these domes is a particularity of the NW Himalaya; they have been described in Pakistan (Pognante and Spencer, 1991; Fontan and Schouppe, 1994; Le Fort et al., 1997) and in Rupshu (Berthelsen, 1953). This early high pressure, low

temperature metamorphism results from the subduction of the Indian slab below the Asian plate and has been dated at around 55 Ma (Tonarini et al., 1993; De Sigoyer et al., 1998).

Remarks on these subdivisions

This classical description of the Himalaya might raise some problems. If the first subdivisions effectively correspond to tectonic units (i.e. subhimalaya, Lesser Himalaya, LHCZ), this is not the case for the overlying zones (HHCZ, TH and NHCZ). Contrary to what has been sometimes proposed in the literature, the HHCZ and NHCZ are not the basement of the TH sedimentary cover. It has been shown that there is only one stratigraphic sequence, which is overprinted by the Himalayan metamorphism at various grades. Moreover the limits between the Crystalline Zones and the Tethyan Himalaya cannot be defined when the metamorphism decreases progressively. For this reason it is impossible to give a good definitions of these three zones. That's why the terms HHCZ, NHCZ and TH will be avoided in the following.

The Lamayuru Unit

The Lamayuru Unit is a stratigraphic sequence of Permian up to Eocene sediments, from the slop of the calcareous platform. While the latter forms the sediments of Spiti and Zanskar, the calcareous and detritic flyschs from the slop form the Lamayuru Unit. The Markha Unit described by Stutz and Steck (1986) NW of this study, is an equivalent of the Lamayuru Unit.

The Indus Tsangpo Suture Zone (ITSZ)

This zone, defined by Gansser (1964), represents the geological boundary between the Indian and Asian plates. The Indus and the Tsangpo rivers follow this zone of relatively tender rocks, before they find a suitable way to turn south towards the Indian Ocean. The ITSZ is formed by:

-The Dras arc Complex made of arc extrusives, volcano-clastic and tuffaceous sediments intercalated with turbiditic siltstones and limestones. This complex is a relic of a middle Late Cretaceous volcanic island arc formed within the Neotethys, above a subduction zone (Robertson and Degnan, 1994).

-The Jurassic-Cretaceous Ophiolite Melanges are chips of the basaltic floor of the Neotethys ocean, intercalated with flyschs and ultramafites (Gansser, 1980).

-The Indus Molasses are mainly continental sequences derived from the post-collisional erosion of the emerging Himalayan belt to the south and from the Ladakh

Batholith to the north. Red beds, conglomerates and lacustrine deposits suggest deposition in intermontane basins (Mascle et al., 1986; Garzanti and Van Haver, 1988).

The Trans-Himalayan Batholith (TB)

Located on the Asian plate, this batholith has formed in several magmatic phases from 100 Ma to Late Paleocene (Schärer et al., 1984). It is due to partial melting of the subducting Neo-Tethyan slab beneath the Asian margin (Honegger et al., 1982). This ultrametamorphism generates a composite I-type plutonic complex ranging from gabbro through diorite to granite. The Trans-Himalaya is divided from west to east in the Kohistan, Ladakh, Kailash, Gandese and Mishimi blocks.

1.4/ Geological settings

The area investigated shows a very contrasting geology ranging from the very low grade metasediments of the Mata nappe in the SW, to the high grade metapelites of the Tso Morari nappe in the NE. Several authors suggested that a tectonic accident, either a thrust or a normal fault, separates the high grade from the very low grade metasediments (Thakur and Virdi, 1979; Thakur, 1983; Guillot et al., 1997). Our observations show that only late normal faulting of little influence exists locally but usually the transition between the two domains is gradual.

1.4.1/ The Mata nappe

In the SW, the frontal part of the Mata nappe is made up of very low grade metasediments which preserved their sedimentary facies. These metasediments can be broadly subdivided into two parts. A southern domain with Upper Triassic to Upper Cretaceous sediments, which can be compared to what is described in Spiti or Zanskar, and a northern domain that ranges from Precambrian to Middle Triassic and which shows many differences with the "classical" Spitian stratigraphy. The main differences come from the lack of several Paleozoic formations and from the different sedimentation rates during Permian and Triassic. Both domains are separated by an important top-to-the-SW-directed thrust, the Kum Tso Thrust, which stacks up Ladinian to Carnien marls and limestones of the northern domain, over Norian to Jurassic massive limestones of the southern domain.

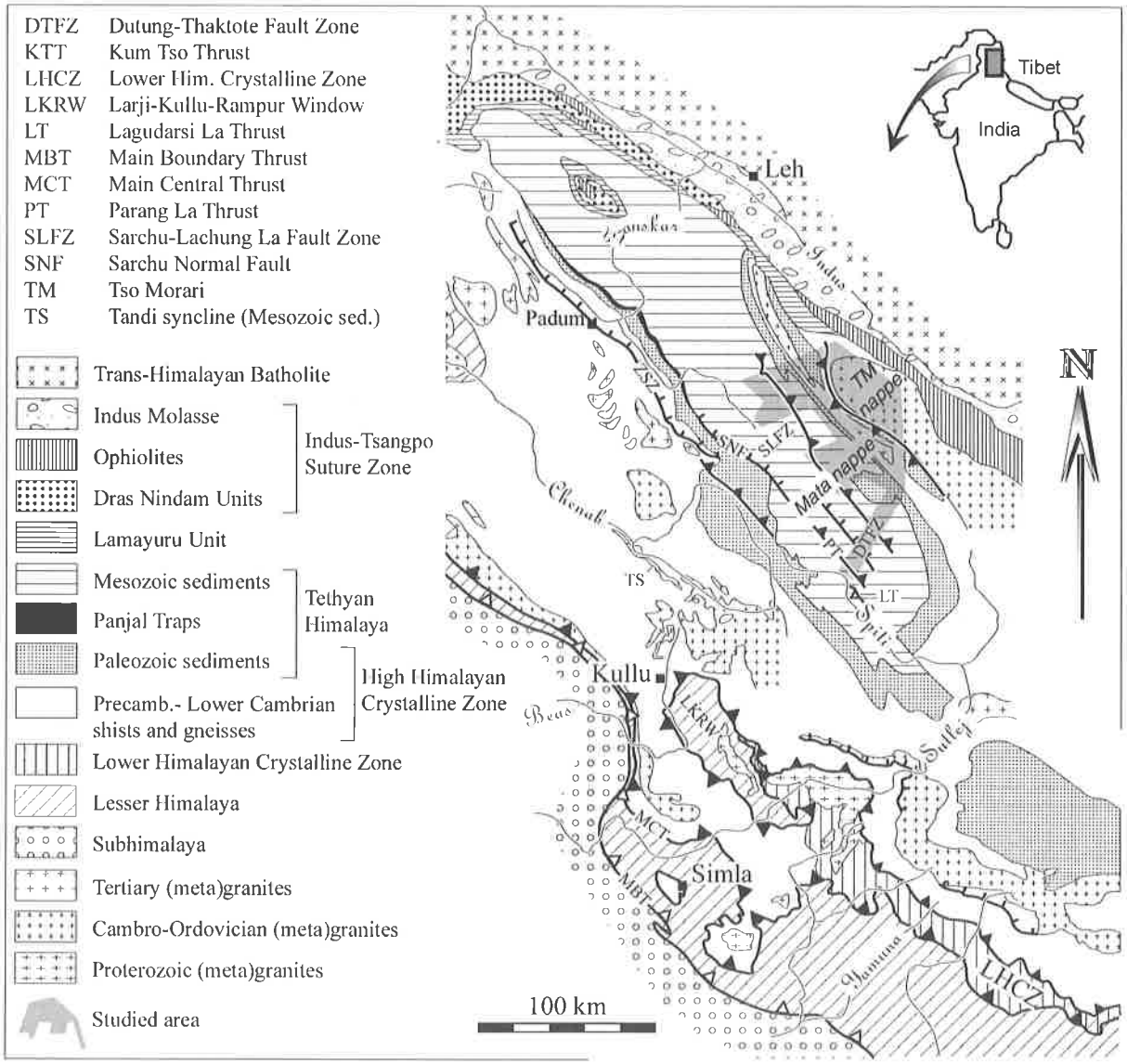

Fig. 1.2: Geological map of NW India, between Simla and Leh. Modified after Frank et al. (1973), Steck et al. (1993), Vannay (1993), Frank et al. (1995), Steck et al. (1998), Vannay and Grasemann (1998), Dèzes et al. (1999), Wyss et al. (1999) and including our own data. The area studied is presented in grey.

In both domains the sediments are folded and overthrust and belong either to the SW-verging Mata nappe (Steck et al., 1998), or to its western equivalent, the Nyimaling Tsarap nappe (Steck et al., 1993). As these nappes are not cylindrical, their fronts are out of line. The Mata nappe shows its frontal thrust (the Parang La Thrust, (Steck et al., 1998) north of the Spiti river, within the investigated area (Plate 1.2), while the frontal thrust of the Nyimaling Tsarap nappe is located more south than the limits of this field (Baralacha La Thrust, (Steck et al., 1993; Vannay and Steck, 1995).

An important synorogenic extension zone cross cut the main structures of compression. These extension zones, the Dutung Thaktote normal Fault Zone and the Sarchu Lachung La normal Fault Zone, have been correlated with the South Tibetan Detachment

System (Burchfiel et al., 1992). It has been shown that theses extensional shear zones are coeval with thrusting along the MCT, at the front of the belt (Hodges et al., 1992; Harrison et al., 1995; 1996; Dèzes et al., 1999).

The sediments of the Mata nappe are weakly metamorphic in the SW. However, they still have been buried during nappe emplacement, which generates an anchizonal to epizonal metamorphism. The regional metamorphic gradient is complicated by normal faults, which lowers diagenetic sediments between epizonal zones. Towards NE, in the more internal parts of the Mata nappe, the metamorphism grade increases progressively to reach the garnet zone.

The Ordovician Rupshu granite intrudes Precambrian to Cambrian sediments. Although coeval with the Tso Morari gneiss emplacement (described below), the alkali-calcic Rupshu granite is clearly different from the latter. In the western continuation of the Rupshu granite lies the Ordovician Nyimaling granite (Stutz and Thöni, 1987). This S-type granite is also clearly different from the Rupshu granite, as revealed by contrasting zircon typology (Girard and Bussy, 1999).

1.4.2/ The Tetraogal nappe

Near Karzok, a lentil of ultrabasics, metabasics and chromite outcrops within the mainly carbonaceous Karzok Formation (Berthelsen, 1953; Steck et al., 1998). Below the lentil, the sediments are in a normal stratigraphic position, while above it they are in an inverse position. The existence of those ultrabasics, about 40km south of the Indus Suture Zone, raises some problems. Berthelsen (1951) suggests that there is two successive sutures. Steck et al. (1998) proposed that they have been swept along the thrust between the Mata and Tetraogal nappe (which could also be a basal slice of the Mata nappe). Fuchs and Linner (1996) correlate this lentil with the Permian Panjal Traps. However the Panjal Traps do not usually contain ultrabasics. On the other hand, geochemical analyses of metagabbros from the Karzok complex, show similarities with analyses made on basic rocks from the Indus Suture Zone (Mahéo et al., 2000).

As the metasediments of the inverted limb of the Mata nappe and those of the Tetraogal nappe are similar, the thrust between those nappes can only be identified when the ultrabasics are present (i.e. near Karzok). The other way to map this thrust would be to follow the limit between the normal and inverted stratigraphy.

1.4.3/ The Tso Morari nappe

It is difficult to trace precisely the limit between the Mata and the Tso Morari nappes, because the same lithologies are found on both sides of the thrust. However the Tso Morari nappe can be distinguished from the Mata nappe by the presence of eclogites and eclogitic

paragneisses (Berthelsen, 1953; Guillot et al., 1995; De Sigoyer et al., 1997; 1997). The age of eclogitisation is 55 ± 17 Ma (U/Pb, (De Sigoyer et al., 2000).

The Tso Morari nappe covers the Tso Morari dome, which consists of a core of a metamorphosed Ordovician granite (Girard and Bussy, 1999) intruding Precambrian to Cambrian sediments of the Phe Formation. The Tso Morari gneiss is not homogeneously deformed and large volumes of its granitic protolith are preserved.

1.4.4/ The Lamayuru Unit and the Indus Suture Zone

They border the northern slope of the Tso Morari dome. Locally a normal fault separates the Indus Suture Zone from the Tso Morari dome (e.g. the Ribil fault, Steck et al. (1998) or Zildat fault of Thakur and Virdi (1979). We did not study these zones which mark the northern limit of the area investigated. For a more complete description of these units see Fuchs and Linner (1995; 1996).

1.5/ History of geological investigations

The first geological descriptions of the Tso Morari area are those from Stoliczka (1866). During his PhD thesis he described the cross section between the Spiti valley and the Indus, passing via the Tso Morari. Special attention is paid to the stratigraphy and we owe him several formations' names, some of which are still in use today. I was seized by some kind of admiration when walking on the trails of this pioneer, who in 1865, realized an incredible expedition across NW India. During his 6 month trip from Simla to Kargil, via Kulu valley, Keylong, Leh, and Padum, he walked back the Tsarap river up to the Pangpo La, and reached the Tso Morari by the large basin of the Phirse Phu, taking a detour through the Lanyer La. Since then, nobody had gone to the Phirse Phu basin and the upper Tsarap valley had only been visited by Raina and Bhattacharyya (1974). Oldham (1888) was the next geologist who visited the Rupshu area. He has been followed by Hayden (1904), who reached the Tso Morari from the Spiti valley by a new route. He has described the Triassic rocks of the Tethyan Himalaya and the metamorphics of the Tso Morari dome. He introduced the new terms Tso Morari gneiss and Rupshu granite. The same author, accompanied by Dr Burrard (Burrard and Hayden, 1908), drew what is probably the first geological section between Simla and the Indus river. Unfortunately this publication is difficult to find. When the wars stopped in Europe, European geologists began once more to investigate the Rupshu area. After his expedition between the Sutlej river and the Indus valley passing by the Tso Morari, Berthelsen (1951) published a new geological section of NW India. Two years later, he published the results of a more detailed study of the Rupshu area, with a special interest in

petrography (Berthelsen, 1953). After this hegemony of European géologists, Indians began to investigate the area. These are the works of Gupta et al. (1970), Sharma and Kumar (1978) and Virdi et al. (1978). The latter published the first biostratigraphic age for the Taglang La Formation (considered as the upper part of the Tso Morari Crystalline), on the basis of Permian conodonts. Then Thakur and Virdi (1979) published a geological map of the Rupshu area. They subdivided the Tso Morari dome in the Puga and the Taglang La Formations. Later on came the work of Thakur (1983) who recognized three tectonic phases and four metamorphic episodes in the Tso Morari Crystalline Complex. More recently, as the Rupshu district became once more open to foreigners, Austrians and French geologists have taken an interest in this area. The results were the papers of Fuchs and Linner (1995; 1996) who described a cross section along the Zara river and who have particularly studied the northern part of the Tso Morari dome. The French school is particularly active at this time and has published several papers about metamorphism and more particularly about the thermobarometry and the age of the eclogitic episode (De Sigoyer, 1995; De Sigoyer et al., 1997; Guillot et al., 1997; 1998; 2000). Excepting the work of Gupta et al. (1970), no studies have been made on the area of the Lachung La, and very few data concern the area of Kum Tso. All the work of the last 150 years seems to have been done on the Tso Morari dome and its surrounding rocks.

1.6/ Purpose and methods of the study

This work comes within an overall study of the NW Himalaya, undertook since 1979 by the University of Lausanne, mainly lead by Prof. A. Steck and H. Masson. It resulted in the publication of five PhD Thesis (Stutz, 1988; Spring, 1993; Vannay, 1993; Dèzes, 1999; Wyss, 1999), the one presented here, and 3 more which are under way (M. Robyr, M. Schlup and V. Baudraz). Together with several papers, these PhD thesis have attempted to produce detailed structural and geological maps of NW India. As the Tso Morari opened to foreigners only recently, very few modern works concern it, and this PhD thesis will partly fill this gap. A large part of this study was devoted to fieldwork and geological mapping, using SPOT satellite images as topographic background. Three geological expeditions allowed us to better understand the structural framework, the metamorphism and the particular stratigraphy of the area. The observations of the author have been completed by the fieldwork realized in 1996 by A. Steck, J.L. Epard, J.C. Vannay, M. Robyr and A. Morard in the area of the Parang La and Lagudarsi La (Steck et al., 1998).

Several questions were open at the beginning of this study:

- Is there a nappe tectonic, as observed further west in the Nyimaling area?
- Are there important stratigraphic differences with the classical series of Spiti?
-What is the Karzok Formation introduced by Fuchs and Linner (1996), and what is its extent?
-What is the nature of the transition between the North Himalayan Crystalline Zone and the Tethyan Himalaya?
-What is the geographical extent of the early eclogitic metamorphism?
- How is the regional metamorphism and are there metamorphic breaks due to nappe tectonics or to an extensional fault zone as observed in Zanskar?
- What are the ages and origins of the metagranites from Rupshu and are they linked with the Nyimaling granite?
- Are there traces of a pre-Himalayan tectono-metamorphic event?

To answer these questions a detailed study of the tectonic structures, the metamorphism and the stratigraphy has been studied in the field, and completed with several methods in laboratory.

Apart from classical petrography on thin sections, the metamorphism was studied by illite crystallinity and Qtz-Cc isotopic thermometry in the very low grade metasediments of the Tethyan Himalaya, and by analytical thermobarometry using different thermodynamic datasets, as well as by Qtz-Grt or Qtz-Ky isotopic thermometry in the North Himalayan Crystalline Zone. Moreover, a complete determination by electron microprobe of the metamorphic paragenesis in the metabasites gives precious information on the regional metamorphic grade.

Three sets of samples of distinct metagranites, namely the Rupshu granite, a granite from the Polokongka La and its deformed equivalent the Tso Morari gneiss, have been dated by U/Pb method on abraded zircons. Their petrography, zircons typology and whole rock geochemistry allowed us to identify their origin and relationships.

2/Stratigraphy

One day in the life of Brahma is equivalent to the time a pendulum would need to erode a bronze mountain, brushed once a century.

The stratigraphy of the northern part of Rupshu is quite different from that of Spiti and Zanskar. While those areas contain the proximal facies of the northern border of India, the Rupshu, as well as the Nyimaling area, contain more distal facies. In the following lithostratigraphic descriptions, we will separate on one hand the Tso Morari nappe from the Mata nappe, and on the other hand the northern domain from the southern domain of the Mata nappe.

The scarcity of fossils, particularly in the north, does not allow a very precise stratigraphy, and most formations names are ascribed on the basis of lithologic correlations and stratigraphic positions. To curb the proliferation of useless names in the Himalayan literature, we intentionally did not introduce new formation names.

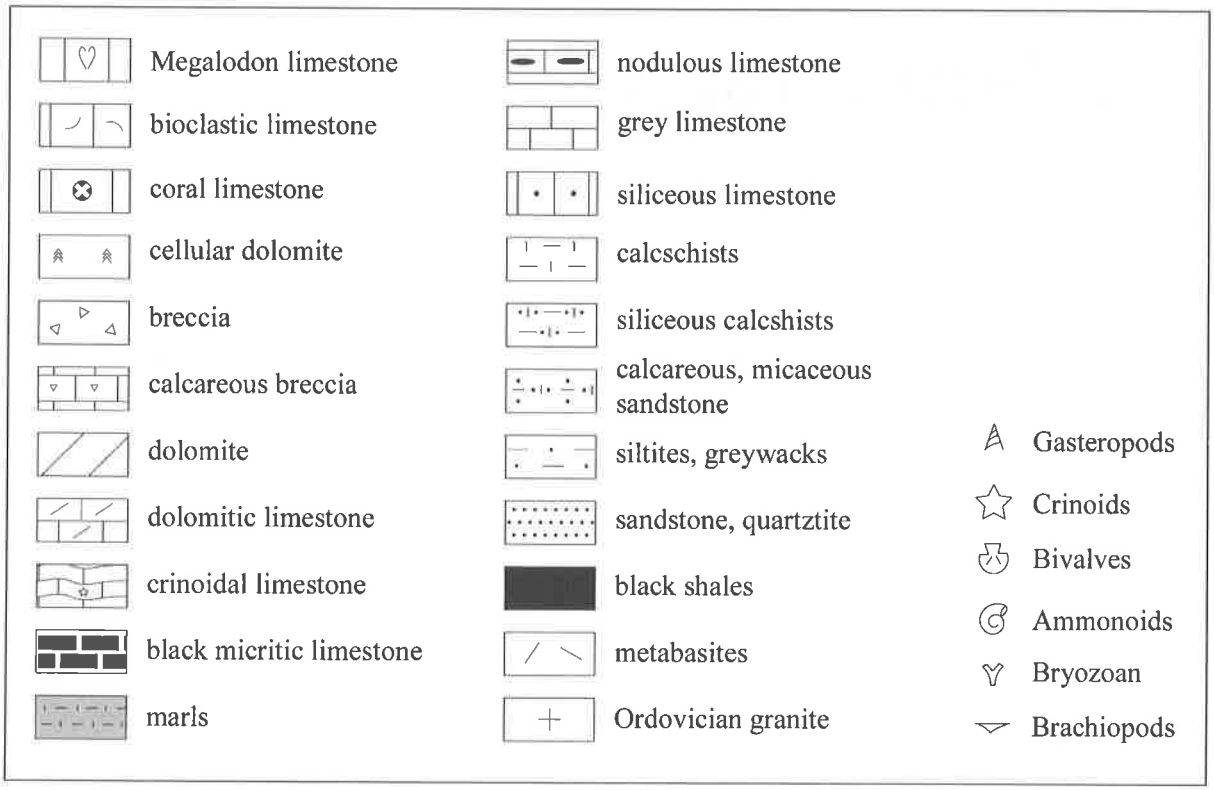

Fig. 2.1:Legend of the symbols used in the stratigraphic logs.

2.1/ The stratigraphy of the Tso Morari nappe

The Tso Morari nappe is entirely made of highly metamorphic metasediments, from the garnet zone up to the onset of the sillimanite zone. Thakur and Virdi (1979) divided the Tso Morari crystalline into the Puga and the Thaglang La Formations. According to the map presented in Thakur (1983), the Puga Fm. more or less corresponds to the Tso Morari orthogneiss and the intruded metasediments, while the Thaglang La Fm. includes all the

overlying metasediments up to the Triassic marls and limestones, without any distinctions. On the basis of Permian conodonts, found on the northern slope of the Thaglang La, Virdi et al. (1978) assign a Permian age for the whole Thaglang La Fm. As it will be shown on the following chapters, this simplistic view is not supported by our observations and the terms Puga and Thaglang La Formations have no stratigraphic meaning.

2.1.1/ The Phe Formation (Nanda and Singh, 1976)

Synonymy: *Haimantas* (Griesbach, 1891); *Dogra Slates* (Wadia, 1934), *Lolab Fm.* (Kumar et al., 1984); *Shumahal Fm.* (Srikantia and Bhargava, 1983); *Kunzam La Fm./Debsa Khas Mb.* (Kumar et al., 1984); *Batal Fm.* (Srikantia et al., 1980); *Vaikrita Series* (Griesbach, 1891).

Age: Its age is not very well constrained, due to the scarcity of fossils. None have been found in Rupshu. The existing Himalayan trilobite collection has been reinterpreted and completed by Hughes and Jell (1999). The older trilobites (*Redlichia* and *Paokania*) found in Himalaya are Early Cambrian. This old layer seems to be present in all the major Himalayan basins (Kumaon, Krol-Tal, Spiti, Kashmir and Salt Range). In Spiti, above this level, several early to middle Middle Cambrian trilobites have been found in the Kunzam La Fm. of the Parahio Valley (Huges and Jell, 1999). An **Late Precambrian to Early Middle Cambrian** age for the Phe Formation seems reasonable.

Description: In the Tso Morari nappe, the Phe Formation is highly metamorphic and mainly presents quartz rich metapelites and subordinates mica-schists. These rocks derive from siltstones, fine argillaceous sandstones, greywacks and shales. Boudins of eclogites retrogressed in amphibolites are intercalated in the metapelites. As the intense deformation could be responsible for their nowadays concordance with the stratigraphy, it is difficult to say if these basic rocks intrude the sediment or if they are coeval. De Sigoyer et al. (2000) compare these basic rocks to the Permian Panjal Traps, on the basis of similar initial epsilon Hf values.

The Phe Formation is intruded by the Ordovician Tso Morari granite, now deformed into a gneiss. Thin discontinuous metasedimentary levels within the orthogneiss suggest a multiple granite intrusion, the original intrusive contacts being subsequently transposed parallel to the schistosity during the main deformation.

As the base of the Phe Formation does not outcrop in Rupshu, it is impossible to estimate its total thickness. Proposed estimations reach 10 km, but it seems that large variations occur along the belt.

Type of sedimentation: The Phe Formation is classically interpreted as deposited in a shallow water intracontinental sea (Baud et al., 1984; Gaetani et al., 1986; Garzanti et al., 1986; McElroy et al., 1990; Vannay, 1993).

2.1.2/ The Karsha Formation (Nanda and Singh, 1976)

Synonymy: *Parahio Series* (Hayden, 1904), *Kunzam La Fm., Upper Mb.* (Srikantia et al., 1980).

Age: No fossils have been found in the Karsha Fm. of Rupshu. However the age generally admitted is **Middle Cambrian** according to its stratigraphic position (Garzanti et al., 1986) and to the trilobites fauna described in Zanskar (Huges and Jell, 1999). In the Nyimaling dome, a poorly preserved trilobite (*Asaphidae*) has been found in the dolomites (Stutz and Steck, 1986). If this identification is correct, it means that the top of the Karsha Fm. could reaches the Late Cambrian in this area.

Description: In the Tso Morari nappe, the Karsha Fm. only outcrops near the Tso Kar, where the formation reaches a thickness of about 300 m. This is probably not representative of their real thickness, as intense shear-deformation affects these rocks. The Karsha Fm. is principally made of massive dolomites of the Thidsi Member, particularly well developed in the Tso Morari nappe. The underlying Mauling Member is limited to about 30 m. of siltstones, sandstones and greywacks with subordinate dolomite and intercalated greenstones.

The base of the formation contains apophysis of the Ordovician Tso Morari granite. The contact between the granite and the sediments is parallel with the bedding, itself parallel to the main schistosity.

Type of sedimentation: In areas of lower metamorphic conditions (Lahul, Zanskar, Spiti), several structures (mudcracks, undulating stratification...) and palaeontological criterias (ichnofossils, stromatolithe) indicate inter- to subtidal shallow level conditions (Kumar et al., 1984; Garzanti et al., 1986; Stutz and Steck, 1986; Vannay, 1993).

2.2/ Stratigraphy of the Mata and Tetraogal nappes

The Mata nappe covers a wide range of metamorphic zones so that the older sediments are highly metamorphosed while the upper part is made of very low grade limestones, the transition being gradual. The Mata nappe will be divided in two domains, that differ by their sedimentation type. These domains are separated by the Kum Tso Thrust.

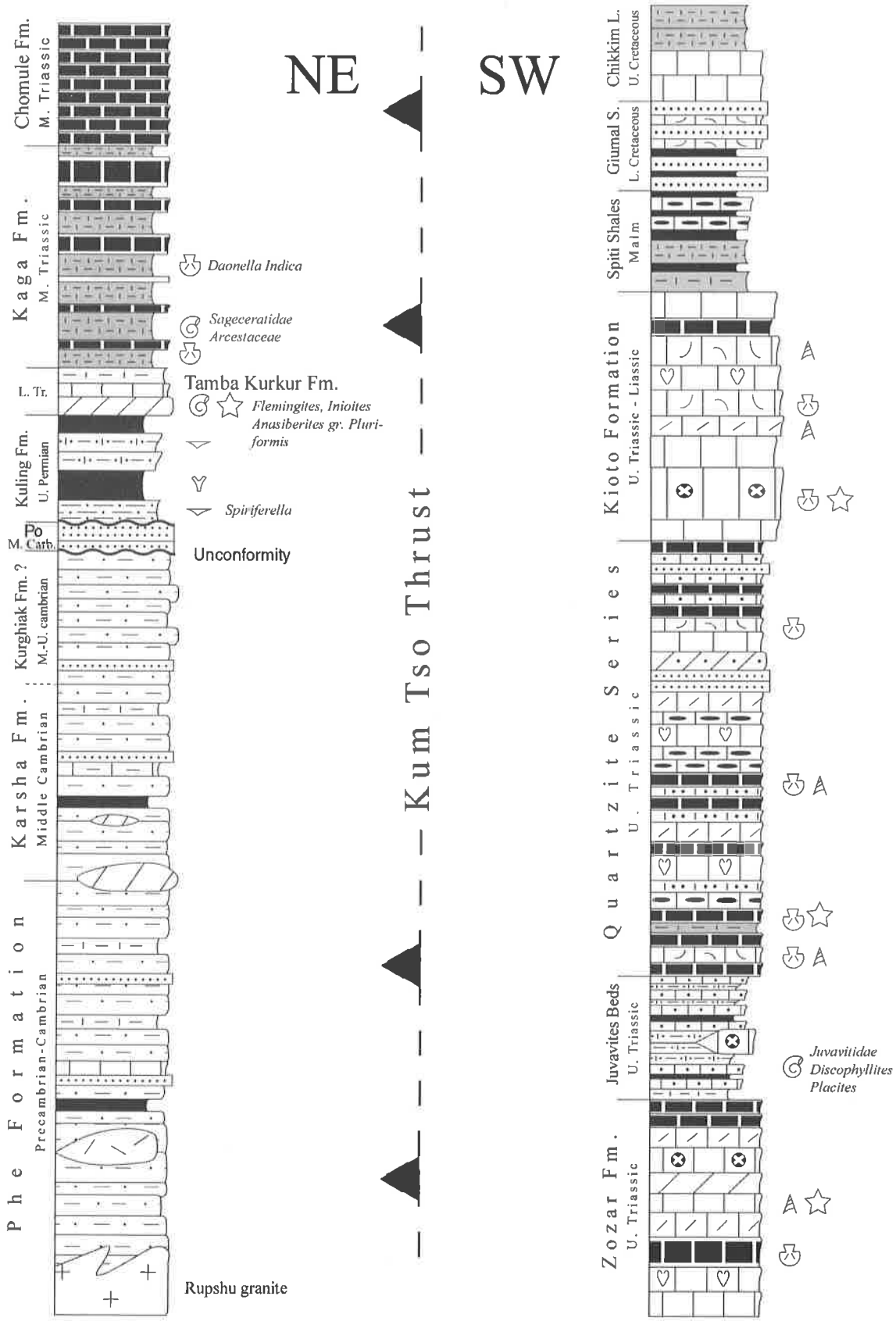

Fig. 2.2: Synthetic stratigraphic log of the Mata nappe, showing the formations that crop out NE and SW of the KTT. Main fossiliferous beds are indicated. Carb. = Carboniferous. L. = Lower, M. = Middle, U. = Upper, Tr. = Triassic.

Northeast of the Kum Tso Thrust

2.2.1/ The Phe Formation (Nanda and Singh, 1976)

Age: Late Precambrian to early Middle Cambrian, see chap. 2.1.1 for more details

Description: In the Rupshu area, the thrust that separates the Tso Morari nappe from the overlying Tetraogal and Mata nappes superposes the Phe Formations of both nappes. So that the upper part of the formation is probably lacking in the Tso Morari nappe, and the base lacks in the Mata nappe. In the latter, the Phe Formation is also made principally of monotonous series of meta- siltstones, sandstones and greywacks. The mineralogy of these layers is strongly controlled by the metamorphism, and detritic minerals are completely recrystallised. The main minerals are quartz, phyllosilicates (Chl and/or Phe and/or Bt) and feldspar (principally plagioclase). Several layers of discontinuous shales, calcschists and greenstones occur occasionally. The thickest basic beds have well-preserved magmatic textures, despite the strong metamorphic recrystallisation. In Lahul, similar amphibolites layers have been interpreted as Late Precambrian to Early Cambrian (Wyss and Hermann, submitted).

The Ordovician Rupshu and Nyimaling granites intrude the metapelites of the Phe Fm. Nowadays the granites are apparently concordant with the metasediments, but this could be the result of the strong Tertiary deformation. Along the upper contact, contact metamorphism generated a quartz-rich fine grain metasediment.

2.2.2/ The Karsha Formation (Nanda and Singh, 1976)

Age: Middle Cambrian, see chap. 2.1.2 for more details.

Description: There is a gradual change in the carbonate supply between the Phe and the Karsha Formations. The lower boundary of the Karsha Fm. is defined by the first occurrence of dolomitic beds. This formation is usually subdivided in the Mauling, Thidsi and Teta Members. In Rupshu, the Mauling Mb. is principally metapelitic and shows similarity with the Phe Fm., except the presence of the dolomites. The latter are thicker and more abundant at the base of the formation than further up. Their thickness vary between zero and 10 meters, because of initial thickness variations and/or intense shearing. The dolomites have been metamorphosed to slightly siliceous, white massive marbles, with a characteristic orange beige weathering colour. Thin layers of calcschists and slightly calcareous siltstones are also present in minor amount. The two other members of the Karsha Fm. are absent or very reduced.

2.2.3/ The Kurgiakh Formation (Garzanti et al., 1986)

Age: Based on trilobites discovered in the lower member, the proposed age for this formation in Zanskar is **Middle to Late Cambrian** (Gaetani et al., 1986; Garzanti et al., 1986; Huges and Jell, 1999). No fossils have been found in Rupshu.

Description: The important black shales, that usually define the lower member of the Kurgiakh Fm. (Surichun Mb.), do not exist in Rupshu. As the last members of the underlying Karsha Fm are also absent, it is difficult to assess if the Kurgiakh Fm is present or if all the rocks that overlie the main dolomites of the Karsha Fm are still part of it. Whatever the reality, the limit between the Karsha and Kurgiakh Formations is impossible to trace on the field.

Type of sedimentation: The pelitic siltstones and sandstones of the upper member of the Kurgiakh Fm. has been interpreted as the result of distal turbidites-deposits. This sedimentary evolution testify to an active tectonic subsidence, leading to a deepening of the sedimentation (Garzanti et al., 1986).

2.2.4/ The Po Formation (Hayden, 1904)

Synonymy: *Tanze Fm./ Mb C* (Nanda and Singh, 1976); *Fenestella Series* (Middelmiss, 1910); *Ganeshpur Fm.* (Srikantia and Bhargava, 1983)

Age: Garzanti et al. (1996a) proposed a **Middle Carboniferous** age in Spiti. The same age has been ascribed to the lower member of the Po Fm. of Lahul (Vannay, 1993), while a Late Carboniferous age is proposed in Zanskar from stratigraphic position (Gaetani et al., 1986).

Description: The first marker horizon above the monotonous metapelitic series of the Precambrian to Cambrian formations is a thin discontinuous layer of white massive quartzite (observed in the area of Pogmar). The latter could represent a reduced equivalent of the classical Po Fm. of Spiti (Hayden, 1904), Zanskar (Gaetani et al., 1990) or Lahul (Vannay, 1993). However, the black shales interbeds do not exist in Rupshu. In the Nyimaling dome, Stutz (1988) describes also a very lacunary and reduced occurrence of the Po Fm, which is only present in the Langthang valley, about 50 km NW of Sangtha.

Type of sedimentation: In more proximal areas (Zanskar, Spiti, Lahul) the Po Fm. reflects shallow epicontinental shelf conditions. The Rupshu area being more distal, this

formation might not be present or very reduced. The same situation has been described in the Nyimaling area (Stutz and Steck, 1986).

2.2.5/ The Kuling Formation (Stoliczka, 1866b)

Synonymy: *Zewan Fm* (Middelmiss, 1910); *Sarchu Fm.* (Nanda and Singh, 1976); *Productus Shales* (Hayden, 1904).

Age: Several brachiopods have been found in the calcareous quartzarenite near Pradong, the Kum Tso and Sangtha. Bryozoan are also present in the shales near the Pogmar La. An age of **Late Permien** (Late Sakmarian to Djulfian in Spiti) is usually attributed to the Kuling Fm. (Gaetani et al., 1986; Stutz, 1988; Vannay, 1993; Garzanti et al., 1996b).

Description: The Permian lithologies show strong lateral variations (Fig. 2.3). In the eastern part of the investigated field, i.e. south of the Tso Morari, we observed a thick succession (~1 km) of shales, marls and limestone metamorphosed to calcschists, with subordinate sandstones and siltstones (see Steck et al. (1998) for more details). Further west calcareous quartzarenites, sometimes containing brachiopods, become dominant. In the Zogoang and Sumkhel Lungpa, the Permian is represented by crinoid bearing calcschists, quartzite and black shales with phosphatized nodules and millimetric pyrite. At the western extremity, i.e. south of Sangtha, a large inverted anticline of Permian is made of dark brown, coarse grained, calcareous sandstones, sometimes rich in brachiopods. A correlation with the Gechang and Gungri Members described in Spiti and Zanskar can be proposed. The black shales show many similarities with the Gungri Member, but the Geshang Mb. is somewhat different in Rupshu than in Spiti. The micro-conglomerates and sandstones of Spiti pass to fine-grain sandstones and to shaly limestones. As already observed by Stutz (1988) in the Nyimaling area, towards north, the clastic deposits decrease and are replaced by argillaceous limestones and black shales.

Type of sedimentation: The base of the Kuling Fm. is marked by a major unconformity almost all along the Himalaya (Hayden, 1904; Heim and Gansser, 1939; Srikantia et al., 1980; Fuchs, 1982; Gaetani et al., 1986; Garzanti et al., 1996b). In the adjoining Nyimaling area, the Late Permian Kuling Fm. lies directly on the Carboniferous Po Fm. (Stutz and Steck, 1986) or on the Late Cambrian Kurgiakh Fm. In Rupshu, the same gap has been observed.

In Spiti, Zanskar and Lahul, the microconglomerates and sandstones of the Gechang Mb. are interpreted as shallow-water transgressive deposits, and the black shales of the Gungri Mb. represent a deepening (Gaetani et al., 1990; Vannay, 1993; Garzanti et al.,

1996b). The total thickness of these two members does not exceed 50 m in Zanskar and 100 m in Spiti. This is about 10 times less than in certain parts of Rupshu, where the lateral variations, both in thickness and lithologies, are much more important. Due to these differences, we think that the Kuling Fm. of Rupshu has been deposited in a more distal environment. The lateral variations shows that it does not seal homogeneously the rift sequence, probably because the newly formed rift still contains high stands.

2.2.6/ The Karzok Formation (Fuchs and Linner, 1996)

Age: No fossils have been found in this formation. Fuchs and Linner (1996) proposed a Permian age for this formation because Linner et al. (1997) showed that the volcanics it contains, have geochemical affinities with the Panjal Traps. However, If both magmatism might be comparable they are not necessarily coeval. In the recent paper of Steck et al. (1998) we proposed a Permo-Mesozoic age. Early Permian conodonts have been discovered in Parang Sumdo, north of the Thaglang La (Virdi et al., 1978). Unfortunately it is difficult to know exactly what these authors dated as they grouped all the metasediments of the Tso Morari dome in only one formation (Thaglang La Fm).

Description: The Karzok Fm. is surrounded by the Phe Formation. If the Permian age of the Karzok Fm. is confirmed, this position implies an important gap from Cambrian to Permian. The upper and lower limits do not show clear evidences of tectonic contacts, except north of Karzok, where the lower limit is locally the base of the Mata nappe. The facies of this formation vary along the strike, but dolomites, quartzites, greenstones and limestones occurs everywhere in different proportions (Fig. 2.3). Near Karzok, the formation is mainly carbonaceous with subordinate amount of quartz-schists and greenstones. A coarse detritism produces breccias with plurimetric pebbles of dolomites and polygenic breccias. These facies disappear further west. A lentil of metabasics, serpentinites and chromite outcrops near Karzok. It marks the thrust between the Tetraogal and Mata nappes at this place (Steck et al., 1998). Elsewhere, this thrust is difficult to find because it juxtaposes similar rocks of the Karzok Formation or Phe Formation. In Rinang, the Karzok Fm. is much more quartzitic, the amount of limestones decreases, and greenstones are still very present. The large amount of Ca-minerals (Ep + Cc) and the presence of a layering in some greenstones, suggest a vocano-sedimentary origin for these layers.

In the landscape, the Karzok Fm. is recognizable by the light colored limestones and dolomites that contrasts with the dark colored quartz-schists of the Phe Formation. It forms a discontinuous ribbon that can be seen on SPOT satellite imagery.

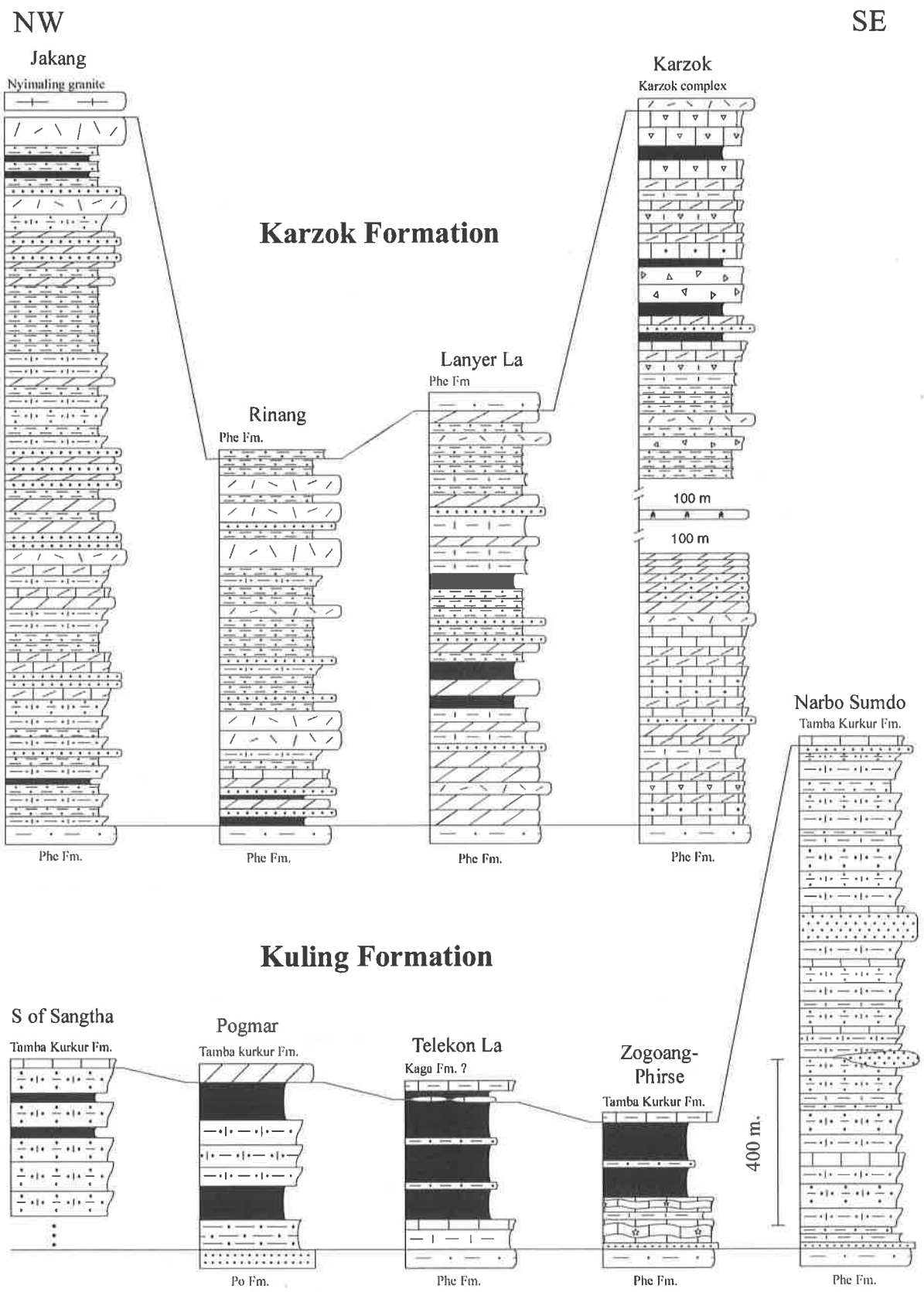

Fig. 2.3: Stratigraphic logs showing the NW - SE lateral variations of the Karzok Fm. (Permian?) and Kuling Fm. (Permian). See Plate 1.1 for places names.

2.2.7/ The Tamba Kurkur Formation (Srikantia et al., 1980)

Synonymy: *Zangla Fm.* (Nanda and Singh, 1976). In Nyimaling, Stutz and Steck (1986) have introduced the term *Samlung Series* for the Lower Triassic series that crops out between the Permian Formation and the Late Triassic Khar Fm. These series include the Tamba Kurkur Fm.

Age: In Spiti, the base of the Triassic is well dated at **Early Griesbachian to Early Dienerian** by several ammonoids and conodonts (Garzanti et al., 1995). According to the same authors, the Tamba Kurkur Fm. extends up to the Lower Anisian. In Zanskar, Late Anisian conodonts (*Gondolella eotrammeri)* was found at the top of the formation (Gaetani et al., 1986). In Rupshu, it is not possible to reach such a precision due to the scarcity of fossils. Two ammonoids (*Flemingites*, determination H. Bucher) have been found, about 10 meters above the last Permian outcrop, in the Kurgiep valley (sample G9866 on Plate 1.3). Some badly preserved Early Triassic ammonoids can also be found near Sangtha, where the Tamba Kurkur Fm. is locally present. The area of Pradong, in the Parang valley, has been studied in detail by Hugo Bucher (in prep.). It seems here that the Lower Triassic formations are present but very reduced, compared to the Spiti valley. The ammonoids *Anasiberites Pluriformis* and *Inionites* have been described by Steck et al (1998) at this locality.

Description: The Tamba Kurkur Fm. lies over the Permian Kuling Formation. It marks a net increase of carbonate supply. The base of the formation is made of massive black micritic limestones, that sometimes contain ammonoids. These lithologies are very reduced equivalents of the Spitian Tamba Kurkur Fm. Therefore the characteristic Nodular Limestones of Spiti are lacking in Rupshu. The Tamba Kurkur Fm. is well exposed in the western and eastern extremities of the field, but are usually lacking or very thin elsewhere. For this reason it has not been mapped everywhere and has been often included in the overlying formation.

Type of sedimentation: The Tamba Kurkur Fm. of Zanskar and Spiti represents a pelagic sedimentation on the outer shelf to upper slope, with low sedimentation rate. The glauconitic condensed horizon found at the top of the formation in these areas, is interpreted as a major regional transgression around the Anisian/Ladinian boundary (Gaetani et al., 1986; Garzanti et al., 1995). In Rupshu, the Tamba Kurkur formation records deeper sedimentation conditions and a very low sedimentation rate that reaches nearly zero at some places. The transgression at the top of the formation does not affect the area, where the transition to the overlying formation is gradual.

2.2.8/ The Kaga Formation (Bhargava, 1987)

Synonymy: *Daonella shales* (Hayden, 1904), *Hanse Fm./ H1 Mb.* (Vannay, 1993), *Zangla Fm.* (Nanda and Singh, 1976).

Age: Very few and badly preserved ammonoids have been found near Pang. These are one *Sageceratidae* and one *Arcestaceae* (det. H. Bucher). However the presence of daonellids bearing layers allows us a correlation with the Kaga Fm of Spiti, dated at **latest Early Ladinian** by conodonts (Garzanti et al., 1995) at the base, while the top of the formation yield **Late Ladinian** ammonoids in Zanskar (Baud et al., 1984; Gaetani et al., 1986). The fauna found in Rupshu is coherent with a Middle Triassic age.

Description: The Kaga Fm. is made of an alternation of argillaceous black marls and massive beds of marly dolomitic limestones. The latter are black and micritic with a brown-ochre weathering color. The limestone / clay ratio increases upwards, so that the massive beds become more and more abundant. The lower limit, with the Tamba Kurkur Formation, is usually difficult to define without fossils.

Type of sedimentation: The Hanse Group of Spiti, which also include the next formation, is deposited in a deep and low-energy offshore shelf environment (Garzanti et al., 1995). The deep, monotonous and almost unfossiliferous facies of Rupshu, confirm this proposition.

2.2.9/ The Chomule Formation (Bhargava, 1987)

Synoymy: *Daonella Limestones* (Hayden, 1904), *Hanse Fm./ H2 Mb.* (Vannay, 1993), *Zangla Fm.* (Nanda and Singh, 1976).

Age: This formation is absolutely fossil-free in Rupshu, but its lithologies and its position above the Kaga Fm. permit us a good correlation with the **Ladinian** Daonella Limestones of Spiti (Hayden, 1904).

Description: The base of the Chomule Fm. is defined by the last apparition of the argilaceous marls of the Kaga Fm. Over this limit, the lithologies are more monotonous and form a regularly bedded succession of decimetric layers of black micritic limestones, sometimes slightly dolomitic, with a brown weathering color. Marly schistose interbeds are rare and very thin. A gradual increase of calcareous input from the base of the Kaga Fm. up to the Chomule Fm. leads to the almost complete clearing of the argillaceous component.

Type of sedimentation: The Chomule Fm. records a strong decrease in the clay supply, which generates lower sedimentation rate, in a pelagic environment.

Southwest of the Kum Tso Thrust

Southwest of the KTT the stratigraphy can be more easily correlated with the Spiti's descriptions (Fig. 2.2). The lithologies are mainly Late Triassic, but the Chomule Fm. has been seen locally, west of the Lachung La (Plate 1.2). It is also made of black micritic limestones, as in the northern series.

2.2.10/ The Zozar Formation (Baud et al., 1984)

Synonymy: *dolomitic limestone* (Hayden, 1904), *Nimaloksa Fm.* (Srikantia et al., 1980; Garzanti et al., 1995), *Sanglung Fm / Mb. B* (Bhargava, 1987), *Zangla Fm.* (Nanda and Singh, 1976).

Age: Foraminiferal assemblages indicate a **Norian** age for the Upper Member of the Nimaloksa Fm. of Spiti (Garzanti et al., 1995).

Description: The Zozar Fm. is characterized by massive metric to plurimetric beds of coral-bearing, clear white-blue limestones and dolomites, megalontid-bearing black micritic limestones, oolitic beds and biocalcarenites with gastropods, brachiopods, bivalves and crinoids. These lithologies can create steep cliffs.

Type of sedimentation: As in Zanskar and Spiti, the Zozar Fm. of Rupshu represents a shallow-subtidal, open marine carbonate platform, characterized by massive bioclastic limestones.

2.2.11/ The Juvavites Beds (Hayden, 1904)

Synonymy: *Quartzite Series / Mb. a* (Gaetani et al., 1986), *Sanglung Fm / Mb. C* (Bhargava, 1987), *Zangla Fm.* (Nanda and Singh, 1976).

Age: Ammonoids occur at several places in the Juvavites Beds. *Juvavitidae* (G96130, Gata), *Discophyllites* (G96133, Gata) and *Placites* (G9834, W Phorang La) allow us to

propose a **Norian** age. This is coherent with the age obtained by Diener (1908) with Spitian fauna.

Description: The Juvavites Beds form a good marker horizon, that contrasts with the massive limestones of the formations above and under. They generate a smooth topography and terraces between cliffs. They are characterized by a net increase in the detritic components, mainly quartz and mica. This forms brown-ochre calcareous sandstones or quartz mica bearing limestones and marls. They sometimes contain brachiopods, bivalvia and belemnites and some well preserved ammonoids.

Type of sedimentation: The distinct increase in terrigenous detritus reflects the influence of storms and tidal currents on a shallow-water shelf.

2.2.12/ The Coral Limestone (Hayden, 1904)

Synonymy: *Quartzite Series / Mb. b* (Gaetani et al., 1986), *Hangrang Fm.* (Bhargava, 1987), *Zangla Fm.* (Nanda and Singh, 1976).

Age: In Spiti, this formation has been dated at **Early/Middle Norian** by conodonts (Garzanti et al., 1995).

Description: It consists of white and massive coral limestone that occur as discontinuous lenses. These are present along the Spiti - Tso Morari and the Sarchu - Pang transects. Their thickness never exceed about 10 meters. This layer is not represented on the geological map.

2.2.13/ The Monotis Shales (Hayden, 1904)

Synonymy: *Alaror Fm.* (Bhargava, 1987), *Quartzite Series / Mb. b* (Gaetani et al., 1986), *Zangla Fm.* (Nanda and Singh, 1976).

Age: ammonoids of **early Middle Norian** age have been described in Spiti (Garzanti et al., 1995).

Description: As these lithologies are very similar to the Juvavites Beds it is difficult to distinguish them when the Coral Limestone are absent. For this reason the Monotis Shales have been included in the Juvavites Beds on the geological map.

Type of sedimentation: Similar to the Juvavites Beds, according to the similarity of facies.

2.2.14/ The Quartzite Series (Hayden, 1904)

Synonymy: *Nunuluka Fm.* (Bhargava, 1987), *Quartzite Series / Mb. c* (Gaetani et al., 1986), *Zangla Fm.* (Nanda and Singh, 1976), *Takh Fm.* (Spring, 1993), *Tsatsa Fm.* (McElroy et al., 1990).

Age: The fossil content of the Quartzite Series of Zanskar indicate **Norian/Raethian** age (Gaetani et al., 1986).

Description: the Quartzite Series are mainly carbonaceous with white or black massive limestones and dolomites, sometimes siliceous, and subordinate calcareous sandstones. Real quartzites are rare and thin. Megalontid-bearing black micritic limestones, oolitic beds and biocalcarenites are similar to those of the Zozar Fm. The Quartzite Series usually form the base of the Kioto Fm cliffs.

Type of sedimentation: The strong increase in abundance and grain size of quartzo-feldspathic detritus observed in Spiti and Zanskar is less marked in Rupshu. This results from the more distal situation of the Rupshu, which is less influenced by the terrigenous supply.

2.2.15/ The Kioto Formation (Hayden, 1908)

Synonymy: *Megalodon Limestone* (Hayden, 1904), *Simokhambda Fm.* (Srikantia et al., 1980). *Para Limestone* (Stoliczka, 1866a).

Age: Foraminiferal assemblages point to a Rhaetian age for the base of the unit in Spiti (Garzanti et al., 1995). In Zanskar, Jadoul et al. (1990) propose a **Rhaetian to Liassic** age based on fauna and flora of the Kioto Fm.

Description: The Kioto Fm. creates steep cliffs and gorges due the large amount of massive limestones and dolomites. The lithologies are quite similar to those of the Quartzite Series, so that the exact limit between the two formations is sometimes arbitrary. However the Kioto limestones are characterized by thicker beds and by a lesser amount of quartzose component. White coral limestones, black Megalodon limestones and dolomitic limestones are the principal lithologies of the formation.

Type of sedimentation: The Kioto Fm. marks the installation of a carbonate platform. It is characterized by a progressive decrease of the siliciclastic supply during the end of the Triassic. In Rupshu this event seems to occur sooner, as the quartzo-feldspathic grains amount already decreases in the underlying Quartzite Series.

2.2.16/ The Spiti Shales (Stoliczka, 1866b)

Synonymy: *Kibber Group* (Srikantia, 1981)

Age: In Spiti the lower Member is dated as **Late Oxfordian** (Arkell, 1956), and the top is of **Early Tithonian** age (Arkell, 1956; Gaetani et al., 1986).

Description: This formation is mainly made of black marly shales. At its top, some siliceous and nodulous limestones are intercalated between the black shales. Nice ammonoids can be preserved in the nodules.

Its only occurrence is near Chikkim, on the left side of the Spiti valley. However, it is possible that this formation is also present on some summits, above the Kioto Fm. Stoliczka (1866b) mention the presence of some Spiti Shales and younger formations on both side of the Pangpo La. Raina and Bhattacharyya (1974) describe these formations in the upper Tsarap valley. In the Pangpo La area, we did not see these Upper Jurassic-Cretaceous formations outcropping, but they might be locally present on some summits.

Type of sedimentation: This unit was deposited on an undisturbed mid-outer shelf only episodically affected by major storm events, responsible for the coarser beds (Gaetani et al., 1986).

2.2.17/ The Giumal Sandstone (Stoliczka, 1866b)

synonymy: *Kibber Group* (Srikantia, 1981)

Age: A **Early Cretaceous** age has been proposed for the Giumal Sandstones of Zanskar (Fuchs and Willems, 1990). It seems that the top of the formation can reach Late Cenomanian (Gaetani et al., 1986).

Description: The base consists of rust-colored, massive quartzites, with fine pelitic interbeds. The top of the series is made of an alternation of green quartzites and dark bioclastic limestones. These beds occur only near Chikkim, in the Spiti valley.

Type of sedimentation: According to Gaetani et al. (1986) the Giumal Sandstone of Zanskar reflects the multiple progradation of clastic detritus, brought by deltaic systems onto a shelf influenced by storm-wave action.

2.2.18/ The Chikkim Limestones (Stoliczka, 1866b)

Age: Santonian to Early Campanian foraminiferal assemblage has been described in the Tsarap valley by Spring (1993). It seems that the Chikkim Limestones spans the time from **Late Albian to Cenomanian** and, in other places, **Cenomanian to Campanian** (Fuchs and Willems, 1990).

Description: They consist of well-bedded, white foraminiferal limestones, free of terrigenous detritus. Above these limestones come more marly facies that form the Chikkim marls. Both of those lithologies are present only near Chikkim.

Type of sedimentation: The Chikkim Limestones were deposited in upper bathyal pelagic environment poor in oxygen and with low sedimentation rate (Gaetani et al., 1986).

2.3/ Conclusions

The observations exposed above show that the Rupshu stratigraphy stretches from Late Precambrian up to Late Cretaceous. Only the Mata nappe contains the whole series; the Tso Morari nappe containing only (meta)sediments older than the Lower Paleozoic. No significant differences exist between the formations that are present in both of the nappes.

The northern domain of the Mata nappe shows a Paleozoic series that is very lacunary. Correlation with the southern areas of Spiti and Zanskar are difficult due to the absence of several marker horizons. The three Precambrian to Cambrian Formations (Phe, Karsha, Kurgiakh) are undistinguishable without the Karsha dolomites. Moreover it is impossible to separate the different members of those three formations. Above the Cambrian, a large gap results from the absence of the Thaple, Muth and Lipak Formations. This gap seems to be more reduced in the Nyimaling dome, where the Lipak Fm. exists (Stutz and Steck, 1986).

The Cambrian-Ordovician boundary is often described as a major unconformity in the Himalayan stratigraphy (Hayden, 1904; Fuchs, 1982; Baud et al., 1984; Garzanti et al., 1986; Brookfield, 1993). In Rupshu, a large gap (or a very reduced and local sedimentation), stretches from Ordovician till Late Permian. The Carboniferous Po Fm. is very reduced and present only in the west (Sangtha - Pogmar La). The overlying Ganmachidam conglomerates and the volcanics of the Panjal Traps are absent. Finally the Late Permian Kuling Fm. marks

the resumption of deposition, with sedimentation rates that are sometimes higher than further south.

A major change in sedimentation seems to occur when going across the Kum Tso Thrust. NE of this thrust the Late Precambrian to Middle Triassic formations are typical of the northern, distal basins of Nyimaling. While SW of the KTT, the Late Triassic to Late Cretaceous formations look like those of the southern basins of Spiti or Zanskar. However, as none of the formations outcrops on both sides of the Kum Tso Thrust, it is impossible to directly compare both domains. Therefore, we can't say whether the sedimentation conditions that occur during Paleozoic to Middle Triassic in the northeastern domain of Rupshu, are getting similar to those of Zanskar and Spiti, when the sediments become younger (Late Triassic to Cretaceous) or when they are located more south.

3/ The Ordovician granitic intrusions

Two granitic plutons, the ***Tso Morari gneiss*** and the ***Rupshu granite***, crop out in the Tso Morari area (Plate 1.2). The ***Polokongka La granite***, classically interpreted as a young intrusion in the Tso Morari gneiss, has been recognized as the undeformed facies of the latter. However we separated granitic samples from the Polokongka La from the gneissic samples of the Tso Morari gneiss, in order to confirm our field observations with geochronological, geochemical and zircon typology characteristics. The detailed results of this study are presented in Girard et al. (1999). Here are presented only the main results.

3.1/ Main results

Conventional isotope dilution U-Pb zircon dating on single-grain and small multi-grain fractions yielded magmatic ages of **479 ± 2 Ma** for the Tso Morari gneiss and the Polokongka La granite, and **482.5 ± 1 Ma** for the Rupshu granite (Fig. 3.1). There is a great difference in zircon morphology between the Tso Morari gneiss (peraluminous type) and the Rupshu granite (alkaline type). This difference is confirmed by whole-rock chemistry. The Tso Morari gneiss is a typical deformed S-type granite, resulting from crustal anatexis. On the other hand, the Rupshu granite is an essentially metaluminous alkali-calcic intrusion derived from a different source material. This particular character differentiates the Rupshu granite not only from the Tso Morari gneiss but also from the peraluminous Nyimaling granite, which is yet in its western extension (Stutz and Thöni, 1987).

3.2/ Interpretation

Data compilation from other Himalayan Cambro-Ordovician granites reveals huge and widespread magmatic activity all along and beyond the northern Indian plate between 570 and 450 Ma, with a peak at 500-480 Ma. The Tso Morari gneiss is a typical example of this mainly peraluminous granitic belt. On the other hand, the Rupshu alkali-calcic granite which probably derived from a different source, also intruded during this period. The Ordovician Kaghan gneiss from Pakistan (Greco et al., 1989; Spencer, 1993) seems to be another example of an alkali-calcic activity. Such a huge and widespread granitic magmatism could only be generated by a major thermal anomaly, linked to a large-scale geologic event.

The Himalayan context during Ordovician is reminiscent of a post-orogenic extensional regime, such as that found at the end of the Variscan orogeny in Western Europe (e.g. (Schaltegger and Corfu, 1995). About 60 to 80 Ma after continental collision, the thickened Variscan continental crust underwent a transtensional to extensional tectonic regime. Both S- and I-type granites intruded, with a general evolution towards alkali-calcic, then post-orogenic alkaline, and finally anorogenic alkaline granites (Bonin et al., 1998). In

the Dora-Maira massif (Northern Italy), late-Variscan peraluminous and alkali-calcic granites are contemporaneous (Bussy and Cadoppi, 1996), in the same way as the Himalayan Tso Morari and Rupshu plutons are. The post-orogenic alkaline Kaghan metagranite from the High Himalaya, which seems to be younger than most of the surrounding peraluminous intrusions (Trivedi et al., 1986) is in line with this evolutionary trend. In conclusion, the Cambro-Ordovician granite magmatism in Himalaya definitely has more common features with post-orogenic than with anorogenic extensional settings. Several authors have suggested that a pre-Himalayan orogeny occurred during Cambro-Ordovician. Their arguments are either sedimentary (Garzanti et al., 1986; Valdiya, 1995), metamorphic (Ferrara et al., 1983; Garzanti et al., 1986; Pognante and Lombardo, 1989; Valdiya, 1995; Argles et al., 1999), or geochemical (on granites) (Frank et al., 1977; Le Fort et al., 1986). but these clues are rather rare along the Himalayan belt, and moreover all of them might also be explained without an orogeny. Indeed the Ordovician unconformity and uplift could be explained with a paleo-tethyan rifting; the metamorphic ages of Argles et al. (1999) or Ferrara et al. (1983) might be the result of a contact metamorphism generated by granitic intrusions.

Nevertheless the timing of the Cambro-Ordovician Himalayan magmatism (mostly around 500-480 Ma) corresponds to the end of the Pan-African event that affects almost all Gondwanian terrain. This is slightly younger than the closest Pan-African belt of the Arabian-Nubian shield (Windley et al., 1996), which suggests that there has been an eastward shift with time of the orogenic activity in eastern Gondwana. The exact nature of the inferred orogenic activity in northern India is difficult to assess. Typical subduction-related rocks are lacking, but if the analogy with the late-Variscan extensional setting is valid, then crustal thickening must have occurred in some way, followed by isostatic readjustment, exhumation and extension. A closer look at other Cambro-Ordovician granites in Himalaya should allow to further test this hypothesis.

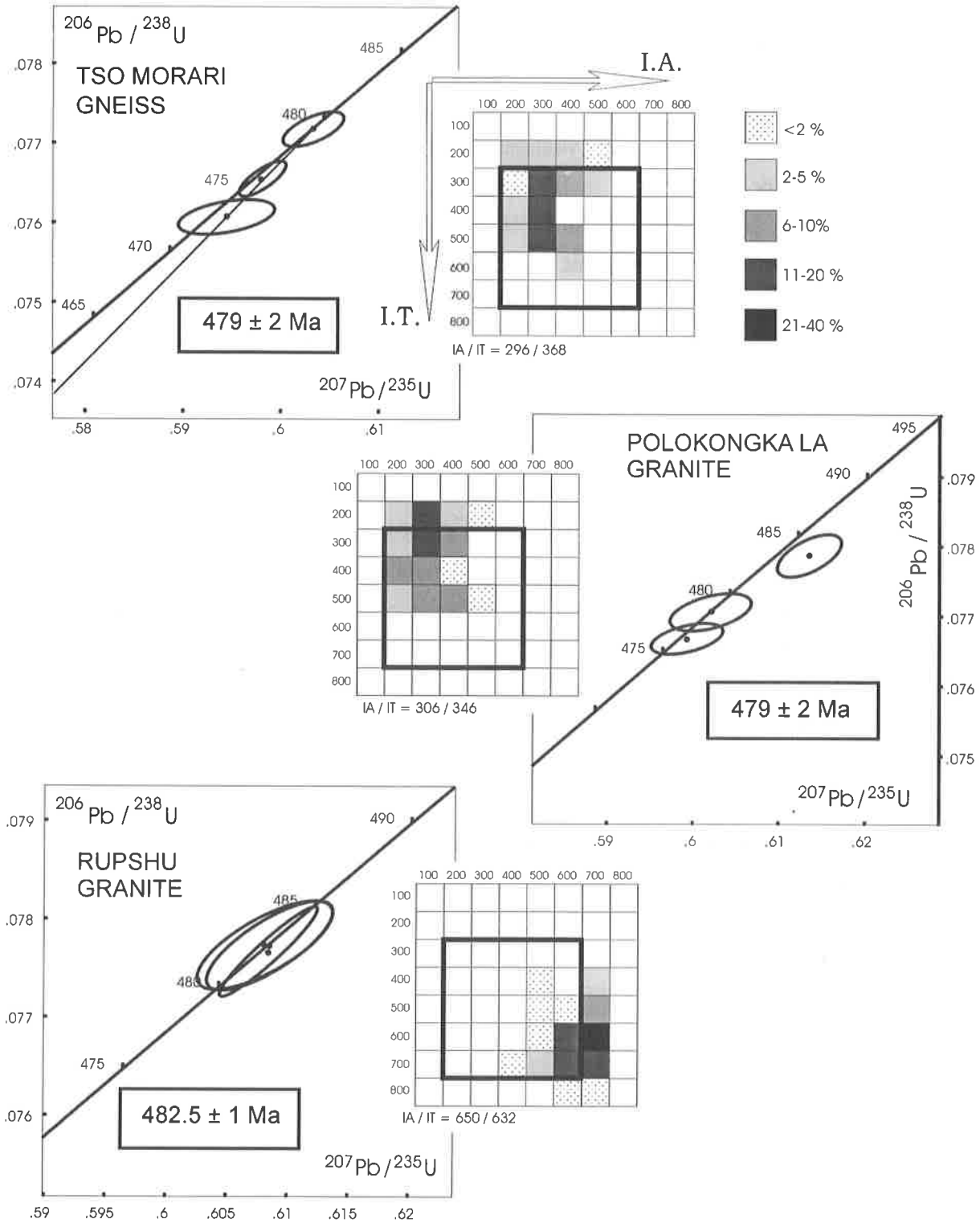

Fig. 3.1: U/Pb ages and Zircon typology (based on the Pupin (1980) method) for three different granitic samples, showing the similarity between the Tso Morari gneiss and the Polokongka La granite and their differences with the Rupshu granite. Preferred ages are in boxes. For More details see Girard and Bussy (1999).

4/ Tectonics

Odin said: Tell me this first, if your intelligence is able to
And if you know it, Vafthrudnir.
Whence spring the earth and the canopy of heaven
At the origin of time, O giant sage?
Vafthrudnir said: It is with the Ymir's flesh that earth was created,
And from the bones formed the mountains;
With the cold giant of hoarfrost's crane was build the canopy of heaven,
And the sea waves are made of his blood.

Song of Vafthrudnir, Edda from the 13th century

The area investigated can be subdivided in four tectonic units, the Tso Morari, Tetraogal, Mata and Shikar Beh nappes (Steck et al., 1998) (Fig. 4.1). These nappes show different metamorphic histories. The eclogitic event recorded by the Tso Morari nappe is missing in the overlying nappes.

Nappe tectonic in NW Himalaya has been described for the first time by french geologists (Bassoullet et al., 1980). Since then it has been supported by the Lausanne team since the beginning of their investigations in this area (Baud et al., 1984; Stutz, 1988; Steck et al., 1993; Vannay and Steck, 1995; 1998; Dèzes, 1999; Wyss et al., 1999). However it is still much debated by Fuchs and Linner (1995) who disagree with the term nappe, because the formations are roughly found in a normal stratigraphic order. This is indeed what we observe, but it does not exclude a nappe tectonic, as explained in Steck et al. (1993). Fuchs and Linner prefer the term "schuppen belt" to the term "nappe" for the structures observed between the Nyimaling dome and the Baralacha La, where the Nyimaling - Tsarap Nappe has been defined by Steck et al. (1993). For us, a displacement of 90 km, such as it has been estimated with a simple shear model for the Nyimaling-Tsarap Nappe (Steck et al., 1993), justify the term nappe. With a simple shear deformation this displacement is possible without disturbing the stratigraphy.

In addition to the "nappe debate", another problem is still hardly discussed between Himalayan geologists. The discord point is the occurrence or not of an ante-Tertiary tectono-metamorphic event. The occurrence of such event is not obvious in Rupshu.

We will describe below the main tectonic structures that outcrop in different areas. This puzzle of information allows us to reconstruct a cinematic model which describes the succession of the different tectonic phases.

4.1 The ante-Tertiary structures

As seen in the previous chapter, an ante-Himalayan event probably occurred at circa 550 Ma, more or less coeval with the Pan African event. If the granites seem to well testify for this event, structural signs are usually difficult to find in Himalaya. In Rupshu, we have not find any tectonic structure that could testify of a Cambro-Ordovician orogeny. The only ante-Tertiary structures found are either sedimentary (e.g. bedding in the low-grade limestones) or magmatic as observed in some undeformed massive boudin of basic rock with relics of magmatic Pigeonite and Olivine (Fig. 4.2).

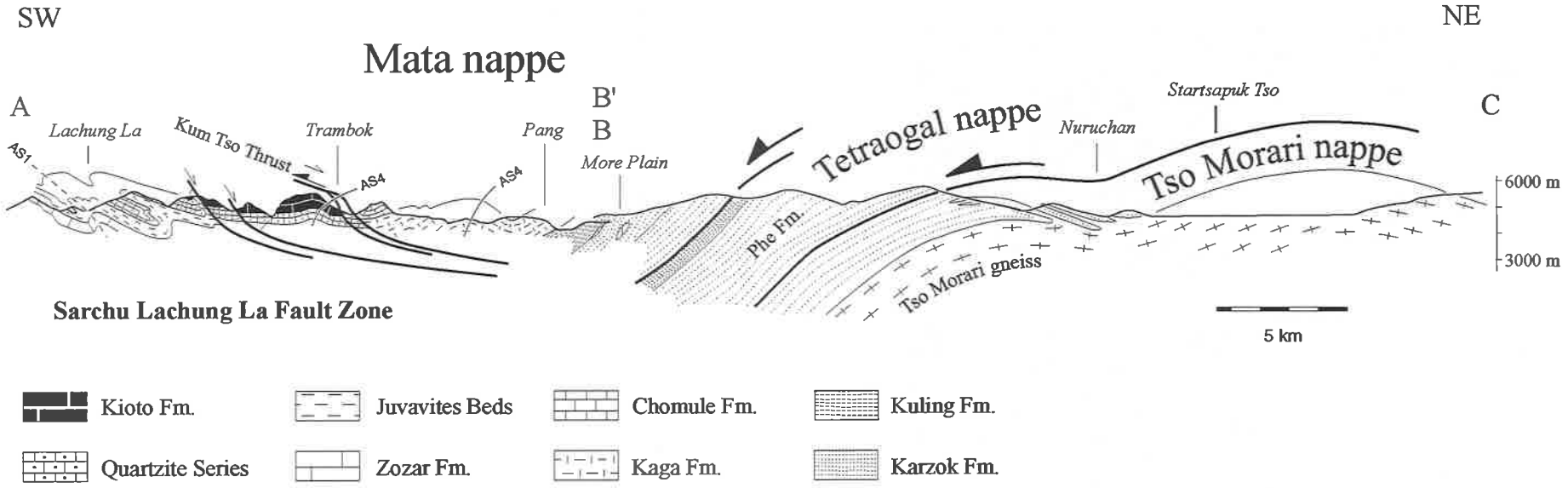

Fig. 4.1: Tectonic cross section AB and B'C between the Tsarap River and the Tso Kar plain. See plate 1.2 for precise location.

Fig. 4.2: Thin section of the metagabbro G9827 with needles of plagioclases (Pl) and coarse grains of Pigeonite (Pig) and rare alterated olivine. The initial magmatic texture is well preserved.

4.2 The Tertiary structures

The Himalayan tectonic of the Rupshu area has been studied by Thakur (1983), Guillot et al. (1997) and Steck et al. (1998). Many divergences exist between those three papers. If the doming structure of the Tso Morari massif is accepted by everybody, a nappe tectonic is only proposed by Steck et al. (1998). In the following chapters we will describe the structures observed and show that they support the model exposed by the latter authors.

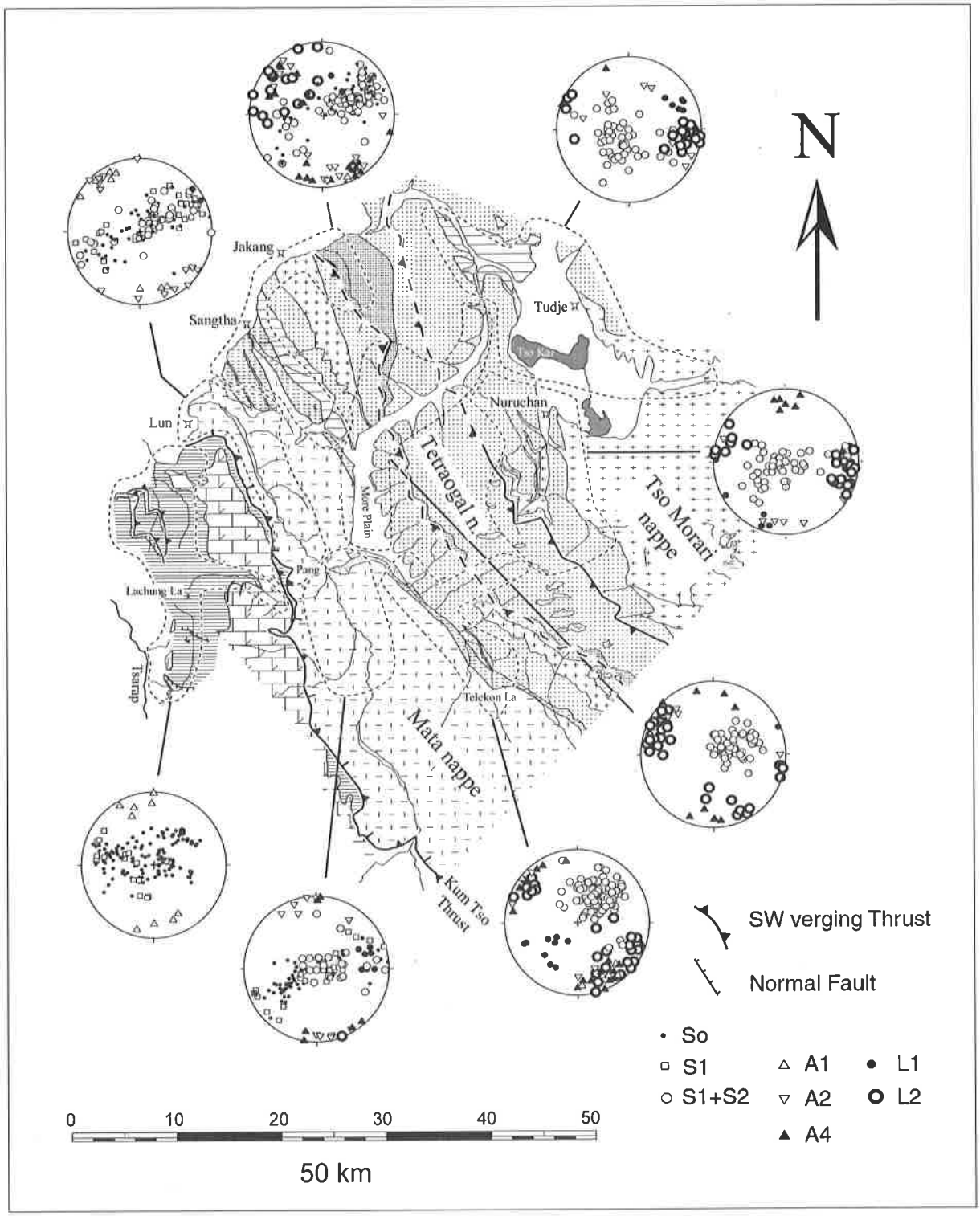

Fig. 4.3: Structural data of the NW area. Lambert projection, lower hemisphere. See Plate 1.2 for lithologies. A = fold axes, L = stretching lineation, S = schistosity.

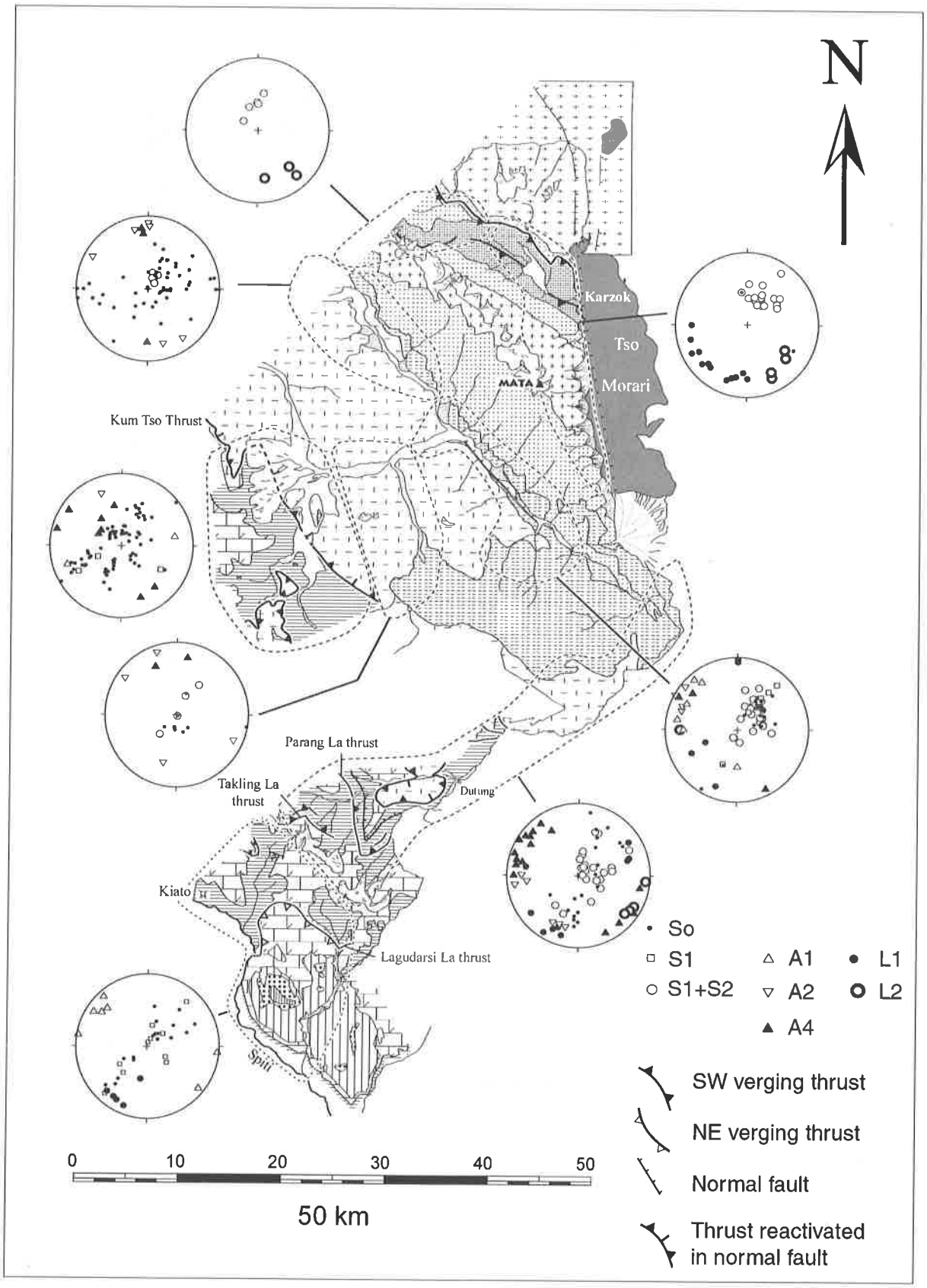

Fig. 4.4: Structural data of the SE area. Lambert projection, lower hemisphere. See Plate 1.2 for lithologies. A = fold axes, L = stretching lineation, S = schistosity.

4.2.1 The Lagudarsi La Thrust

The Lagudarsi La Thrust (Steck et al., 1998) can be observed in Spiti, on the northern side of the valley (Plate 1.2). It outcrops along the trail which connects the Lagudarsi La with the village of Kioto. The thrust superposes Kioto Limestones over Kioto Limestones, what complicates its identification. A SW plunging lineation and calcite fibres indicate a NE-directed overthrusting. This important thrust is the oldest Himalayan structure found in this area. Interference structures with a younger SW-vergent phase can be observed along the way to the Parang La (Steck et al., 1998). Because of the weak metamorphism of the area where the Lagudarsi La thrust outcrops, no penetrative NE-vergent schistosity has been observed.

4.2.2 The SW-verging structures

The main schistosity observed in the Tso Morari and Tetraogal nappes and in the internal part of the Mata nappe, is usually the sum of two successive schistosities S1 and S2. This can be seen in microlithons and in hinges of some folds. The S1 schistosity carries a NE-SW stretching lineation L1 at some places (Fig. 4.3 and 4.4). Shear sense criteria usually indicate a top-to-the-SW movement, but the opposite criteria has also been observed. First generation isoclinal folds (F1) can be seen in pelitic lithologies, but large scale F1 folds are absent. The large scale SW-vergent folds are clearly associated with the second schistosity. The Pradong recumbent fold, described by Steck et al. (1998), is a good example of such a fold. The synclinal bend, which crops out in the Parang valley, shows that a second schistosity is in axial surface of the fold (Fig. 14 in Steck et al. (1998)). In the Toze Lungpa, spectacular isoclinal F2 folds can be observed in the Triassic Kaga Formation. They affect an older S1 schistosity and are folded by NE-vergent backfolds (Fig.4.5). F2 folds are also responsible for the complex structure found near Sangtha and which will be described below. A sub-horizontal NW-SE stretching lineation L2 exists in the Tso Morari nappe and in the internal part of the Mata nappe. This lineation overprints the older L1 stretching lineation (Fig. 4.6). In the same outcrop shear sense criteria indicate sometimes both top-to-the NW or top-to-the SE movement.

In the frontal parts of the Mata nappe, only one schistosity develops in the low-grade metasediments (diagenesis to anchizone). It is still associated to SW-vergent folds, but a brittle tectonic begins to take place. Good examples of such folds can be observed in the area of Lachung La and Parang La (Fig. 4.7). Together with these folds, thin-skinned thrust structures develop. Along the Tso Morari -Spiti transect a succession of SW-directed thrusts creates an imbricate structure that ends with the Parang La thrust and with its lateral equivalent the Takling La Thrust. This Parang La Thrust front interferes with the older NE-vergent structures, associated with the Lagudarsi La Thurst.

Along the Tso Kar - Sarchu transect we observe the same transition from an internal part, composed by the Tso Morari nappe and the northern part of the Mata nappe, where the deformation is highly ductile and where two parallel schistosity develop, to an external part, where only one schistosity develops and where important thrusts appear.

Fig. 4.5: Interference structure between F2 and F4 folds in the Toze Lungpa, W of Pang.

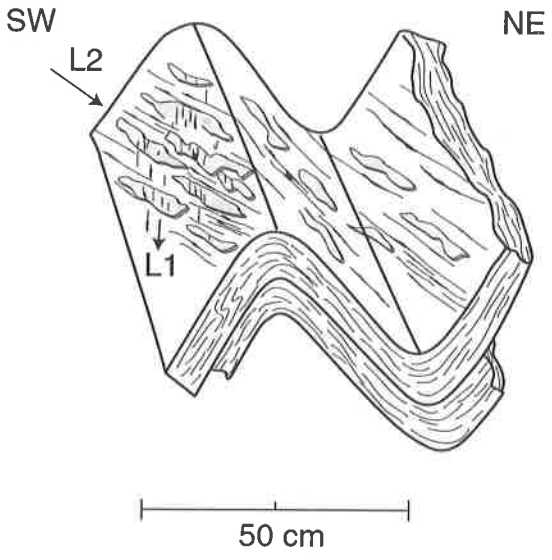

Fig. 4.6: Calcschist sample from the Permian Kuling Formation, with both of the lineations L1 and L2. Both are marked by quartz fibers. The S1+S2 schistosity is refolded by F4 folds.

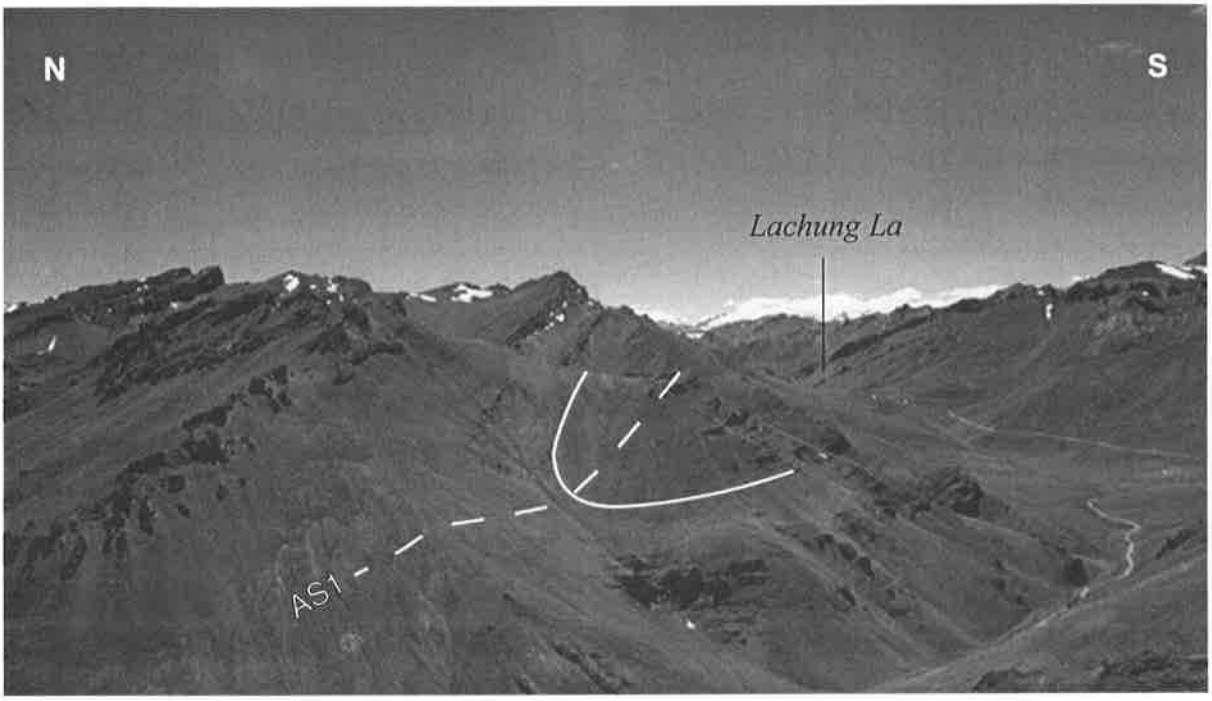

Fig. 4.7: Example of a SW vergent syncline associated to the emplacement of the Mata nappe, in the Upper Triassic.

4.2.3 The Kum Tso Thrust (KTT)

This important structure can be followed from the Tso Morari - Spiti transect, where it crops out near Dutung, up to the eastern extremity of the investigated field, in the Zara valley (Plate 1.1). The Kum Tso Thrust usually superposes the Middle Triassic Kaga or Chomule Formations above the Upper Triassic Juvavites Beds or Quartzite Series or even above the Liassic Kioto Formation. On the western side of the Zara valley, one can easily see the dark limestones of the Chomule Fm. overthrusting the Upper Triassic to Liassic clear massive limestones (Fig. 4.8). The Kum Tso Thrust also outcrops along the Manali -Leh road at Trambok. At this particular place the thrust is doubled, and a slice of quartzite series is taken in-between both thrusts. The Kum Tso Thrust is verticalized by younger NE vergent folds, but on the top of the mountain on can see that the dark Chomule Fm. is above the Kioto Limestones. In the Phirse Phu accumulation basin, where lies the small Kum lake, outcrop conditions allow us to see that the Kum Tso Thrust creates a mylonitic textures with calcite veins and with top-to-the SW shear sense of thrusting (C'-S structures). The amount of initial displacement along this thrust is difficult to evaluate as it has been reactivated as a normal fault (see below). But as it put in contact two different domains with important differences in the sedimentation conditions (see chapter stratigraphy for more details), thrusting along the Kum Tso Thrust might have been important. The subsequent reactivation of the KTT as a normal fault, generates a cataclastic structure (Fig. 4.9) associated with top-to-the NE shear sense criteria marked by very small folds in calcite veins.

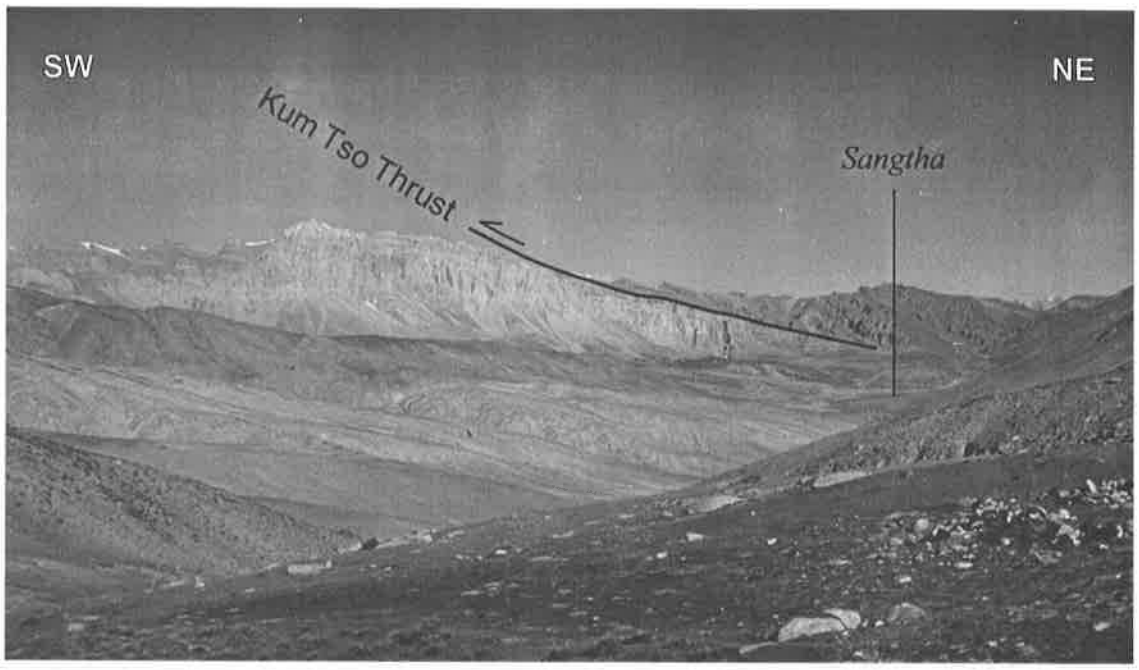

Fig. 4.8: Dark Middle Triassic formations overthrusting along the Kum Tso Thrust (KTT), the white Upper Triassic to Liassic Kioto Limestones, on the western side of the Zara valley, above Sangtha.

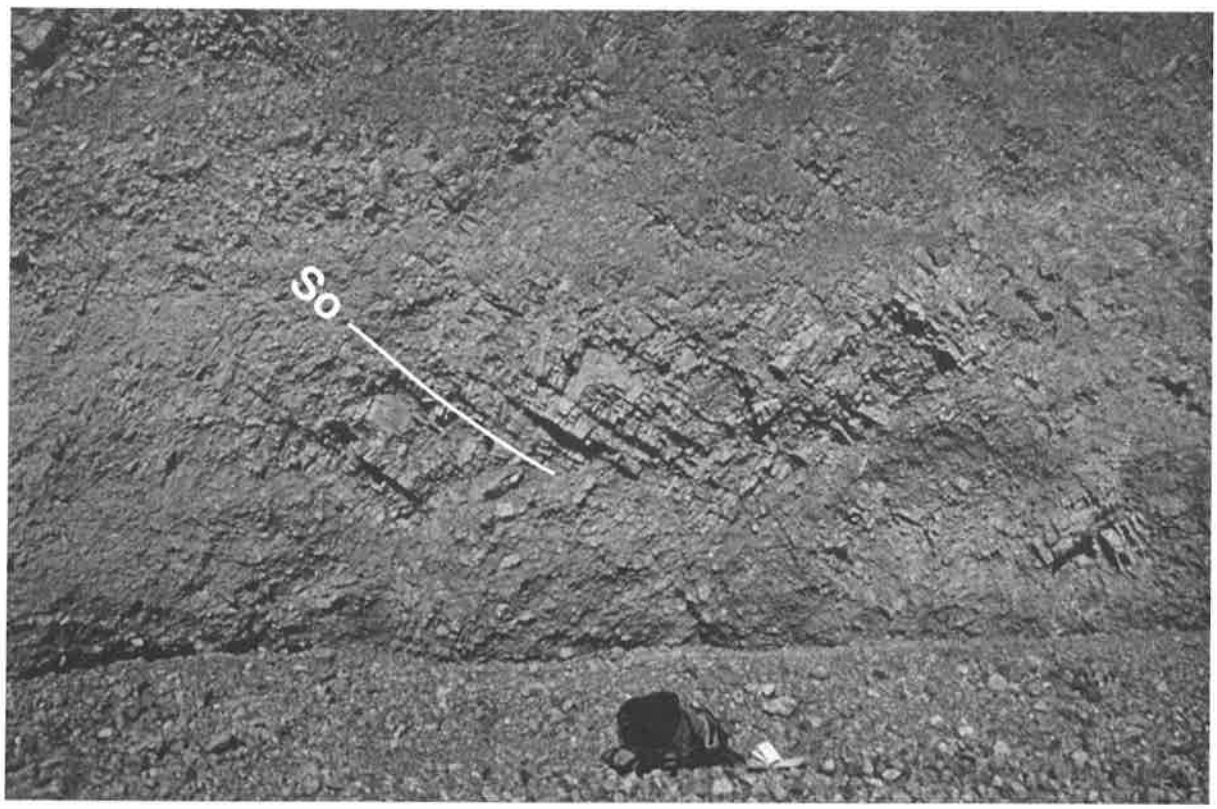

Fig. 4.9: Picture of a cataclastic texture in the hanging wall of the Kum Tso Thrust. This texture is generated by the reactivation of the thrust in a normal fault. Outcrop situation is near Trambok (western area). Mountain backpack for scale.

4.2.4 The late SW-vergent folds

In two places, it has been possible to distinguish a third phase of SW-vergent folding that creates F3 folds. In the Phirse valley, a third phase of folding has been proposed by Steck et al. (1998) to explain the style difference between the isoclinal Pradong recumbent fold and the open fold that affects the limestones of the Chomule Fm., on the southern side of the valley. Near Sangtha a three phase interference structure also allow us to distinguish F2 from F3 folds. Although these are the only places where F3 folds can be really identified, it does not mean that this folds are rare. It is possible that in many places, it is only impossible to distinguish them from the F2 folds.

4.2.5 The structure of Sangtha

This particular structure is worth a detailed explanation, as it reveals a lot of information about the different phases. It is a complex three phases interference structure that crops out over a field of about 10 km^2. The detailed map and a cross section are given on Fig. 4.10. To better understand the structure, we have to unfold the successive phases. The first phase present in this structure creates very isoclinal SW-vergent F2 folds (Fig. 4.11a). A second SW-vergent phase refolds the synclinal heads of the F2 folds (Fig. 4.11b). Such an F3 hinge crops out above Sangtha. This outcrop shows a folded S2 schistosity, parallel to the folded bedding. This hinge is the anchor of the structure as it is the only one that really crops out. The last phase creates large-scale NE-verging open folds. It folds the whole structure and places the Permian in a synform (Fig. 4.11c). When descending the Zara valley to the south, the Triassic reappears two times within the large Permian synform. These thin bands show that the Triassic has been folded several times, but it is difficult to assign these folds to a particular phase, as no hinges outcrop. However, according to their isoclinal style, it is highly possible that they are also F2 folds.

During their geological traverse of Eastern Ladakh, Lahul and Chamba, Fuchs and Linner (1995) describe the structures of the Sangtha area. Their interpretation is completely different from our, as they place the Permian that lies south of Sangtha, in an antiform position. However Fig.4.10 shows that the structure is much more complicate than what they draw on their cross section. The simplification of the Fuchs and Linner's map permitted to put the Permian in an antiform position, but this is no more possible if we take in account all the data given by detail mapping. Drawing an antiform would lead to define a first phase of deformation with isoclinal NE vergent folds (Fig. 4.12). Such an early NE vergent phase is not documented anywhere in Rupshu nor in the adjacent Nyimaling area (Stutz and Steck, 1986).

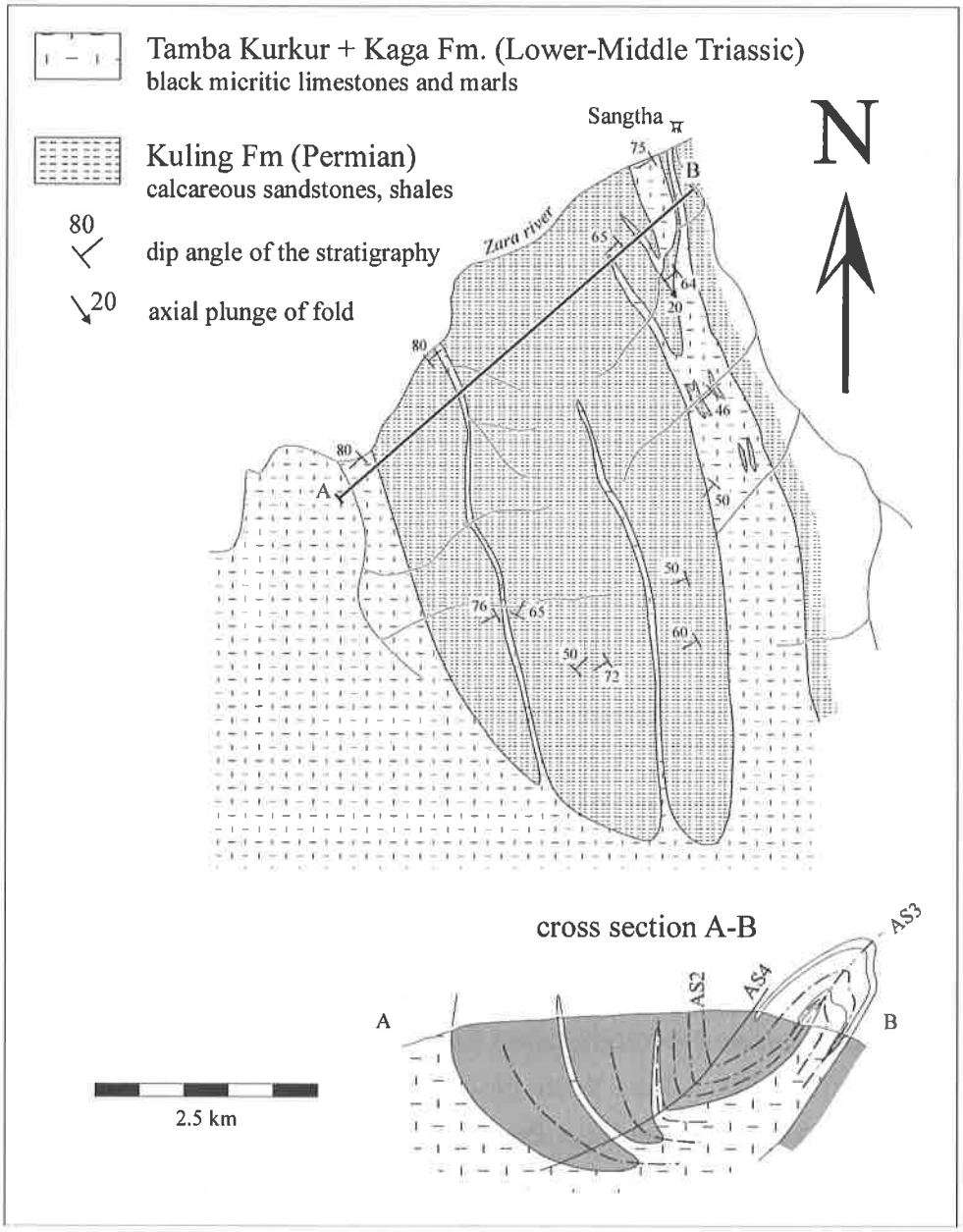

Fig. 4.10: Detailed geological map and cross section of the area of Sangtha, showing the complex interference structure between F2, F3 and F4 folds. F4 fold creates the large synform. AS = axial surface.

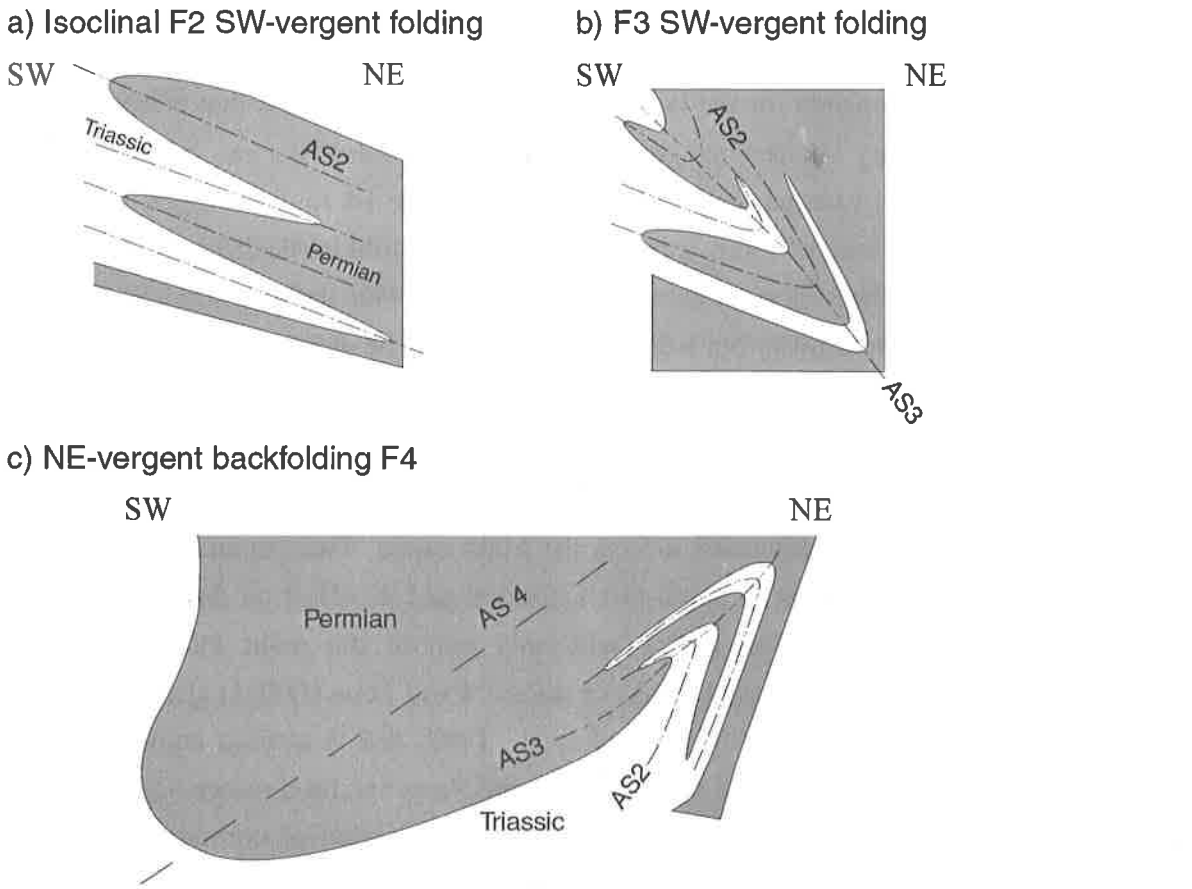

Fig. 4.11: Explanation of the interference structure of Sangtha, with the three successive phases. In c) the isoclinal folds in the main F4 syncline (see Fig. 4.10) have not been drawn.

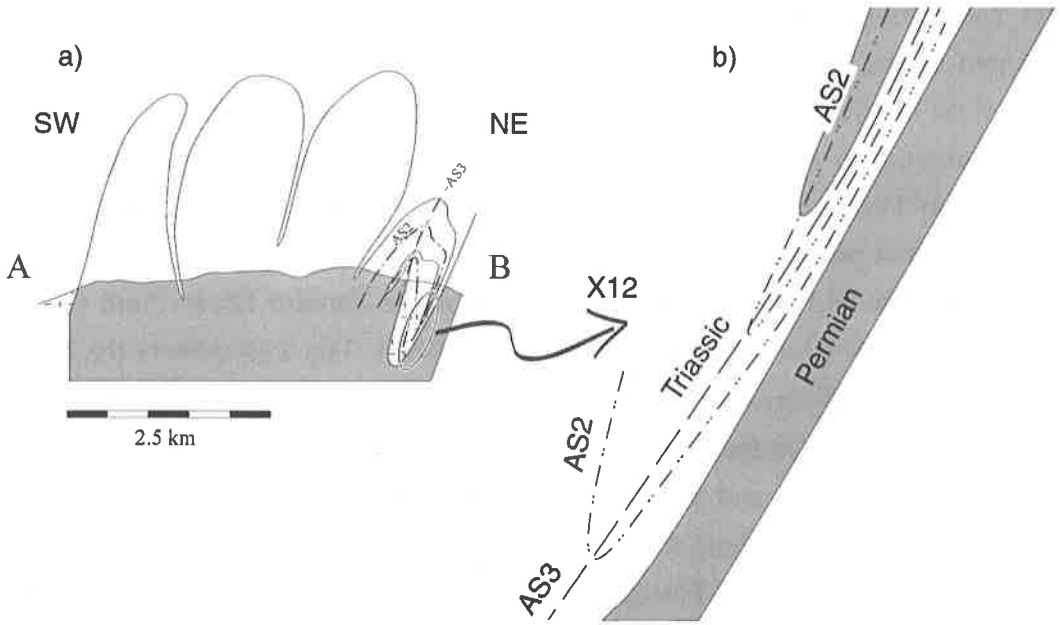

Fig. 4.12: a) Cross section across the interference structure of Sangtha, placing the Permian in an antiform position. As this solution implies an early NE vergent phase 2, it has to be rejected. b) This 12 times enlargement of the NE part shows that this solution also implies that three axial traces have to stand in the narrow band of Triassic marls.

4.2.6 The NE-verging backfolds

This phase is responsible for the large scale NE-vergent backfolds that affect both of the nappes. It creates many interference structure with older folds. This can be particularly well observed in the Toze Lungpa, below Pang (Fig. 4.5). The F4 folds are open folds and exist at different scales. South of Pang, a large scale F4 open fold verticalizes the Kum Tso Thrust. Further west, the thrust is even overturned (near Lun). This deformation usually does not develop a penetrative schistosity but a discrete cleavage can be observed at several places.

4.2.7 Extensional structures

An important phase of extension affects the Mata nappe. Two papers (Girard et al., 1999; Girard et al., in press) treat in detail this extension and its effect on the metamorphic grade, deduced by illite crystallinity. We will only expose the main features of this extensional phase. It creates the Dutung Thaktote normal Fault Zone (DTFZ) along the Spiti-Tso Morari transect (Steck et al., 1998; Girard et al., 1999) and it western equivalent, the Sarchu Lachung La normal Fault Zone (SLFZ) along the Pang-Sarchu transect (Girard et al., in press). Both of the fault zones are characterized by a succession of normal faults along some kilometers (Fig. 4.13). The S1 schistosity and thrust surfaces of the Mata nappe (e.g. the Kum Tso Thrust or the Parang La Thrust) are crosscut or reactivated by the NE dipping normal faults. As indicated by illite crystallinity and by cataclastic textures, normal faulting occurs under brittle diagenetic conditions. It is difficult to say whether normal faulting occurs before or after backfolding. Along the Spiti-Tso Morari transect, backfolds occur in the internal ductile part of the Mata nappe, while normal faulting is restricted to the external brittle part, so that no interference can be observed. We concluded that these two structures are two different answers to a same and coeval tectonic process. Along the Pang-Sarchu transect, the Kum Tso Thrust is backfolded. Although backfolding probably occurs before normal faulting, we cannot prove it.

The DTFZ and the SLFZ are eastern equivalent of the Zanskar Shear Zone (ZSZ) described further to the SW (Herren, 1987; Dèzes et al., 1999). The ZSZ affects the High Himalayan Crystalline Zone-Tethyan Himalaya transition and is active at a deep structural level, under ductile conditions. On the opposite, The DTFZ and the SLFZ are situated within the very low-grade metasediments and are active at a shallower structural level, under brittle conditions. However all of them belong to the extension system found almost all along the Himalaya, usually known as the South Tibetan Detachment System (STDS) (Burchfiel et al., 1992) or the North Himalayan Shear Zone (Pêcher, 1991). Several extension zones of the STDS show that this system was active during the 24-20 Ma time interval: Zanskar Shear Zone = 22.2 - 19.8 Ma (Dèzes et al., 1999), Deorali detachment ≈ 22.5 Ma (Hodges et al.,

1996), Dudh Kola - Chame detachment = 24-21 Ma (Coleman, 1996), Manaslu detachment ≈ 22 Ma (Guillot et al., 1994), Qomolangma detachment = 22 - 19 Ma (Hodges et al., 1992). As thrusting of the HHCS along the MCT is active between 23 and 6 Ma (Hubbard and Harrison, 1989; Harrison et al., 1995; Hodges et al., 1996), the normal faulting along the STDS is coeval with the thrusting along the MCT.

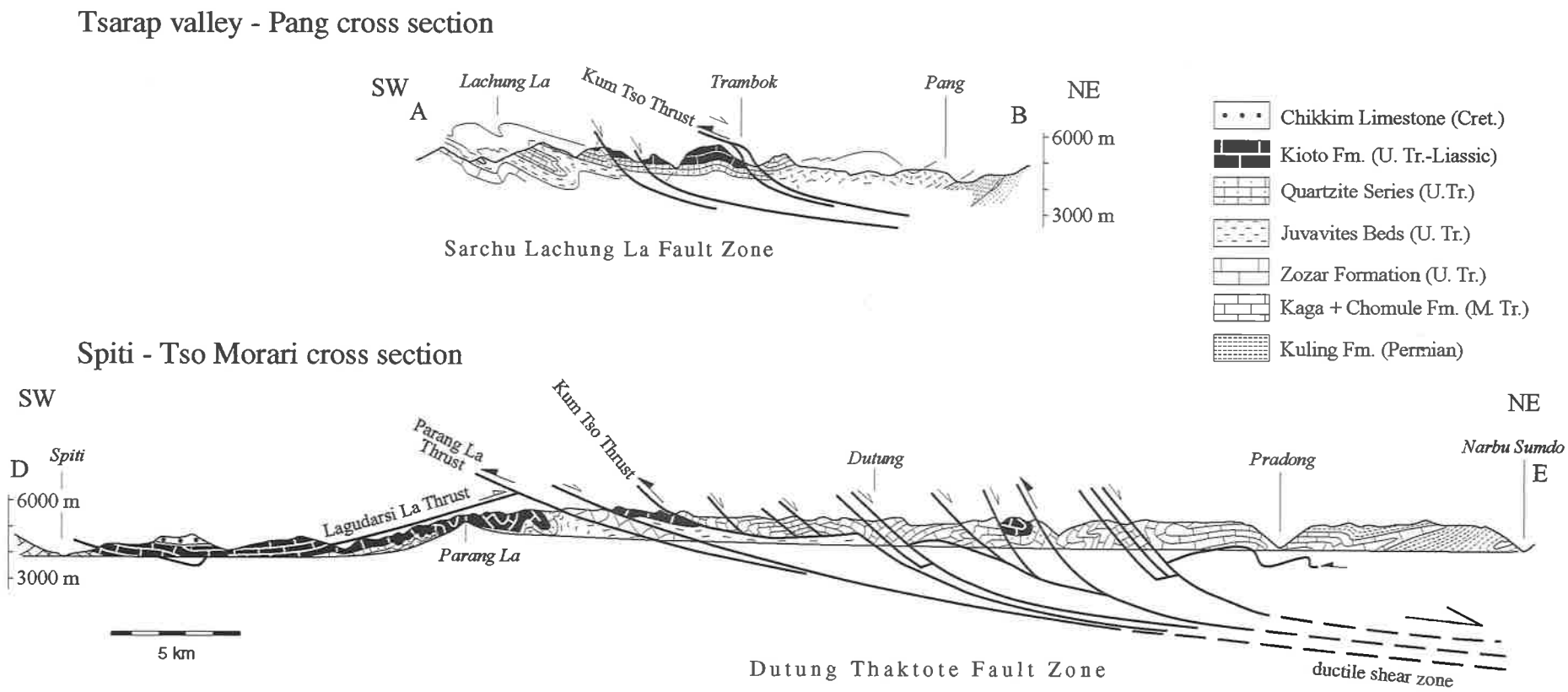

Fig. 4.13: Cross sections through the Sarchu Lachung La normal Fault Zone and Dutung Thaktote normal Fault Zone. See plate 1.2 for locations.

4.2.8 The Tso Morari dome

A late tectonic creates a large-scale dome and basin structure that is responsible for the doming of the Tso Morari massif and for the wide syncline of the Phirse basin. As shown by the important plain filling of the Phirse basin, as well as by the active rivers erosion from the Tso Morari massif that creates steep gorges, this phase is still active today. Several N-S normal faults are linked to the doming. This is the case of the Tso Morari normal fault system described by Steck et al. (1998). The hot sulfur springs of Puga is related to these faults. The normal fault situated in the lower Phirse Valley southeast of Manechan, is also due to this phase (Fig. 4.4). The Tso Morari is situated in a pull-apart structure, related to dextral strike-slip movements parallel to the Indus Suture Zone. These movements are responsible for the N-S oriented normal faults and for the oblique NW-striking dome and basin structure.

4.3/ Conclusions

The area investigated is large enough to well document a complex polyphase tectonic. Even though the pre-Himalayan tectonic structures are absent, such an event might have affected the area. If this event did not generate a high-grade metamorphism and strong deformations, it can be easily overprinted by the subsequent Himalayan phases, which are better documented. They can be subdivided in 7 phases of deformation. The first NE vergent phase is present only in the SE extremity of this field, in Spiti. The three subsequent phases are ductile SW-vergent phases (D1-D3), linked to the nappes emplacement. It is followed by a NE vergent phase of backfolding that affects the whole field. During or after backfolding, brittle extensional structures affect the frontal part of the Mata nappe. The last phase creates a dome and basin structure, that can be seen only at the map scale.

The occurrence of eclogites in the Tso Morari nappe shows that this set of rocks has extruded over a vertical distance of about 70 km. Although this extrusion have an important vertical component, the shear sense criteria indicate that an horizontal component with top-to-the-SW movements is also present during exhumation. Moreover the overlying Mata nappe with its internal ductile part, and its frontal brittle part, characterized by successive thrusts, is a good example of a nappe structure.

5/ Metamorphism

The metamorphism of the Tso Morari dome has been intensively studied due to the presence of eclogitic basic lenses within the Tso Morari nappe. Together with the Kagan, Neelum and Stak eclogites of Pakistan (Pognante and Spencer, 1991; Le Fort et al., 1997; Fontan, in prep.), the Tso Morari eclogites are the only witnesses of a High Pressure-Low Temperature (HP-LT) metamorphic phase in Himalaya. As the eclogitic phase has been analyzed with modern techniques by the French team, we focused our interest on the regional metamorphism that follows this HP-LT metamorphism. An important metamorphic gradient exists between the very low-grade metasediments in the SW, which recorded a diagenetic to epizonal metamorphism, and the high-grade metapelites of the Tso Morari nappe in the NE.

Within the calcareous lithologies of the external part of the Mata nappe, in very low-grade metamorphic terrain, we tried to quantify the metamorphism with the isotopic Qtz-Cc geothermometer (Sharp and Kirschner, 1994). The results showed that the assemblage was not in equilibrium, and it has not been possible to draw conclusions. Therefore we resort to the "illite crystallinity" method to semi quantify this very low-grade metamorphism.

In the northeastern area, the abundance of metapelites and metabasites within the Paleozoic formations permits us a good control of the metamorphic gradient between the chlorite and sillimanite zones. We will expose below different thermobarometric methods that where compared to the petrographic observations made in thin sections.

List of mineral abbreviations

Ab	Albite	Ms	Muscovite
Act	Actinolite	Oli	Oligoclase
Alm	Almandine	Omp	Omphacite
An	Anorthite	Pg	Paragonite
And	Andesine	Phe	Phengite
Andr	Andradite	Phl	Phlogopite
Ann	Annite	Pl	Plagioclase
Bt	Biotite	Prp	Pyrope
Cc	Calcite	Qtz	Quartz
Chl	Chlorite	Rt	Rutile
Dol	Dolomite	Sill	Sillimanite
Ep	Epidote	Sps	Spessartine
Gln	Glaucophane	Std	Staurolite
Grs	Grossular	Ttn	Titanite
Grt	Garnet	Zo	Zoisite
Hbl	Hornblende		
Ky	Kyanite		
Mgn	Magnetite		

5.1/ The High Pressure - Low Temperature metamorphism

This early metamorphism, linked with the subduction of the Indian plate below Asia, has been strongly retrogressed by the subsequent metamorphic phases, linked to the extrusion of the Tso Morari nappe. Relics of this HP-LT metamorphism are only found in eclogites lenses and eclogitic metasediments of the Tso Morari nappe. The Mata nappe, which overlies the Tso Morari nappe, is devoid of such relics and thus did not record this metamorphism.

We did not studied this metamorphism in detail, and we will only expose here the main results obtained by the French team concerning the eclogites and the eclogitic metasediments found north of Karzok. The main paragenesis of the eclogites is Grt + Phe + Omp + Gln + Rt + Zo + Qtz + Pg. Using the *Thermocalc* calculations of Powell and Holland (1988; 1994), De Sigoyer et al. (1997) estimate a pressure of 21 ± 4 kbar and a temperature of 580 ± 60°C. In metapelites, a relict paragenesis has been found as inclusions within some garnets. This jadeite-chloritoid-paragonite-garnet assemblage indicates pressure between 18 and 22 kbar and a minimum temperature of 520 - 550°C (Guillot et al., 1997). A Lu/Hf age of 55 ± 12 Ma, a Sm/Nd age of 55 ± 7 Ma and an U/Pb age on allanite of 55 ± 17 Ma have been obtained for this eclogitic episode (De Sigoyer et al., 2000). This age is coherent with the 49 ± 6 Ma (Sm/Nd, garnet-clinopyroxene) obtained for the Kaghan eclogites of Pakistan (Tonarini et al., 1993).

5.2/ The Barrovian metamorphism

After the HP-LT metamorphism that affects only the Tso Morari nappe, the whole nappe stack was affected by a regional metamorphism of Barrovian type. In the Tso Morari nappe, this metamorphism has been dated at 47 ± 2 Ma by Sm/Nd, Rb/Sr and Ar-Ar on amphibolites and garnet bearing metapelites (De Sigoyer et al., 2000).

This metamorphism decreases towards the SW and isograds are oblique to the nappes or formations boundaries. This results from the existence of a thermal dome that is partly controlled by the tectonic doming of the Tso Morari massif. At some places, the retrogressive metamorphism linked to the nappes extrusion, has strongly overprinted the peak temperature mineral assemblages.

The Barrovian metamorphism has been particularly studied along the transect between the Tsarap River and the Tso Kar Plain, where an important gradient can be observed. We will expose below the different metamorphic zones observed from SW to NE.

5.2.1/ The very low-grade metamorphism

Between the Tsarap River and the More Plain, the mainly carbonaceous Permian to Lower Jurassic sediments recorded a very low-grade metamorphism between diagenesis and epizone. The typical paragenesis is **Cc ± Dol, Qtz, illite, smectite, kaolinite, chlorite, illite/smectite and corrensite**. Kaolinite is more abundant in diagenetic zones, but it can also occur in the anchizone. Measurements of the illite crystallinity on the (001) diffraction peak of illite (Kübler index) makes it possible to put forward an important zone of extension, that lowers diagenetic limestones in-between anchizonal limestones (the Sarchu Lachung La normal Fault Zone, SLFZ). More details of this zone can be found in Girard et al. (in press).

Similar conditions have been found along a subparallel cross section between the Spiti valley and the Tso Morari, where the Dutung Taktote normal Fault Zone (DTFZ) has been described (Steck et al., 1998; Girard et al., 1999).

5.2.2/ The chlorite zone

The last calcareous samples along both aforesaid profiles indicate epizonal conditions in the Middle Triassic marls and limestones. Below these sediments, the first pelitic lithologies are those of the Cambrian Karsha and/or Kurgiakh Formations. These metapelites are quartz rich gneisses or schists with a strong penetrative schistosity. They contain the stable paragenesis **Qtz-Ms-Chl-Ab**, with Ms and Chl within the S1 + S2 schistosity. The chlorite zone is very thin and the first biotite appears on the right side of the Sumkhel Lungpa and NE of Pogmar (Plate 5.4).

5.2.3/ The biotite zone

Metapelites of the biotite zone contain the critical paragenesis of **Qtz-Ms-Bt-Ab-Chl**. Biotite is found either as thin minerals within the S1 + S2 schistosity planes, or as bigger post-kinematic porphyroblasts. The transition between the chlorite and the biotite zone is gradual, with an increase in the amount and size of the biotite. Some chloritoide has also been found near the Pogmar La and SE of the Tso Morari, in metapelites of the biotite zone (Plate 5.4).

More or less along the biotite in isograd, lenses of **metabasics** show a stable paragenesis of **hornblende-actinolite-albite-epidote-chlorite**. The amphiboles and chlorite mark the S1 + S2 schistosity. The coexistence of hornblende and actinolite is well illustrated in sample G9855, where two different kinds of amphibole occur (Fig.5.1). Large porhyroclasts are strongly zoned and show actinolitic green to pale green core with Mg-hornblende blue green rims. Thin needles are usually blue green with hornblende compositions, although some green actinolitic needles also occur. This indicates a prograde

metamorphism from the greenschist facies to the lower part of the epidote amphibolite facies. Sample G96 101, from the area of Traktagol, also contains some barroisite in coexistence with Hbl and Act (Fig. 5.1). Some massive bodies of metagabbros, found in the Phe Formation near Numah, have preserved a magmatic texture with idiomorphic plagioclase, altered olivine and pigeonite (Fig 4.2). No schistosities appear in these rocks but chlorite and actinolite begin to replace the magmatic minerals.

5.2.4/ The garnet zone

The first appearance of garnet is well documented in the More Plain, where the garnet-in isograd is situated just above the Nyimaling Granite (Plate 5.4), in the **metapelites** of the Phe Formation. The typical paragenesis is **Qtz-Bt-Ms-Grt-Pl**. Muscovite and biotite mark the S1 + S2 schistosity, and garnet sometimes contain sygmoidal inclusions. Garnet occurs in the more pelitic lithologies, while the quartz-rich paragneisses only contain biotite. The transition between the biotite and the garnet zone is gradual. Garnet is small and few abundant in the first garnet bearing samples. The garnet-in isograd cross cut the formations boundary west of the More Plain, as no garnet occur in the area of Pangjin and Rinang, where much metapelites would be susceptible to host some. This clearly reflects a thermal doming around the Tso Morari dome.

On the Tso Morari lake side, the first garnet appears above the Rupshu granite. There is no more garnet further north until the end of the Morari lake. As neither the Rupshu granite nor the Karzok Formation contain abundant metapelites, This lack of garnet might partly results from a chemical control. However as indicated by the metabasites found around Karzok (see below), it seems that this area has been strongly overprinted by a greenschist facies metamorphism during its exhumation.

The **metabasics** found within the garnet zone have not preserved magmatic relics. The critical assemblage contains **hornblende-plagioclase (Oli-And)-garnet (65% Alm, 20% Grs, 7% Sps, 3% Prp)-biotite**. The amphibole vary in the same sample from an Fe-tschermakite to an Mg-hornblende (sample G9625 and V963 on Fig. 5.2). Small size garnets (<2mm) are quite homogenous in both of the analyzed amphibolitic samples G9625 and V963 (Fig. 5.3). They show flat composition traverses reflecting a chemical homogenization through diffusion at high temperature. Sample G986 differs from the other metabasics by its greater amount of dark ferromagnesian minerals and its very low content of plagioclase. The paragenesis is hornblende-garnet-epidote-quartz-magnetite/hematite-apatite-calcite-titanite-albite (Fig. 5.4). Hornblende grows as a symplectite with quartz and calcite, with numerous idiomorphic magnetite and/or hematite inclusions. Garnet has similar compositions than in the other metabasites, but shows a stronger compositional zoning characterized by a core to rim Grs increase, parallel with an Alm decrease (Fig. 5.3). The high modal percentage of calcic

minerals suggests that this rocks is the metamorphic product of a marls. Moreover this sample comes from a zone where several marbles and calcschists are intercalated in metapelites. The texture of this sample remind an eclogitic texture, but the garnet is very poor in Prp (<10%) compared to garnets analyzed in the eclogites of the Tso Morari nappe (De Sigoyer et al., 1997). The dolomite of the Karsha Fm. in the area of Shingbuck sometimes contain needles of tremolite. However this diagnostic mineral is rare due to the low abundance of quartz in the dolomite.

5.2.5/ The kyanite + staurolite zone

This zone is restricted to a small area near Nuruchan, in the Tso Morari nappe. The **metapelites** contain the assemblage **Qtz-Bt-Ms-Ky-Std-Grt-Pl**. This assemblage develops during the main phases of deformation D1 and D2 linked to the nappe emplacement, and post date the eclogitic metamorphism. It has not been possible to delimit a smaller zone where kyanite or staurolite alone would be present, as both of the minerals coexist throughout the whole zone. Kyanite without garnet and staurolite has been described within Mg rich metapelites, east of the Polokongka La (Guillot et al., 1997). This kyanite is interpreted as resulting from the HP-LT metamorphism by Guillot et al. (1997). South of the Kiagar La, that is east of the investigated area, kyanite and sillimanite gneisses have been described by Thakur (1983) in the Tso Morari nappe.

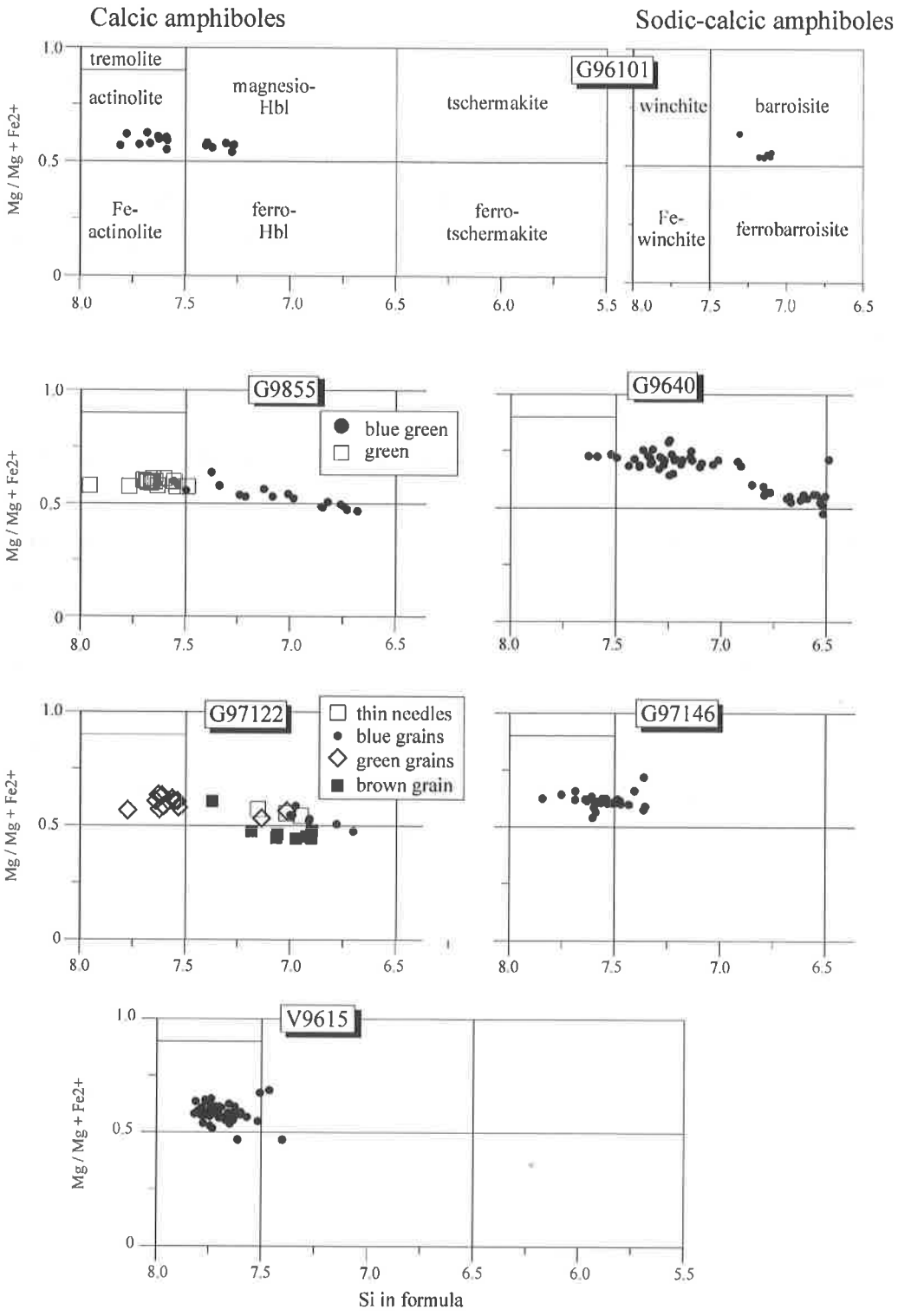

Fig. 5.1: Amphiboles compositions of 6 samples that contain hornblende and actinolite. Classification diagrams after Leak et al. (1997). Diagram parameters for calcic amphiboles are: $Ca_{(B)} > 1.5$; $(Na+K)_A < 0.5$; $Ca_{(A)} < 0.5$ and $(Na+K)_A < 0.5$; $(Ca+Na)_B > 1$; $0.5 < Na_B < 1.5$ for sodic-calcic amphiboles. Fe^{2+} is estimated on the basis of a 13 cations normalisation. See Plate 5.3 for samples locations.

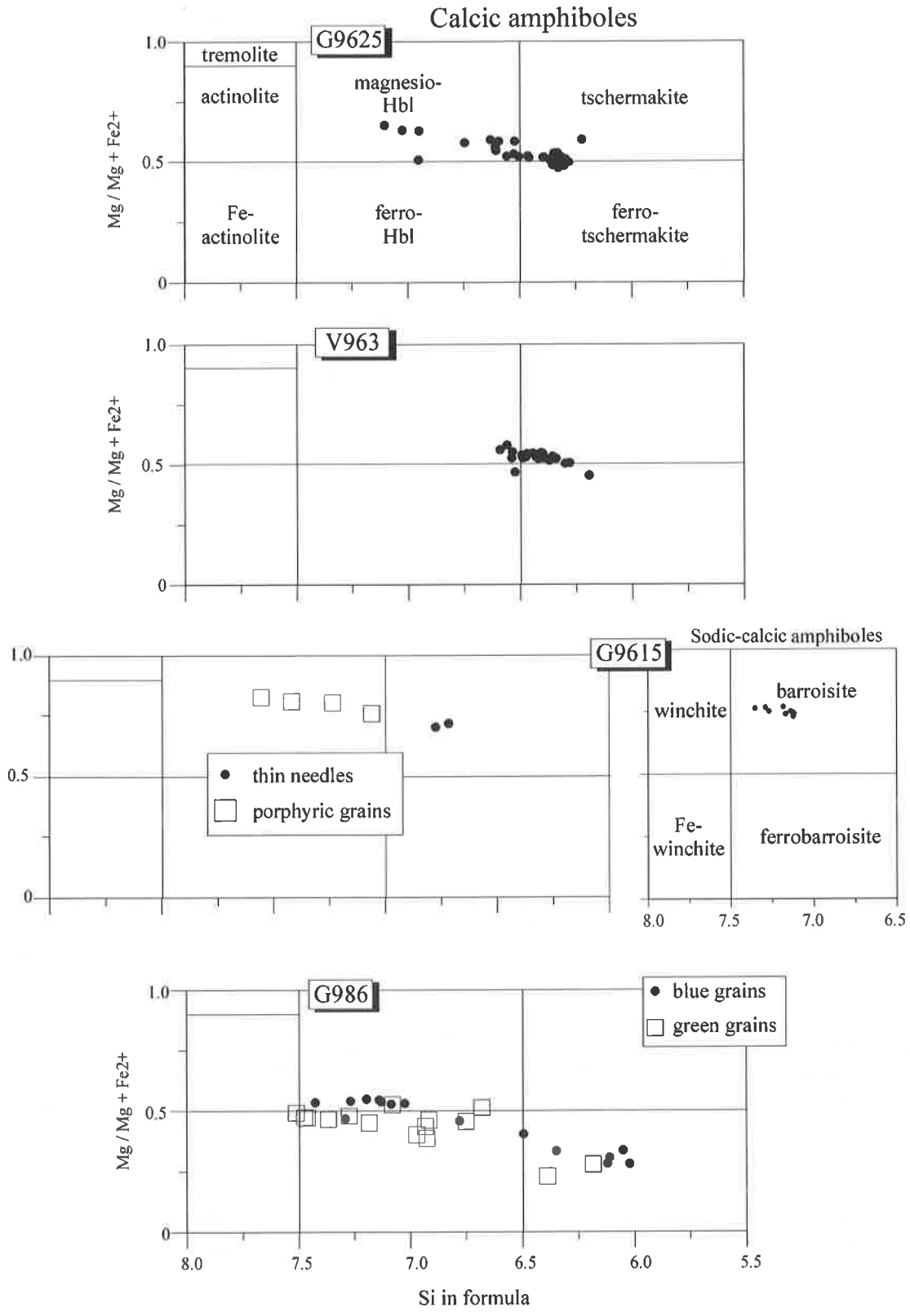

Fig. 5.2: Amphiboles compositions of 4 samples that contain hornblende without actinolite. Classification diagrams after Leak et al. (1997). See Fig. 5.1 for diagram parameters. Fe^{2+} is estimated on the basis of a 13 cations normalisation. See Plate 5.3 for samples locations.

An **amphibolite** from the kyanite + staurolite zone contains the stable assemblage of **hornblende + labradorite** and large clasts of probable albite completely damouritized. The stable plagioclase contains the highest anorthite content from the investigated area.

Tremolite-actinolite has also been found in calcschists layers intercalated in the metapelites of the Phe Fm. near Nuruchan.

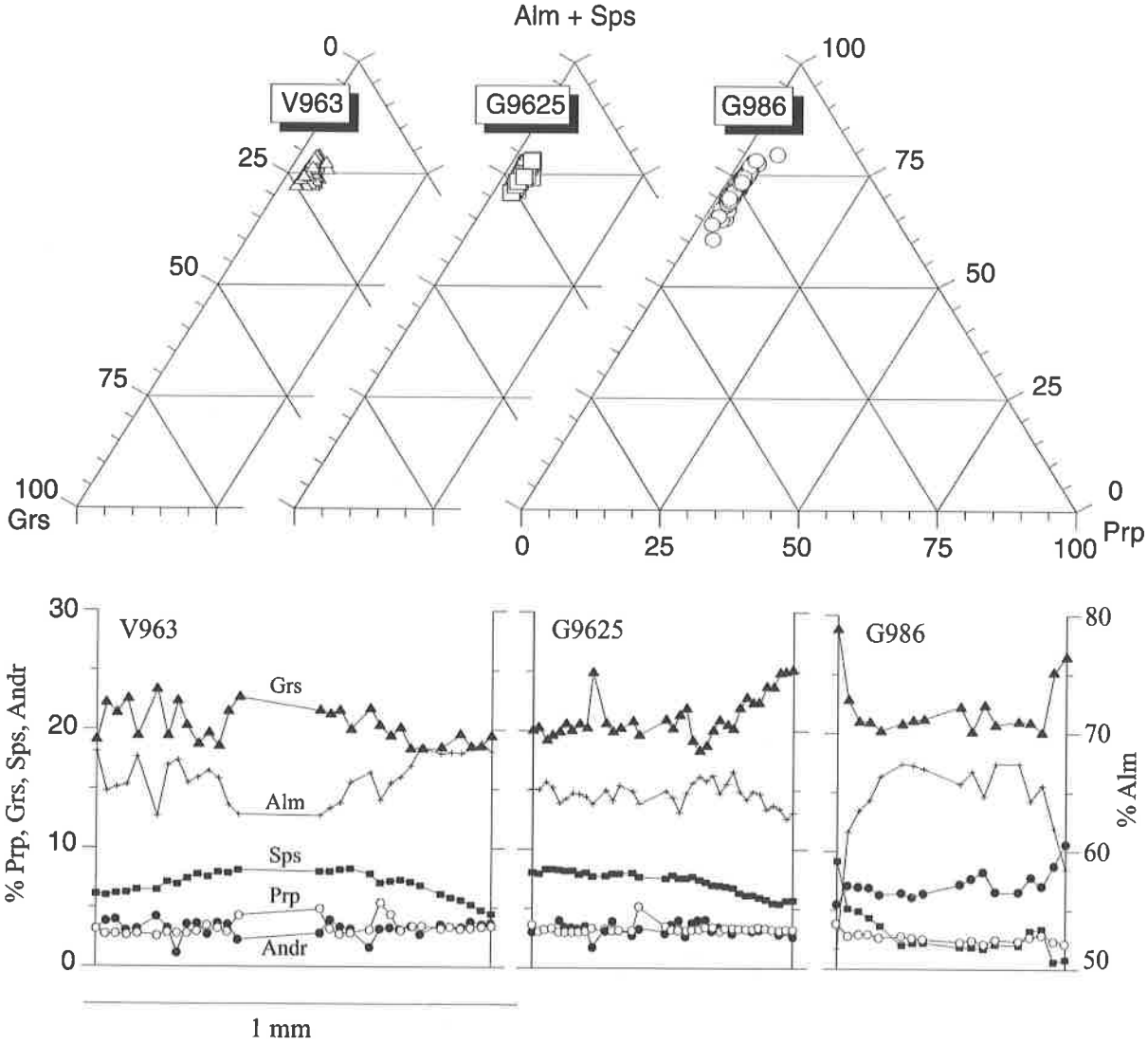

Fig. 5.3: Projections of garnet compositions from 2 metabasics (V963 and G9625) and one metamarls (G986) in ternary diagrams. Rim to rim compositional profiles of those garnets are also presented. See Plate 5.3 for samples emplacements.

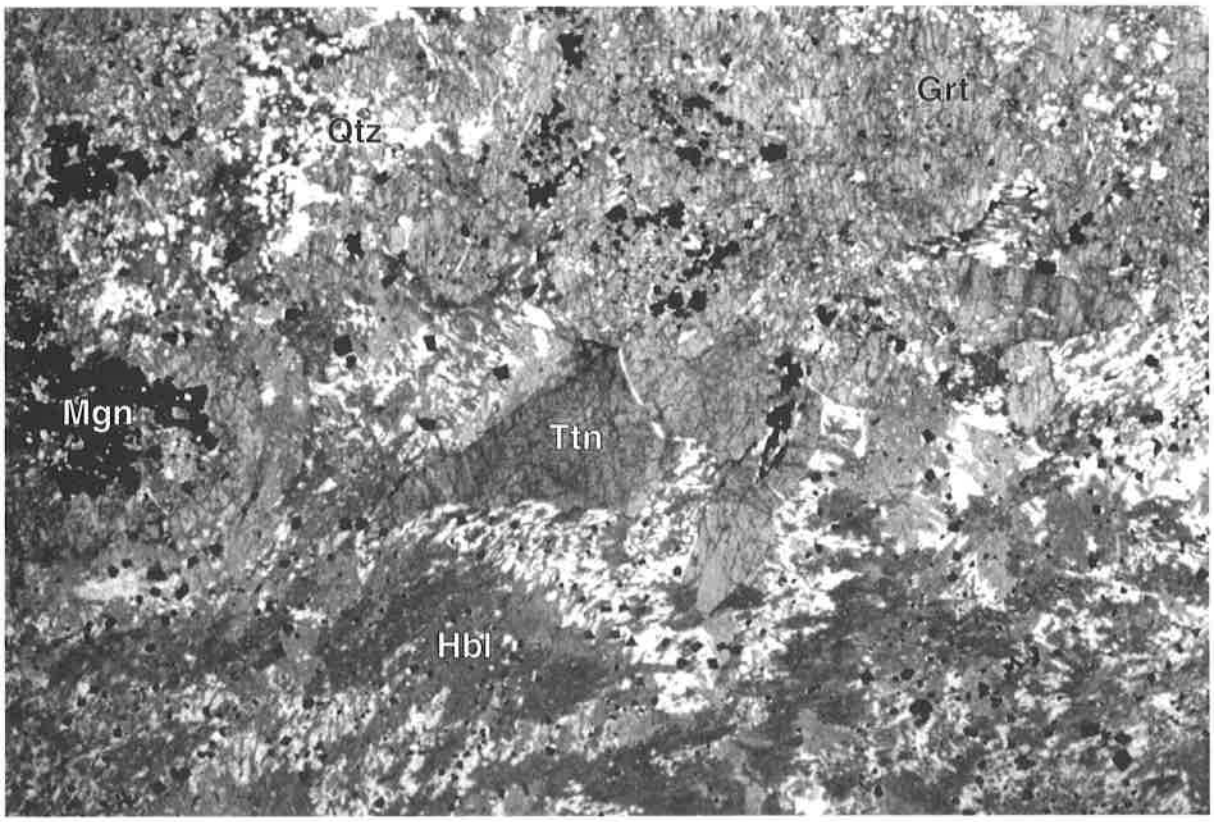

Fig. 5.4: Thin section of the metamarls G986. With large garnet (Grt) and titanite (Ttn). White minerals are almost all quartz (Qtz) and isotropic minerals are magnetite or hematite (Mgn). Dark mineral in the bottom are hornblende (Hbl).

5.2.6/ The sillimanite zone

Two samples taken south of Sangtha, in the valley west of Horlam La, contain the paragenesis **Qtz-Bt-Ms-Ky-Sill-Pl ± Grt**. Sillimanite grows at the expense of biotite. It occurs as fibrolite, oriented along the same schistosity than Bt, Ms and Ky (S1 + S2). Although the sillimanite growing postdate the kyanite growing, both of these minerals seem stable. Moreover, as the sillimanite bearing samples have been collected very close to Ky + Std bearing samples, the metamorphic grade just reaches the onset of sillimanite zone.

5.2.7/ The retrogressive metamorphism

The area of Karzok merits a particular attention because the retrogressive metamorphism has been particularly active. Everything seems to indicate that it only reaches the biotite zone, even though it is surrounded by higher grade zones (Plate. 5.4). The metapelites of the Karzok - Karzok La - Lanyer La area contain Qtz-Bt-Ms-Chl or Qtz-Chl-Ms assemblages. The metabasics indicate greenschists facies conditions with Ab-Chl-Ep ± Act assemblages, and the dolomitic limestones are devoid of tremolite. However one basic

sample from Karzok (AS9691) contains small needles of hornblende within the schistosity, that are altered by chlorite. This sample has a prasinitic texture attesting its strong retrogressive metamorphism in the greenschist facies.

A single chemical control cannot explain the absence of the diagnostic minerals of a higher metamorphic grade, because metapelites and metabasics exist in the Karzok Fm. and in the Phe Fm. It seems more plausible that this zone has been subjected to a more intense retrogressive metamorphism during its exhumation, and that the metamorphic peak has been almost totally overprinted.

5.3/ Thermobarometry

The metapelites from the profile Tsarap River - Tso Kar have been analyzed with a Cameca SX50 electron microprobe. The internally consistent thermodynamic data sets of Holland and Powell (1998) and of Berman (1988) have been used to calculate pressures and temperatures of the peak metamorphism, using computer programs *Thermocalc 2.75* (Powell and Holland, 1999) and *TWQ 2.02* (Berman and Brown, 1997). We also compared these two methods to another independent thermometer based on the differences between the isotopic ratios of oxygen in quartz and garnet and in quartz and kyanite (Sharp, 1995).

In the metabasics, amphibole, garnet and plagioclase have also been analyzed with the electron microprobe to qualitatively determine the metamorphic facies and to use the geothermometer based on the Ti content in amphibole (Colombi, 1989).

The very low-grade limestones have been analyzed by X-Ray diffraction to measure the illite crystallinity of the clay fraction (<2 μm). These analyses give semi- quantitative temperatures for the southwestern extremity of the profile. These results can be found in Girard et al. (in press).

5.3.1/ The Thermocalc calculations

Conventional thermobarometry usually consists of locating the intersection between two different calibrated reactions such as the Garnet-Biotite geothermometer combined with the Garnet-Muscovite-Annite-Plagioclase geobarometer. As the *Thermocalc* computer program (Powell and Holland, 1999) (*http://www.esc.cam.ac.uk/astaff/holland/index.html.),* uses an internally consistent thermodynamic data set (Holland and Powell, 1998), it has the advantage of using all available experimental information, rather than just a subset. A method has been developed to calculate the average P-T from all the possible independent set of reactions, for a given mineral assemblage (Powell and Holland, 1994). The choice of the independent set of reactions does not influence the P-T result, because the method considers

the correlation among the reactions used. Moreover several diagnostics permit us to investigate the influence of the input data on the calculated P-T, and eventually to modify these data when an outlier end member exists.

As this method also takes in account the uncertainties of the data set, the propagated uncertainty represents the accuracy and not only the precision of the method. This explains why the uncertainty ellipses are so large on Fig. 5.7. *"Precision is a measure of the reproducibility of observations of a samples thought to be representative of a population. Accuracy is a measure of how well the sample represents the population"* (Mc Kenna and Hodges, 1988). However as we are mainly interested in the metamorphic gradient, the precision, which mainly depends on the quality of the analyses, is sufficient to compare the values between them. The accuracy given by *Thermcalc* is five to ten times bigger than the precision (Worley and Powell, 2000)

Selection of the analyses

Calculations have only been made for metapelites from the garnet zone to the sillimanite zone (Table 5.2). Metapelites with only Qtz-Ms-Bt does not have enough minerals to sufficiently constrain the P-T conditions. Several composition profiles have been realized through one or two garnets per sample (Fig. 5.5 and 5.6). Only three samples (V96 25, G98 21 and G97 164) have preserved a good bell-shape compositional profile, characterized by core to rim Fe^{2+}/ Fe^{2+}+Mg (Fe^{2+} estimated by normalization) and X_{Sps} decrease, and parallel X_{alm} and X_{Prp} increase. These are typical growth zonings that have not been re-equilibrated. Those three samples come from the kyanite + staurolite and from the sillimanite zones and in all three, garnets are greater than 1 mm. Although both of these conditions seem to be necessary to preserve a growth zoning, they are not sufficient as bigger grains or grains from the same zone also show homogenous compositions. When a growth zoning (or a partially re-equilibrated growth zoning) is present, a mean of the analyses with the lower ratios Fe^{2+}/ Fe^{2+}+Mg have been selected for the thermobarometry (Tab. 5.1). These selected analyses are always close to the garnet rims. Homogenous composition profiles indicate a diffusion through the garnet at high temperature, and the peak compositions are susceptible to be lost (Spear and Selverstone, 1983). In this case, the calculated temperature should underestimate the peak temperature. The outermost rims usually show a retrograde zoning characterized by an increase of the Fe^{2+}/ Fe^{2+}+Mg ratio (e.g. G97 197 on Fig. 5.6). Those analyses have been avoided in the thermobarometric calculations.

	V9623				V9625				V9629				
	Grt	Bt	Phe	Pl	Grt	Bt	Ms	Pl	Grt	Bt	Ms	Pl	Std
SiO2	37.25	35.80	50.37	63.59	37.61	35.90	46.09	63.68	37.40	36.16	46.73	64.46	29.87
TiO2	0.04	1.79	0.34	0.00	0.04	1.76	0.45	0.00	0.03	1.80	0.64	0.00	0.64
Al2O3	20.71	18.77	30.50	23.27	20.89	20.02	37.96	23.25	20.68	20.14	37.51	22.72	50.90
Cr2O3	0.03	0.00	0.05	0.00	0.03	0.00	0.04	0.00	0.03	0.00	0.03	0.00	0.05
FeO	35.57	20.09	0.00	0.14	33.91	18.78	0.00	0.06	33.97	18.08	0.00	0.07	13.68
MnO	1.40	0.07	0.00	0.00	0.65	0.11	0.00	0.00	3.05	0.12	0.00	0.00	0.35
MgO	2.31	9.65	2.30	0.00	3.98	9.92	0.52	0.00	2.95	10.02	0.63	0.00	1.51
CaO	3.60	0.00	0.02	4.63	3.62	0.00	0.01	4.58	2.78	0.00	0.02	4.04	0.01
Na2O	0.00	0.00	0.64	8.85	0.00	0.00	1.21	9.20	0.00	0.00	1.24	9.32	0.00
K2O	0.00	9.29	9.71	0.07	0.00	9.04	9.57	0.10	0.00	9.46	9.62	0.09	0.00
	V9630				**V9634**				**G97128**				
	Grt	Bt	Ms	Pl	Grt	Bt	Ms	Pl	Grt	Bt	Ms	Pl	
SiO2	36.73	35.68	47.52	64.43	37.49	36.16	46.77	63.08	36.88	34.90	48.24	60.75	
TiO2	0.08	0.99	0.27	0.00	0.06	1.68	0.46	0.00	0.09	1.31	0.22	0.00	
Al2O3	20.50	19.04	36.22	22.80	20.79	19.02	37.23	23.72	20.30	19.20	31.09	24.81	
Cr2O3	0.03	0.00	0.03	0.00	0.03	0.00	0.03	0.00	0.04	0.03	0.06	0.00	
FeO	33.01	21.50	0.00	0.11	35.15	19.33	0.00	0.10	33.09	22.59	2.45	0.03	
MnO	5.08	0.14	0.00	0.00	0.86	0.08	0.00	0.00	5.52	0.13	0.01	0.00	
MgO	1.77	9.30	0.92	0.00	3.18	9.90	0.71	0.00	1.36	7.82	1.76	0.00	
CaO	3.25	0.00	0.01	4.08	3.24	0.00	0.01	5.17	3.48	0.00	0.02	6.45	
Na2O	0.00	0.00	0.94	9.32	0.00	0.00	1.55	8.83	0.00	0.00	0.49	7.99	
K2O	0.00	9.02	10.00	0.10	0.00	9.84	9.37	0.10	0.00	9.38	9.92	0.09	
	G97142				**G97148**				**G97151**				
	Grt	Bt	Ms	Pl	Grt	Bt	Ms	Pl	Grt	Bt	Ms	Pl	
SiO2	37.11	35.10	46.95	60.74	37.06	35.53	46.33	58.69	38.67	35.59	45.94	64.07	
TiO2	0.10	1.83	0.22	0.00	0.06	1.21	0.47	0.00	0.03	1.92	0.82	0.00	
Al2O3	20.41	18.69	34.72	24.87	20.59	19.39	35.89	25.11	20.90	20.00	35.79	21.63	
Cr2O3	0.05	0.05	0.05	0.00	0.02	0.00	0.07	0.00	0.03	0.06	0.03	0.00	
FeO	30.15	21.89	2.01	0.05	36.43	19.49	1.05	0.18	33.99	20.35	1.02	0.11	
MnO	7.33	0.59	0.04	0.00	0.58	0.04	0.00	0.00	0.75	0.08	0.02	0.00	
MgO	1.69	7.77	0.92	0.00	1.91	9.96	0.68	0.00	3.50	8.89	0.63	0.00	
CaO	4.00	0.00	0.01	6.49	3.78	0.00	0.00	7.15	3.90	0.00	0.01	2.67	
Na2O	0.00	0.00	0.90	7.95	0.00	0.21	1.08	7.40	0.00	0.00	1.10	9.96	
K2O	0.00	9.59	9.94	0.10	0.00	8.48	9.69	0.07	0.00	9.12	9.71	0.19	
	G97152				**G97158**				**G97164**				
	Grt	Bt	Phe	Pl	Grt	Bt	Ms	Pl	Grt	Bt	Ms	Pl	Std
SiO2	37.25	35.54	50.38	61.22	38.32	35.68	46.28	60.08	37.23	36.07	46.30	62.85	29.84
TiO2	0.07	1.39	0.38	0.00	0.06	1.47	0.66	0.00	0.06	1.34	0.33	0.00	0.51
Al2O3	20.75	19.50	29.62	23.89	20.81	19.39	35.25	25.14	20.70	20.14	36.47	22.76	50.36
Cr2O3	0.03	0.00	0.05	0.00	0.03	0.05	0.08	0.00	0.01	0.00	0.04	0.00	0.05
FeO	34.80	19.28	1.87	0.34	32.80	17.40	1.62	0.09	34.52	17.85	0.86	0.08	14.77
MnO	0.73	0.07	0.01	0.00	1.96	0.11	0.00	0.00	1.90	0.09	0.01	0.00	0.28
MgO	2.84	9.88	2.40	0.00	3.56	11.04	0.72	0.00	2.94	10.68	0.59	0.00	1.83
CaO	3.92	0.00	0.01	5.71	3.96	0.00	0.00	6.70	2.81	0.00	0.01	4.58	0.02
Na2O	0.00	0.24	0.47	8.15	0.00	0.00	1.08	7.72	0.00	0.23	1.56	9.23	0.00
K2O	0.00	9.48	9.89	0.17	0.00	9.38	9.63	0.09	0.00	9.33	8.88	0.10	0.00

Table 5.1: Electron microprobe results (weight % oxides) used for the thermobarometric calculations on metapelites. Analytical conditions: acceleration voltage for all minerals = 15 kV, beam current: 30 nA for garnet, 15 nA for micas and staurolite and 10 nA for plagioclase. See Plate 5.1 for samples location. Limit between Phengite and Muscovite fixed at 6.4 Si p.f.u.

	G97171					G97185				G97195			
	Grt	Bt	Phe	Pl	Std	Grt	Bt	Ms	Pl	Grt	Bt	Ms	Pl
SiO2	37.39	35.83	49.21	59.48	29.50	37.32	35.39	48.43	57.59	38.43	36.19	46.74	64.24
TiO2	0.07	1.35	0.35	0.00	0.57	0.04	0.99	0.39	0.00	0.05	1.49	0.45	0.00
Al2O3	20.71	18.72	28.19	25.38	50.81	20.72	18.65	31.10	26.31	20.91	18.67	33.91	22.50
Cr2O3	0.03	0.00	0.02	0.00	0.06	0.02	0.00	0.05	0.00	0.03	0.04	0.02	0.00
FeO	34.49	18.75	3.69	0.05	14.32	34.53	20.63	2.11	0.08	33.26	19.16	1.64	0.02
MnO	1.21	0.06	0.01	0.00	0.25	0.65	0.06	0.01	0.00	0.47	0.15	0.00	0.00
MgO	2.88	11.38	3.34	0.00	1.64	2.82	10.03	1.96	0.00	2.85	10.01	1.33	0.00
CaO	3.47	0.00	0.01	7.28	0.01	3.75	0.00	0.02	8.64	5.76	0.00	0.01	3.86
Na2O	0.00	0.21	0.58	7.63	0.00	0.00	0.08	0.40	6.70	0.00	0.00	1.02	9.40
K2O	0.00	9.36	9.55	0.08	0.00	0.00	9.36	10.36	0.08	0.00	9.23	9.77	0.10
	G9821					**G97197**							
	Grt	Bt	Ms	Pl	Std	Grt	Bt	Ms	Pl				
SiO2	37.25	36.07	45.98	58.20	30.21	37.86	36.28	47.23	62.12				
TiO2	0.03	1.52	0.47	0.00	0.63	0.07	1.49	0.51	0.00				
Al2O3	20.78	19.06	35.29	26.43	50.96	20.61	19.35	33.84	23.83				
Cr2O3	0.03	0.00	0.04	0.00	0.07	0.03	0.04	0.04	0.00				
FeO	34.76	18.48	1.14	0.05	13.73	35.06	19.44	1.51	0.15				
MnO	0.70	0.04	0.01	0.00	0.18	1.27	0.09	0.02	0.00				
MgO	3.28	10.77	0.71	0.00	1.40	2.20	10.08	1.24	0.00				
CaO	3.46	0.00	0.02	8.51	0.01	4.12	0.00	0.01	5.19				
Na2O	0.00	0.17	0.87	6.93	0.00	0.00	0.00	0.87	8.70				
K2O	0.00	9.42	9.74	0.05	0.00	0.00	9.30	9.85	0.09				

Table 5.1 continued

As biotite is not chemically zoned, the mean of a single grain that touches the garnet and that is as close as possible to muscovite and plagioclase has been used for the thermobarometry. Sometimes muscovite shows large variations of the SiO2 content in the same grain or between grains, without any coherent zonation. The mean value of the best located grain has usually been used. Plagioclase is usually homogenous, except in samples G97 195 and G97 128 where albite coexists with oligoclase. As oligoclase (or even a more An rich phase) was probably the stable phase during peak metamorphism, these analyses have been selected. In the other samples all the analyses indicate oligoclase or andesine.

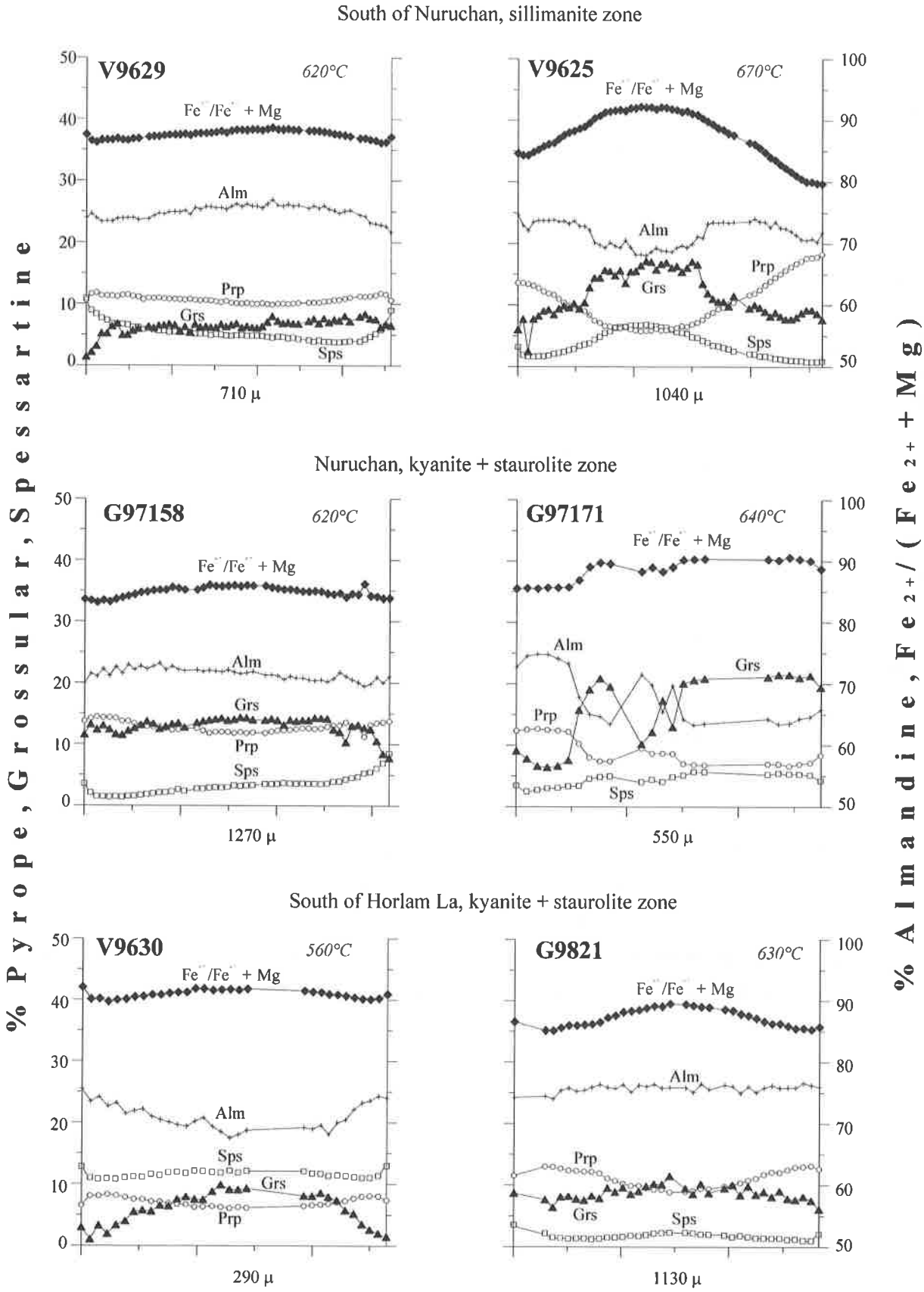

Fig. 5.5: Rim to rim compositional profiles of garnets from metapelites, from the sillimanite and kyanite + staurolite zones. Temperatures obtained with *Thermocalc* calculations are indicated in italics. Samples that give the lower temperature are on the left, to compare them with the garnets that give a higher temperature in the same zone (on right).

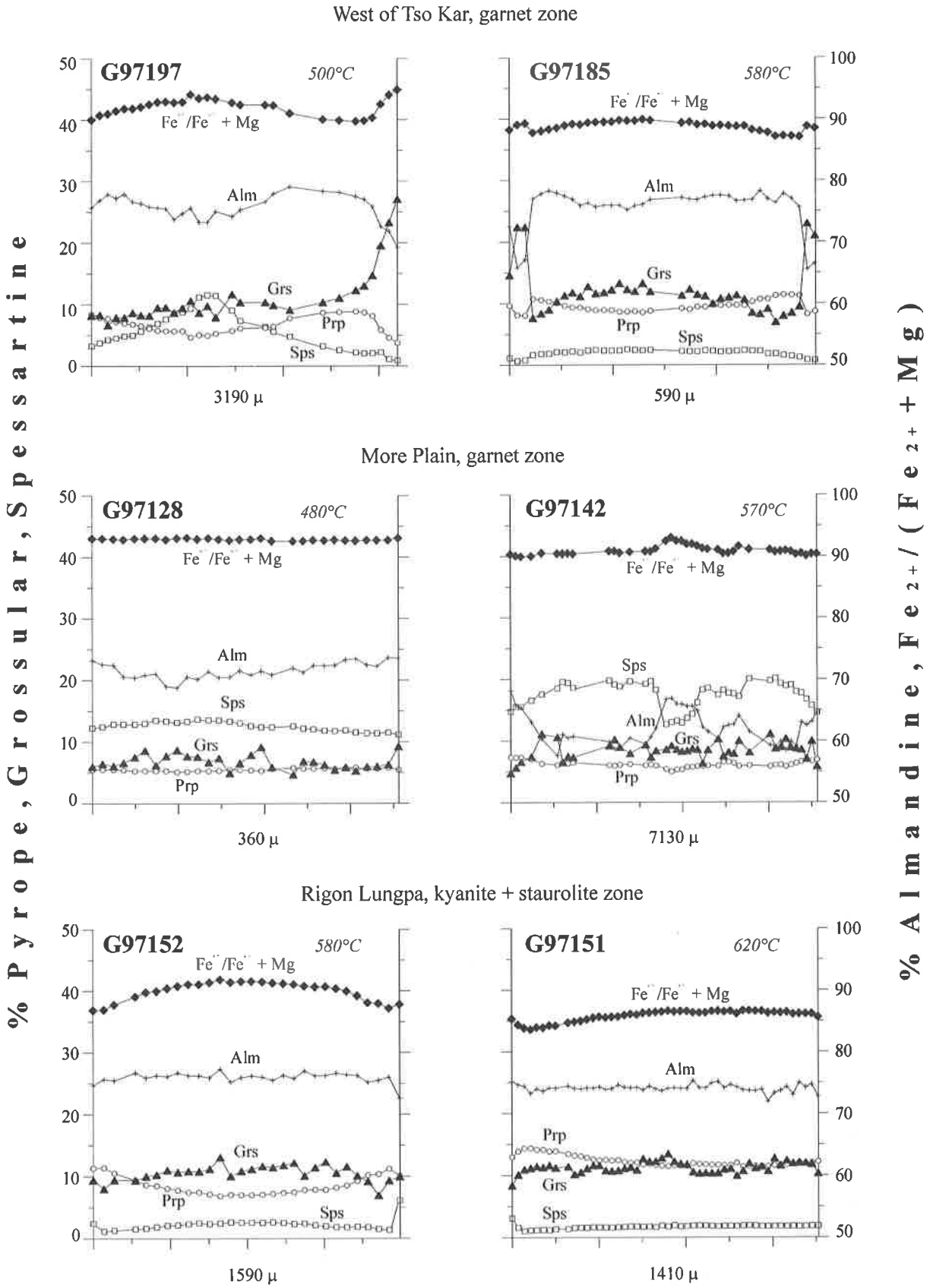

Fig. 5.6: Rim to rim compositional profiles of garnets from metapelites, from the garnet and kyanite + staurolite zones. Same remarks as in Fig. 5.5.

Results

When plotted in a petrographic grid, one can see that the temperatures calculated by *Thermocalc* are coherent with what predicted the petrographic observations (Fig. 5.7). However, two garnet bearing samples are within the biotite zone and one kyanite-bearing sample is within the garnet zone. All the staurolite + kyanite bearing samples fall in the stability field of this assemblage. Three ellipses have been drawn with a 1σ confidence interval, in order to give an idea of the uncertainties given by *Thermocalc* (a double size would represent a 2σ confidence interval). The ellipse of the staurolite bearing are much smaller than the others, because of the greater number of end members taken in account. The other uncertainties ellipses are of the same order of magnitude. But the consistency of the results suggests that these ellipses overestimate the real accuracy, and in any case, precision is much lower.

On the geological map, those results show that the higher temperatures and pressures are actually in the sillimanite zone (9.7 kbar / 670° C) and they decrease towards the garnet zone (boxes on Plate 5.1). The mean calculated field geothermal gradient, assuming a density of 2.75 kg / dm^3, is of 22 ± 3°C/km. One sample shows an inconsistently high pressure and temperature (G97 195: 11kbar / 650°C). This sample comes from the lower limit of the garnet zone, where garnet is very small. This improbable result reflects a non equilibrium between the different phases. This fact is supported by the presence of an altered oligoclase together with albite.

5.3.2/ The TWQ calculations

The TWQ 2.02 computer program developed by Rob Berman is based on a different thermodynamic data set (Berman, 1988), and does not make it possible to estimate the uncertainties on the P/T results. This program can be downloaded from the web site http://www.gis.nrcan.gc.ca/twq.html. A nominal uncertainty of ± 50°C and ± 1kbar has been attributed to all data. In contrast to the *Thermocalc* calculations, where different equilibrium are used, TWQ always uses the same independent reactions. Two reactions are used in the garnet zone:

GARB : Alm + Phl = Prp + Ann
GMAP: Ann + 3An = Grs + Alm + Ms

And one more reaction is used when kyanite is present:

GASP: Grs + 2Ky + Qtz = 3An

sample n°		mineralogy	reaction	TWQ P (kbar)	TWQ T (°C)	Thermocalc P (kbar)	Thermocalc sig. P	Thermocalc T (°C)	Thermocalc sig. T	Thermocalc corr
V96 23	Grt1	**Qtz, Phe, Bt, Grt, Pl**	GARB-GMAP	9.8	570					
V96 23	Grt3		GARB-GMAP	**8.1**	**610**	6.7	1.5	530	85	0.84
V96 25	Grt3	**Qtz, Ms, Bt, Grt, Pl, Ky**	GARB-GMAP	12.7	790					
V96 25	Grt3		GARB-GASP	14	800					
V96 25	Grt4		GARB-GMAP	**12.5**	**790**	9.7	1.7	670	90	0.84
V96 25	Grt4		GARB-GASP	**14**	**790**					
V96 29	Grt3	**Qtz, Bt, Ms, Std, Grt, Ky,**	GARB-GMAP	10.9	720					
V96 29	Grt3	Chl, **Pl**	GARB-GASP	12.1	720					
V96 29	Grt4		GARB-GMAP	**8.9**	**640**	8.3	0.9	620	20	0.15
V96 29	Grt4		GARB-GASP	**9.7**	**650**					
V96 30	Grt2	**Qtz, Bt, Ms, Pl, Grt,** Chl	GARB-GMAP	**7.1**	**560**	7.4	1.8	560	110	0.82
V96 30	Grt3		GARB-GMAP	**8.5**	**560**					
V96 34	Grt1	**Qtz, Ms, Bt,** Chl, **Pl, Grt**	GARB-GMAP	10.3	710					
V96 34	Grt2		GARB-GMAP	12.3	780					
V96 34	Grt4		GARB-GMAP	**9.3**	**690**	8.3	1.5	630	95	0.82
G97 128	Grt1	**Qtz, Ms, Bt, Chl, Pl, Grt**	GARB-GMAP	5.9	629	5.3	1.6	580	110	0.85
G97 128	Grt2		GARB-GMAP	**4.8**	**540**	4.3	1.3	480	80	0.81
G97 142	Grt1	**Qtz, Ms, Bt,** Chl, **Pl, Grt**	GARB-GMAP	**6.2**	**620**	6.0	1.5	570	100	0.85
G97 148	Grt1	**Qtz, Ms, Bt,** Chl, **Pl, Grt**	GARB-GMAP	**6**	**540**	5.7	1.3	490	75	0.80
G97 151	Grt1	**Bt, Qtz, Ms, Grt, Ky,** Pl	GARB-GMAP	**15.7**	**820**	10.4	1.7	620	90	0.83
G97 151	Grt1		GARB-GASP	**18.1**	**830**					
G97 152	Grt2	**Qtz, Bt, Phe, Grt, Pl,** Chl	GARB-GMAP	**8.9**	**670**	7.0	1.5	580	90	0.84
G97 158	Grt1	**Bt, Ms, Chl, Qtz, Ky, Grt, Pl**	GARB-GMAP	8.7	680					
G97 158	Grt2		GARB-GASP	**9.9**	**680**	8.0	1.4	620	80	0.82
G97 164	Grt1	**Qtz, Bt, Ms, Grt, Std, Ky,**	GARB-GMAP	9	650					
G97 164	Grt1	Chl, **Pl**	GARB-GASP	10	650					
G97 164	Grt2		GARB-GMAP	**8.4**	**620**	8.3	0.9	630	20	0.17
G97 164	Grt2		GARB-GASP	**8.9**	**620**					
G97 171	Grt1	**Phe, Bt,** Chl, **Grt, Std, Ky,**	GARB-GMAP	**6.5**	**610**	7.2	0.9	640	20	0.21
G97 171	Grt1	**Qtz, Pl**	GARB-GASP	**7.6**	**620**					
G97 171	Grt2		GARB-GMAP	9.5	700					
G97 185	Grt1	**Ms, Bt, Qtz, Pl, Grt,** Chl	GARB-GMAP	**7.4**	**670**	6.2	1.4	580	95	0.82
G97 195	Grt1	**Qtz, Ms, Bt, Grt,** Pl, Chl	GARB-GMAP	**15**	**730**	10.9	1.9	650	100	0.87
G97 197	Grt1	**Qtz, Ms, Bt, Grt, Pl**	GARB-GMAP	**8**	**600**	6.5	1.4	500	80	0.85
G98 21	Grt1	**Qtz, Bt, Ms, Grt, Std, Pl,**	GARB-GMAP	**7.4**	**660**	7.2	0.8	630	20	0.21
G98 21	Grt1	Chl, **Ky**	GARB-GASP	**8.2**	**660**					

Tab. 5.2: P-T results. Some samples have been analysed twice (e.g. V9623 Grt1 and 3). Mineral abbreviations in bold are stable, other are retrograde minerals. Reactions used by TWQ are indicated. Preferred P-T values are in bold. Sigma P and T are for 1σ confidence level. A nominal uncertainty of ± 50°C and ±1 kbar is assumed for the TWQ calculations. Corr = P-T correlation calculated by *Thermocalc*.

Depending on which geobarometer is used (GMAP or GASP) two different results are obtained. The P/T results showed on Plate 5.1 are the mean values. The choice of the geobarometer can have a large influence on the pressure (up to 2.4 kbar) but has almost no influence on the temperature. The analyses used for the calculations are the same than those used with *Thermocalc* (see above for selection criteria).

Compared to the *Thermocalc* results, TWQ always gives slightly higher temperatures and pressures (Fig. 5.8). Two samples out of the three that contain kyanite without staurolite, give unrealistic too high values for both temperatures and pressures (Fig. 5.7). When reported on the map, one see that once more, sample G97 195 gives much too high values for a sample from the garnet zone, reflecting its disequilibrium. Sample G97 151, situated at the beginning of the kyanite + staurolite zone also shows too high P/T values (17kbar / 825°C). In both of them, the plagioclases have the lowest anorthite content from all samples (<20% An). As also suggested by the petrographic observations, this plagioclase might be partly retrogressed and not in equilibrium with the other minerals. The fact that plagioclase is involved only in one reaction over the five used by *Thermocalc*, might explain the consistent result obtain with *Thermocalc* and not with TWQ (which use only three reactions, two being plagioclase dependents) on sample G97 151. Although sample V96 25 has probably recorded the highest temperature, the 790°C given by TWQ are overestimated for a sample from the lower limit of the sillimanite zone.

Despite these three problematic samples, the results obtained with TWQ are also consistent with the different metamorphic grades observed on the field, although the absolute temperatures are slightly higher than those obtained by *Thermocalc*. The field geothermal gradient calculated with TWQ is of 23 ± 3°C/km, almost like the one calculated with *Thermocalc* (see above).

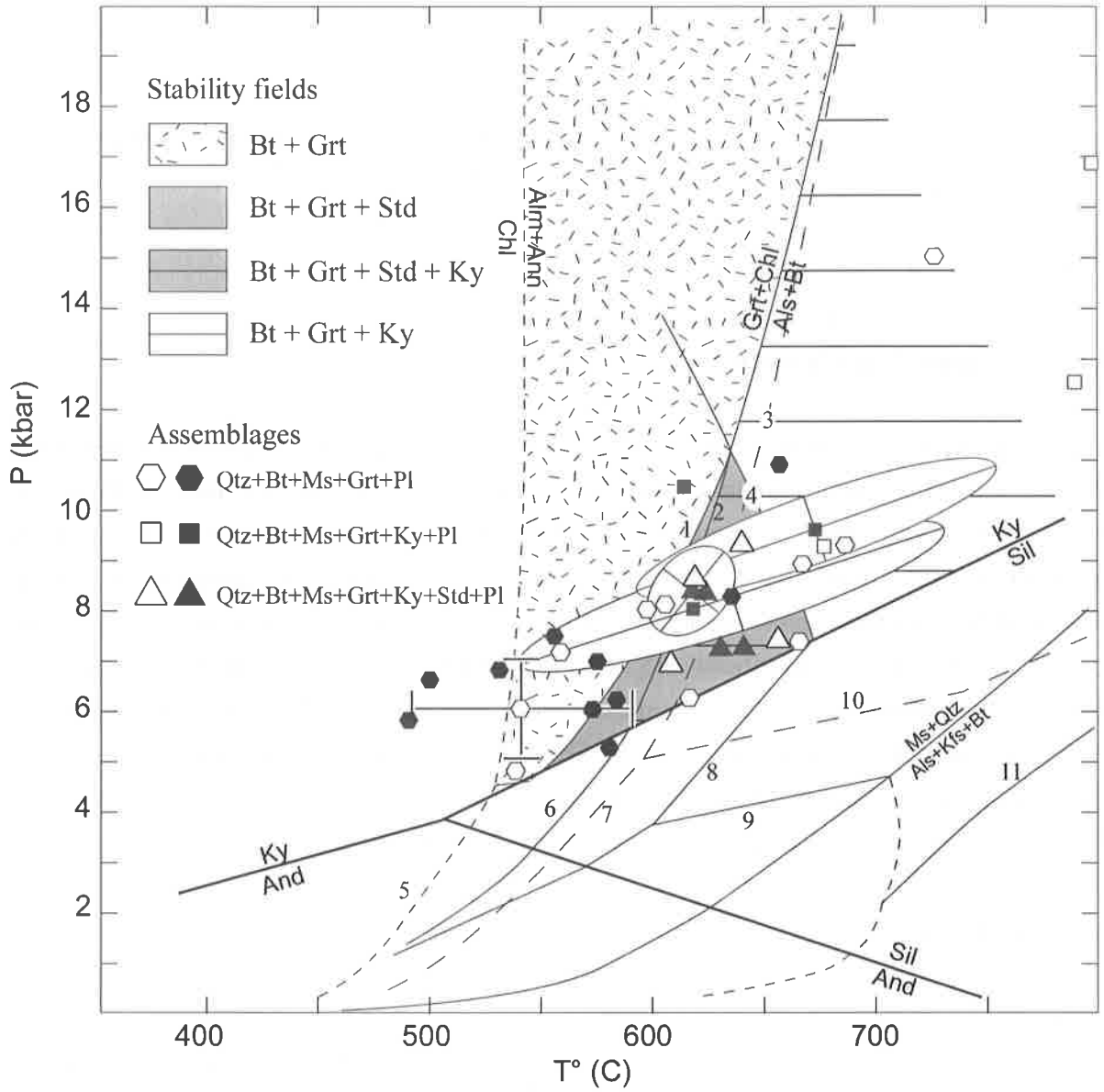

Fig. 5.7: Projections of the P/T results obtained with *Thermocalc* (solid symbols) and *TWQ* (empty symbols) in the petrogenetic grid of Holland and Powell (1998) for the KFMASH system. As biotite is present in excess in all samples, only the biotite involved reactions have been drawn. Three 1 σ uncertainties ellipses have been drawn for the *Thermocalc* results, the other samples have similar uncertainties (see text). A nominal uncertainty of ± 50°C and ± 1 kbar has been attributed for the TWQ results (drawn only for one sample for clarity). Reactions: 1: Grt+Chl = Std+Bt. 2: Std+Chl = Als+Bt. 3: Chl = Als+Bt. 4: Std+Bt = Grt+Als. 5: FeChl = Ann+Cld. 6: Chl+Als = MgCld. 7: Chl = Crd +Bt. 8: Std = Alm+Als. 9: Alm = Ann+Als. 10: Als+Bt =MgCrd 11: Als+Bt = Grt+Crd.

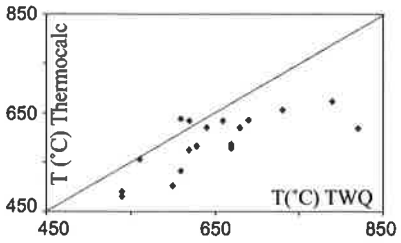

Fig. 5.8: Temperature correlation between *Thermocalc* and *TWQ*.

5.3.3 / The isotopic geothermometers

The isotopic geothermometers are based on the temperature-dependent equilibrium between the isotopic composition of oxygen in two phases. In this case the pairs of phases are quartz - garnet and quartz - kyanite. Those two different geothermometers are independent and both of them should give the same peak temperature, provided the minerals are coeval. The advantages of these geothermometers are that first they are not pressure dependent, and second the isotopic compositions are less susceptible to be reset during retrogressive metamorphism than the chemical compositions. A discussion of the retrograde diffusional exchange that could exist is discussed in Sharp (1995). Due to slow diffusion rates, this phenomenon should not affect the calculated temperatures of more than 40°C (Sharp, 1995). The relation between the isotopic compositions and the temperature is:

$$1000\ \mathrm{Ln}\alpha_{qtz\text{-}grt} = a\ 10^6 / T^2 + b \cong \Delta^{18}O_{Qtz} - \Delta^{18}O_{Grt}$$

where $\alpha_{qtz\text{-}grt} = (1000+\Delta^{18}O_{Qtz}) / (1000+\Delta^{18}O_{Grt})$ and $\Delta^{18}O = {}^{18}O/{}^{16}O_{(sample\ -\ standard)} / {}^{18}O/{}^{16}O_{(standard)}$, and where **a = 3.1 ± 0.2** for Qtz -Grt, and **a = 2.25 ± 0.2** for Qtz – Ky, b = 0 for both of the equilibrium (Sharp, 1995).

Analytical conditions

24 metapelites from the Tso Morari and Mata nappes have been analyzed. All of them except one, contain quartz and garnet and seven contain kyanite. The minerals were selected by hand picking on crushed samples. They have been then washed for several minutes in a bath submitted to micro-sounds. Kyanite and garnet have been treated with HF at room temperature to clean them from small impurities. Quartz has been also treated by HF, but only for one minute. This treatment permits us to distinguish quartz from feldspar, which becomes white.

The selected minerals pairs were then analyzed by the laser fluorination technique of Sharp (1990) at the University of New Mexico (UNM) in Albuquerque, USA. The technique consists of heating with a CO2 laser a very small amount of mineral (1-2 mg, corresponding

here to 3-10 grains) in a fluorine rich atmosphere (obtained here by the injection of BrF5). Oxygen is directly transferred and analyzed in a mass spectrometer. There is no more need to transform the O_2 in CO_2, as described in Sharp (1990). Several internal standards, with a determined value of $\Delta^{18}O$ (SMOW) = 18.1 ‰ (Lausanne 1), are analyzed in the same line than the samples to enable a correction in case of a general drift. Most of the time all minerals from the same sample are analyzed on the same line, and most analyses have been repeated at least twice. For some samples, it has not been possible to double the analysis because of the small amount of mineral. A standard deviation smaller than 0.1 ‰ is usually obtained, but it is greater than 0.2 ‰ for two analyses (Tab. 5.3). However it has to be noted that the absolute value is not important as the temperature is only dependent of the difference between the $\Delta^{18}O$ values. In other words only the precision, i.e. the reproducibility, must be good, but the accuracy can be poor. The mean precision, that take in account only the standard deviation of the analyses, is usually of about 25°C (but can reaches up to 90°C when reproducibility is poor). While the mean accuracy, that also takes in account the uncertainty on the equilibrium fractionation factor *a* (± 0.2), is of about 65°C and can reaches 130°C.

Results

The mean $\Delta^{18}O_{Qtz}$ (SMOW) of all samples is 13.1 ± 1.1 ‰, while $\Delta^{18}O_{grt}$ (SMOW) is 8.8 ± 1.0 ‰ and $\Delta^{18}O_{Ky}$ (SMOW) is 10.9 ± 0.9 ‰. All the values are presented on table 5.3. The temperatures obtained using the equations of Sharp (1995) for the equilibrium between quartz and garnet vary between 520 and 740°C, and those for the quartz - kyanite equilibrium between 500 and 790°C. But both of these last extremes are poorly constrained as the 500°C is based on a single analysis of kyanite and the 790°C has a precision of ± 90°C due to the poor reproducibility of the kyanite analyses. The temperatures obtained with Qtz - Ky are usually slightly higher than those obtained with Qtz - Grt. This could be explained by three ways. Either Qtz, Ky and Grt are not in isotopic equilibrium, or Ky and Grt did not crystallize at the same temperature, or one of the calibrations is incorrect. An isotopic disequilibrium due to a selective diffusion of the $\Delta^{18}O$ of garnet or kyanite is few probable as those minerals have a very slow diffusion rate. Moreover as there is no criteria which indicate that kyanite grows at higher temperature than garnet, the apparent disequilibrium comes probably from an inaccurate calibration of the Qtz - Grt geothermometer, which gives slightly underestimated temperatures in the sillimanite zone. On metapelites of the High Himalayan Crystalline Zone of the Sutlej valley, Vannay et al. (1999), using the same calibrations, also observe that the temperatures obtained by Qtz - Ky are higher than those obtained with Qtz - Grt.

	delta 18 O smow			Std deviation			T (°C)		Precis. 2σ		Accur. 2σ	
				nom. Std dev. = 0.10			fract fact a				a ± 0.2	
							3.10	2.25				
Sample	Qtz	Grt	Ky	Qtz	Grt	Ky	Q-G	Q-K	Q-G	Q-K	Q-G	Q-K
V962	12.91 12.64 12.83	8.41										
average	12.79	8.41		0.11	0.10		573		30		62	
V9616	11.66 11.65	7.47										
average	11.65	7.47		0.00	0.10		592		21		60	
V9617	12.78 12.76	8.49										
average	12.77	8.49		0.01	0.10		582		20		59	
V9623	14.15 14.04	9.71										
average	14.09	9.71		0.06	0.10		573		23		59	
V9625	13.71	9.26 9.44	11.16									
average	13.71	9.35	11.16	0.10	0.09	0.10	575	672	26	53	61	99
V9628	12.89 12.81	8.20	10.13 10.08									
average	12.85	8.20	10.11	0.04	0.10	0.10	548	638	19	36	56	89
V9629	12.37 12.32	7.48 7.76										
average	12.35	7.62		0.02	0.14		541		25		58	
V9630	12.00 11.80	7.85 7.87										
average	11.90	7.86		0.10	0.01		607		22		61	
V9632	12.93 12.82	8.21 8.31										
average	12.87	8.26		0.05	0.05		551		13		55	
G97128	14.57 14.75	10.14										
average	14.66	10.14		0.09	0.10		560		25		59	
G97141	14.20 13.63	9.15 9.15										
average	13.92	9.15		0.29	0.00		538		49		72	
G97148	11.73 11.55	7.57 7.55										
average	11.64	7.56		0.09	0.01		603		19		60	
G97151	13.92 14.34	10.21 10.00										
average	14.13	10.10		0.21	0.10		610		53		78	
G97154	11.48 11.37		8.59 8.58									
average	11.42		8.58	0.06	0.10	0.10		622		37		88
G97158	13.76 13.40	9.26 9.59 9.58	10.65 10.73									
average	13.58	9.48	10.69	0.18	0.15	0.10	601	615	51	64	76	101
G97159	14.30 14.22	9.60	10.47									
average	14.26	9.60	10.47	0.04	0.10	0.10	547	503	19	22	56	72
G97161	12.57 12.52	8.57 8.57	10.69 10.34									
average	12.54	8.57	10.51	0.03	0.00	0.17	615	785	6	93	58	132
G97164	11.68 11.66	7.18 7.56 7.34	9.09									
average	11.67	7.36	9.09	0.01	0.16	0.10	580	665	31	37	63	91
G97165	11.97 12.20	7.57 7.59										
average	12.09	7.57		0.12	0.01		560		22		58	
G97169	14.60 14.63	9.75 9.93										
average	14.61	9.84		0.02	0.09		538		16		55	
G97171	13.43 13.49	8.57 8.35										
average	13.46	8.46		0.03	0.11		519		18		54	
G97185	12.77 12.66	9.67 9.63										
average	12.71	9.65		0.06	0.02		738		20		68	
G97187	15.12 15.30	11.20 11.17										
average	15.21	11.18		0.09	0.01		611		20		60	
G97195	12.89 12.71	8.94 9.02										
average	12.80	8.98		0.09	0.04		633		23		63	

Tab. 5.3: Results of the Δ18O (‰) versus Standard Mean Ocean Water (SMOW) for quartz, garnet and kyanite in metapelites. Obviously wrong analyses have not been reported. Temperatures have been obtained with the quartz-garnet (Q-G) and quartz-kyanite (Q-K) calibrations proposed by Sharp (1995). The precision only takes in account the standard deviation of the analyses, while accuracy also includes the imprecision on the fractionation factor "a". A nominal standard deviation (nom. Std dev.) of 0.10‰ have been attributed to samples analysed only once.

When represented on the geological map (Plate 5.2), the temperatures obtained with the isotopic geothermometers show a coherent metamorphic gradient with temperatures of about 550°C in the garnet zone and going up to 670°C in the sillimanite zone. As already observed with the conventionnal thermobarometry (see above), the sample G97 195 once more gives an unrealistic too high temperature, reflecting its disequilibrium. Sample G97 185, collected near the basal thrust of the Mata nappe, also gives a too high temperature. But its very low ratio $\Delta^{18}O_{Qtz}$ / $\Delta^{18}O_{Grt}$ suggests that the $\Delta^{18}O_{Qtz}$ has been lowered by an isotopically light fluid. A similar fluid alteration is well documented at the base of the Diableret nappe, in the Swiss Alps (Crespo-Blanc et al., 1995). Sample G97 159, from the kyanite + staurolite zone, gives temperatures of 550° and 500°C for Qtz -Grt and Qtz - Ky respectively. These temperatures are obviously too low. But this might come from imprecise analyses, as both of Grt and Ky have only been analyzed once.

Compared to the results obtained with thermobarometry using TWQ and *Thermocalc*, one can see that the temperatures obtained by Qtz - Grt isotopic equilibrium are situated in-between those given by *Thermocalc* and those given by TWQ (Fig. 5.9). As only two samples (V96 25 and G97 158) have been analyzed with both of Qtz - Ky and classical thermobarometry, it is difficult to compare the results. But for both of these samples, the temperatures obtained with *Thermocalc* (670 and 620°C, Plate 5.1) are almost identical to those obtained with Qtz - Ky (670 and 610°C, Plate 5.2). This is not the case when TWQ is compared to Qtz - Ky.

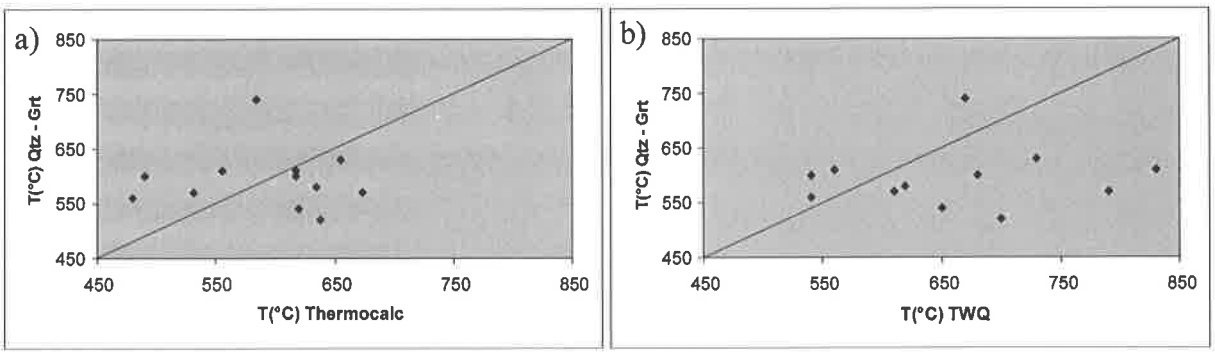

Fig. 5.9: Correlation between the temperatures obtained with the Qtz-Grt isotopic thermometer and with Thermocalc (a) and TWQ (b).

5.3.4/ The Ti content of amphibole

This very easy-to-use thermometer has been empirically calibrated in the metabasics of the Alps by Colombi (1989). It is based on the Ti content of amphibole, a value that is linked to the temperatures by the following empirical equations:

For $Ti_{(norm.)} < 0.08$; $T(°C) = 2816\ Ti + 445$
For $Ti_{(norm.)} > 0.08$; $T(°C) = 980\ Ti + 600$

The Ti contents of amphiboles from metabasites have been analyzed at the University of Lausanne with a Cameca SX50 electron microprobe, with an acceleration voltage of 15kV and a beam current of 15 nA. Ten temperatures ranging between 470 and 600°C, have been obtained with this method (Plate 5.3). These temperatures are coherent as both of the highest ones (570 and 600°C) have been obtained in amphibolites from the garnet zone. No analyses have been made in the higher grade zones. Along the Sumkhel Lungpa and in the More Plain, four samples with coexisting hornblende and albite give similar temperatures around 500°C.

Although these results seem to be coherent they have to be considered with care as the empirical constant 445, in the first equation cited above, already fixes the temperature in a plausible range, and the very low Ti content (<0.05) only slightly influence this constant.

	G9615			G9625			G9640		G96101			
	Barr.	Mg Hbl	Ab	Mg Hbl	Grt	Oli	Mg Hbl	Ab	Barr.	Mg Hbl	Act	Ab
SiO2	50.10	47.27	67.90	45.05	36.98	77.94	49.84	69.57	48.14	49.93	52.95	68.21
TiO2	0.17	0.20		0.31	0.19		0.22		0.12	0.08	0.04	
Al2O3	10.10	10.35	20.27	11.44	20.12	14.00	6.58	19.64	6.57	4.31	1.50	19.80
Cr2O3	0.08	0.06		0.00	0.07		0.03		0.06	0.00	0.03	
Fe2O3	8.27	5.61		6.14	1.83		4.22		10.49	4.80	2.26	
FeO	3.38	6.47	0.04	12.15	28.84	0.14	11.87	0.18	13.19	15.43	16.35	0.23
MnO	0.10	0.10		0.22	3.40		0.25		0.33	0.28	0.23	
MgO	14.55	14.71		9.80	0.77		12.45		8.63	10.92	11.97	
CaO	8.93	11.74	1.33	11.50	8.38	3.37	11.61	0.23	8.49	11.75	11.74	0.10
Na2O	2.52	1.86	11.11	1.06		5.04	0.87	11.92	2.33	0.72	0.42	11.66
K2O	0.19	0.19	0.04	0.42		0.05	0.23	0.04	0.40	0.21	0.12	0.05
Total	98.39	98.56	100.70	98.08	100.59	100.53	98.16	101.58	98.76	98.42	97.60	100.05

	V9615			G97122			G97146		G986			
	Act	Act	Ab	Mg Hbl	Act	Ab	Act	Ab	Tsch	Mg Hbl	Grt	Ab
SiO2	54.06	51.90	83.89	47.81	52.94	68.78	52.09	68.22	40.26	47.28	36.709	65.62
TiO2	0.09	0.33		0.22	0.10		0.16		0.10	0.12	0.135	
Al2O3	2.27	2.68	10.46	8.69	3.18	19.74	4.82	19.81	12.14	7.36	19.494	20.83
Cr2O3	0.05	0.00		0.00	0.00		0.22		0.00	0.03	0.000	
Fe2O3	1.48	4.41		6.45	3.31		0.18		7.50	19.45	3.119	
FeO	15.51	14.76	0.53	13.78	13.48	0.14	16.89	0.09	19.93	3.54	29.429	0.33
MnO	0.27	0.25		0.35	0.33		0.30		0.52	0.63	1.595	
MgO	12.71	11.82		9.33	13.03		11.16		4.09	10.78	0.669	
CaO	11.86	11.54	0.24	10.53	11.96	0.25	11.69	0.60	11.20	8.65	9.198	1.88
Na2O	0.38	0.47	6.15	1.32	0.41	11.71	0.47	11.30	1.50	0.87		10.78
K2O	0.18	0.16	0.19	0.36	0.10	0.05	0.21	0.10	0.71	0.36		0.15
Total	98.86	98.31	101.46	98.83	98.84	100.67	98.20	100.12	97.96	99.08	100.35	99.59

	AS96110		V963		
	Mg Hbl	And	Tsch.	Grt	And
SiO2	42.57	52.16	43.51	36.97	59.58
TiO2	1.97		0.47	0.12	
Al2O3	7.35	29.70	14.22	20.46	25.72
Cr2O3	0.02		0.06	0.07	
Fe2O3	5.45		4.74	1.85	
FeO	20.62	0.67	13.48	30.58	0.15
MnO	0.30		0.18	0.89	
MgO	5.99		8.38	1.24	
CaO	10.42	12.44	11.56	8.30	7.56
Na2O	1.80	4.40	1.05		7.30
K2O	1.03	0.16	0.43		0.08
Total	97.52	99.53	98.08	100.48	100.39

	G9855		
	Mg Hbl	Act	Ab
SiO2	47.74	52.55	68.404
TiO2	0.20	0.05	
Al2O3	6.28	2.55	19.640
Cr2O3	0.11	0.05	
Fe2O3	6.54	3.42	
FeO	13.96	14.85	0.242
MnO	0.30	0.36	
MgO	10.05	12.28	
CaO	11.03	11.89	0.231
Na2O	0.75	0.36	11.689
K2O	0.45	0.15	0.09
Total	97.42	98.50	100.30

Tab. 5.4: Electron microprobe results (weight % oxides) of metabasic rocks. Analytical conditions: acceleration voltage for all minerals = 15 kV, beam current: 30 nA for garnet, 15 nA for amphiboles and 10 nA for plagioclase. See Plate 5.3 for sample emplacements.

5.4/ Conclusions

Four thermobarometric methods have been applied in order to better constrained the P-T conditions of the area and to compare them. As shown by the three maps that expose these results (Plates 5.1, 5.2 and 5.3), all methods give more or less the same picture of the metamorphic gradient between the garnet and the onset of the sillimanite zone. Only the absolute values change slightly. From all methods it is difficult to say if one or the other is better, as all give good and bad results at different places. It seems that TWQ gives more coherent P/T results in the garnet zone than *Thermocalc*, but this is sometimes the opposite in the higher grade zones. The temperatures obtained by the isotopic equilibrium are probably the most representative of the reality, but those temperatures are very sensitive to the precision of the analyses. A good analysis with an excellent reproducibility is absolutely necessary. Between Qtz - Grt and Qtz - Ky isotopic thermometry, it seems that Qtz - Ky gives more realistic temperatures in regards to the metamorphic zones, and moreover they perfectly correlate with the temperatures of *Thermocalc*. This is surprising as the Qtz - Ky has been calibrated assuming a known fractionation factor for Qtz - Grt (Sharp, 1995). The temperatures obtained with the Ti content in amphibole are difficult to correlate as most samples do not come from the same place than the metapelites. However the metabasites V963 and G9625 are very close to the metapelites V962 and V9632 respectively, which have been analyzed isotopicaly. The temperature difference between the samples is smaller than 30°C, showing that despite its empirical calibration, the Ti content in amphibole gives good temperatures.

The pressures obtained with both of the methods using the thermodynamic data sets are strongly correlated to the temperatures. This is illustrated by the identical and more or less constant field geothermal gradients. The calculated geothermal gradients for each sample give cause for concluding that this gradient is more or less homogenous throughout the whole field. In Zanskar, Dèzes et al. (1999) obtain a similar field geothermal gradient of 22 ± 2 °C/km for metapelites from the garnet zone to the migmatite zone, using *Thermocalc* calculations. This field geothermal gradient, characteristic for an orogenic or Barrovian metamorphism, is clearly different than the gradient responsible for the early HP/LT metamorphism, estimated with the data of De Sigoyer et al. (1997) at 7 °C/km. The regional metamorphism increases progressively north eastward, without any metamorphic jumps between the Tethyan Himalaya and the North Himalayan Crystalline Zone, what does not allow us to clearly delimit those two domains. There is also no metamorphic jump between the Mata and the Tso Morari nappes. However while the Tso Morari nappe shows an early eclogitic stage followed by an amphibolitic stage, the Mata nappe is only characterized by a progressive Barrovian metamorphism. The subsequent greenschists facies retrogression affects both of the nappes.

It can be concluded from that discussion, that the use of several independent thermobarometers, coupled with the analysis of the phase equilibrium in thin section, is necessary to obtain a vision of the regional metamorphism as realistic as possible. An attempt of synthesis of all methods permit us to draw approximate isothermal lines that illustrate the metamorphic gradient observed in the field (Plate 5.4). This metamorphic map is well constrained in its western part, where most of the analyses presented above have been made. In the eastern part, the lines are mainly drawn after the paragenesis observed in the field, as no detailed thermobarometry have been realized. The only data come from the "illite crystallinity" measured in the very low-grade sediments, between the Spiti river and Narbu Sumdo (Girard et al., 1999), and from one P/T estimate obtained on retrogressed eclogites north of the Tso Morari, between the Kiagar Tso and Sumdo (De Sigoyer et al., 1997). These authors show that after the eclogitic stage, the sample underwent a strong decompression from 20 kbar to 9 ± 3 kbar accompanied with a small temperature increase to 610 ± 70°C.

At the map scale, it seems that the regional metamorphism creates a thermal dome, with the highest temperatures attained near Nuruchan. The location of the highest grade zones, in the southern border of the Tso Morari gneiss, shows that the thermal doming does not exactly correspond to the tectonic Tso Morari dome, as suggested by Thakur (1983). However this hypothesis is subject to cautions because large parts of the Tso Morari gneiss complex have not been investigated in detail and it is possible that new occurrence of Ky + Std or Sillimanite bearing assemblages will be described. Moreover the area of occurrence of these minerals (near Nuruchan) shows temperatures that are only 30°C higher than some temperatures obtained in the garnet zone. In other words, the thermal dome is not very important and might change its shape when more data will be available.

Combined with the data on the HP-LT metamorphism and on radiochronology of the French team (De Sigoyer et al., 1997; Guillot et al., 1997; 2000), the thermobarometric results exposed above, permit us to draw two different P-T-loops for the Tso Morari and Mata nappes (Fig. 5.10).

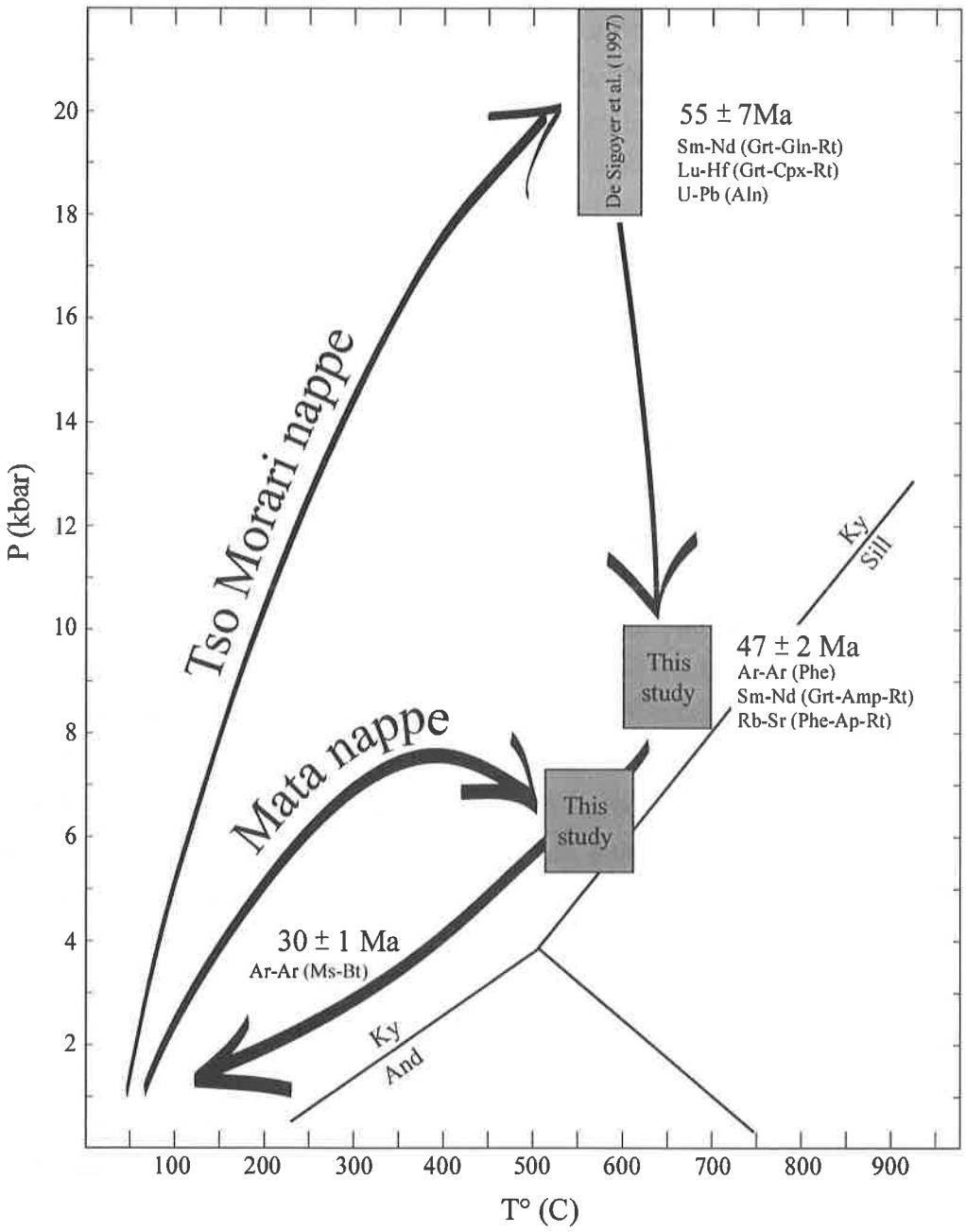

Fig.5.10: P-T paths for the Tso Morari and Mata (+Tetraogal) nappes. Radiochronological data are from De Sigoyer et al. (2000). The 31 Ma ages date the recrystallization of biotite and muscovite under greenschist facies conditions. No precise P-T conditions are available for this event.

6/ Conclusions

"Any real comprehension of the truth cannot be quick. He who understands quickly, is unable to realise that he has not yet really understood."

Albert Jacquard

During this study we attempted to better constrain the geology of the Rupshu area by undertaking large-scale fieldwork. From a sedimentary point of view, the Precambrian to Middle Triassic series of Rupshu have shown many differences with the coeval sediments of Spiti, Lahul or Zanskar. Although the lithologies of the lower Paleozoic formations are similar to those of Spiti, they are much less differentiated, so that the distinctions between those formations is often impossible. The Upper Paleozoic is characterized by important gaps. The same situation is observed in the Nyimaling area (Stutz and Steck, 1986). The Permian series ends these gaps. It shows distal facies with important lateral variations. The Karzok Formation also shows lateral variations, even so it is always characterized by the occurrence of dolomites, quartzites, siltstones and basic layers. The geochemistry of the latter are similar to that of the Permian Panjal Traps of Kashmir (Linner et al., 1997). Then the Lower Triassic is almost absent, while the Middle Triassic Kaga and Chomule Formations are well represented. From the Lower Triassic up to the Chomule Fm., the sedimentation conditions seem to vary progressively from a carbonaceous and detritic environment to a purely carbonaceous environment, so that the formations' limits are not always well defined. The Upper Triassic to Cretaceous sediments exist only in the southwestern area, where the metamorphism is of very low grade. These series are similar to those of Spiti or Zanskar, but the Quartzite Series are much more carbonaceous and less siliceous. Once more, this confirms the more distal environment of the Rupshu sediments.

This reconstructed stratigraphy has been perturbed by an intense deformation that can be subdivided into 7 phases. The tectonic observations made on this field confirm the existence of a nappe tectonic in the NW Himalaya. An equivalent of the early NE-vergent Shikar Beh nappe proposed in several papers of the Lausanne team (Steck et al., 1993; Vannay and Steck, 1995; Dèzes, 1999; Steck et al., 1999; Wyss et al., 1999) only affects a small part of the studied field, in Spiti. This means that this phase does not propagate very far to the NE. On the other hand, the three subsequent SW-vergent phases create a strong deformation and an important Barrovian metamorphism. Three different nappes, The Tso Morari, Tetraogal and Mata nappes, result from these phases. The Tso Morari nappe is the lowermost one. It is characterized by ductile deformation with top-to-the-SW shear, linked to the subduction of the Indian plate below Asia, and with subsequent top-to-the-NE shear, linked to its exhumation. The overlying Tetraogal nappe has been discovered in Karzok, where a basic and ultrabasic complex is interpreted as a slice within the thrust between the Tetraogal and Mata nappes. The Mata nappe shows a gradual change in the deformation style from ductile in the internal parts, to brittle in the external part. Isoclinal folds and two penetrative schistosities characterize the ductile deformation, and an imbricate structure with several thrusts results from the brittle deformation. These characteristics, and its situation in the lateral continuation of the Nyimaling Tsarap nappe, show that the Mata nappe is an equivalent of the latter. However the fronts of these two nappes are not aligned along the

strike. After the nappe emplacement, the Rupshu area recorded an extensional phase, that we correlated with the formation of the South Tibetan Detachment System, found all along the Himalayan belt. In Rupshu this extension does not affect the transition between the Tethyan Himalaya and the High Himalayan Crystalline Zone, as it is usually the case, but is situated within the very low grade metasediments. The extension generates brittle normal faults which lower diagenetic sediments in-between two anchizonal to epizonal zones. Only the "illite crystallinity" method has been able to semi-quantify this very low grade metamorphism, and to reveal the importance of the extensional faults observed during fieldwork. An important phase of backfolding with NE-vergent open folds developed before or during extension. The last deformational phase creates a dome-and-basin structure and is responsible for several N-S striking normal faults.

The transition between the non- to very low grade metasediments of the Tethyan Himalaya and the North Himalayan Crystalline Zone is gradual and associated with an increase of the metamorphic grade. The North Himalayan Crystalline Zone, as well as the High Himalayan Crystalline Zone, are only metamorphic equivalent of the base of the Tethyan Himalaya sedimentary series. In 1964, Gansser already pointed out this problem when he described the geology of the Kumaon Himalaya. He said that if in the south the limit of the Higher Himalayas (in the topographical meaning) seems clear, things become more complicated towards the north where the limit is less clear, both topographically and geologically. "*The geological limit is arbitrarily placed where the fossiliferous sediments of the northern slopes begin their independent tectonics, which roughly coincides with the Middle Palaeozoic outcrops*" (Gansser, 1964, p.104).

The regional Barrovian type metamorphism, linked to the nappe emplacement, follows the High Pressure - Low Temperature phase. While the regional metamorphism affects every nappes, the HP - LT metamorphism only affects the Tso Morari nappe. This important metamorphic difference permits us to distinguish the Tso Morari nappe from the overlying ones. Different thermobarometric methods have been used to estimate the P-T conditions of the regional metamorphism. The strongest metamorphic gradient can be observed between the Tsarap River in the SW, where the very low grade limestones show anchizonal conditions, up to the area of Nuruchan in the NE, where the metapelites are metamorphosed at the onset of the sillimanite zone. From the nappes' front, metamorphic grade increases progressively towards the structurally deepest zones. Under the last epizonal limestones, there is a thin chlorite zone, which ends up with the first appearance of biotite. Then small garnets appear in metapelites. Garnet grain size increases as we reach deeper zones. Temperatures of about 500-550°C and pressures of about 5-6 kbar are obtained for this zone. The contact between the Tetraogal and Tso Morari nappes is within the garnet zone, with no particular metamorphic break. This shows that the regional metamorphism is coeval with the nappe emplacement and that there is no older transported metamorphism. Below the garnet zone, staurolite and kyanite

appear simultaneously. Temperature and pressure conditions obtained for the kyanite + staurolite zone are 600-650°C / 7.5-9 kbar. A small zone contains metapelites with the particular assemblage kyanite + sillimanite. As none aluminium silicate shows instability features, it seems that both of them are stable, and only the onset of the sillimanite zone is attained. The different thermobarometers indicate temperature of 650-670° and pressure of 9.5 kbar for this zone. The field geothermal gradient is estimated at 22 ± 3 °C/km for every nappes, in line with an orogenic (or Barrovian) metamorphism. The metamorphic isograds cut the nappes and formations boundaries obliquely. As the temperatures seem to decrease in all directions from the hottest zone near Nuruchan, the regional metamorphism creates a thermal dome, centered on the southwestern flank of the Tso Morari dome. However, new observations of kyanite + staurolite or sillimanite-bearing metapelites within the Tso Morari gneiss would modify this image.

A Pre-Tertiary tectono-metamorphic phase is not documented in the Rupshu area. However the Ordovician Tso Morari and Rupshu granites (479 ± 2 Ma and 482.5 ± 1 U/Pb on zircon, respectively) seem to set up in a post-orogenic tectonic setting. The coexistence of S-type peraluminous granite (the Tso Morari gneiss) and of metaluminous alkali-calcic intrusion (the Rupshu granite) reminds the extensional regime found at the end of the Variscan orogeny, in Western Europe. As the timing of this magmatism corresponds to the end of the Pan-African event, the Ordovician granites constitute important reminders of the occurrence of a Pre-Himalayan event. At a local scale, the laboratory work realized on samples from the Polokongka La granite and from the Tso Morari gneiss, has confirmed the field observations, which indicated that the former is the undeformed protolith of the latter. The term "Polokongka La granite" used in the literature should be abandoned. On the other hand, zircons from the Rupshu granite show a very different typology from those of the peraluminous Nyimaling granite. Even though the Rupshu granite is in the southeastern continuation of the Nyimaling granite, it seems that each granite derives from a different source.

With all these data summarized above, with the radiochronological data and the P-T estimates for the eclogitic metamorphism of de Sigoyer et al. (1997; 2000), we can propose a tectonic model (Fig. 6.1), which is a modification of the model already proposed by Steck et al. (1998):

The subduction of Neotethyan ocean stopped shortly before 55 Ma. Sm-Nd, U-Pb and Lu-Hf radiometric ages of de Sigoyer et al. (2000) indicate that the subduction of the continental Indian plate generates the eclogitic metamorphism at 55 Ma. The P-T conditions of this metamorphism in the Tso Morari slab implies a burial depth of at least 70 km (De Sigoyer et al., 1997; Guillot et al., 1997). The subduction of the continental crust marks the end of the subduction mechanism and the blocking of the system. Above

the surface of underthrusting, the upper part of the Indian crust is sheared off and accreted, generating the Mata and Tetraogal nappes. More or less at that time, in the internal parts of the Indian margin, the compressive stress generates the NE-vergent Shikar Beh nappe. The thrust plane of this nappe may be created by the reactivation of preexisting extensional faults.

At 47 Ma, the light, mainly quartzo-feldspathic, Tso Morari nappe has been exhumed along the surface of underthrusting, up to a depth of 25 km. The medium pressure - high temperature retrograde metamorphism is of this phase. Above the Tso Morari nappe, the Mata (and Tetraogal) nappes end their emplacement. The Mata nappe front folds the older structures of the Shikar Beh nappe. The overburden of the Mata nappe was greater than 20 km, as indicated by the pressure of 7 kbar (Fig. 5.10). The metamorphism peak of the Mata nappe may have occurred between 55 and 47 Ma.

After 47 Ma, the Tso Morari, Tetraogal and Mata nappes follow the same tectonic evolution. Their exhumation is directed towards the SW, between the thrust surface at the base of the nappe stack and the Ribil fault. Ar-Ar ages on muscovite and biotite indicate a recrystallization under greenschist facies conditions 30 Ma ago (De Sigoyer et al., 2000).

Some 20 Ma ago, the extrusion of the entire crystalline nappe stack generates the initiation of the Main Central Thrust (situated about 200 km south of the Rupshu area). In the central parts of Himalaya, extensional structures develop, as the South Tibetan Detachment System. In the Rupshu area this extension is represented by the normal fault zones situated in the frontal parts of the Mata nappe (i.e. the Dutung - Thaktote and Sarchu - Lachung La normal Fault Zones).

At present time, thrust activity has been transferred towards south, in the Himalayan Frontal Thrust. In more internal parts of the belt, large scale dome and basin structure are generated. N-S striking active normal faults, like those found in the area of the Tso Morari, testify for a transpressional tectonic nearby the Indus Suture Zone.

Guillot et al. (1999) have proposed a diapiric model for the exhumation of the Tso Morari eclogites. For them the Tso Morari unit is extruding vertically, like a salt dome. We refute this model for several reasons. Firstly, it does not explain the existence of the Karzok ultrabasics, which can only come from the Indus Suture Zone in the NE, and thus imply important horizontal translations. Secondly, this model does not take in account the structures and the shear sense criteria observed, which indicate an important component of simple shear with top to the SW sense of movement. And thirdly the diapir model implies the occurrence of a normal fault on both side of the Tso Morari dome. If a late normal fault effectively exists in the northeast (the Ribil fault), none exists on its southwestern side.

On the other hand, the model presented in fig. 6.1 fits better with the observed structures. A SW-verging nappe tectonic is strongly supported by the structural observations and by the important overburden responsible for the orogenic metamorphism observed in the Tso Morari, Tetraogal and Mata nappes. This model is a modification of the one presented by Steck et al (1998). The timing of the previous model has been better constrained by new data of de Sigoyer et al. (2000). And the burial depth during the peak of regional metamorphism has been constrained by our new thermobarometric data. Otherwise the mechanisms of exhumation and nappe emplacement are similar.

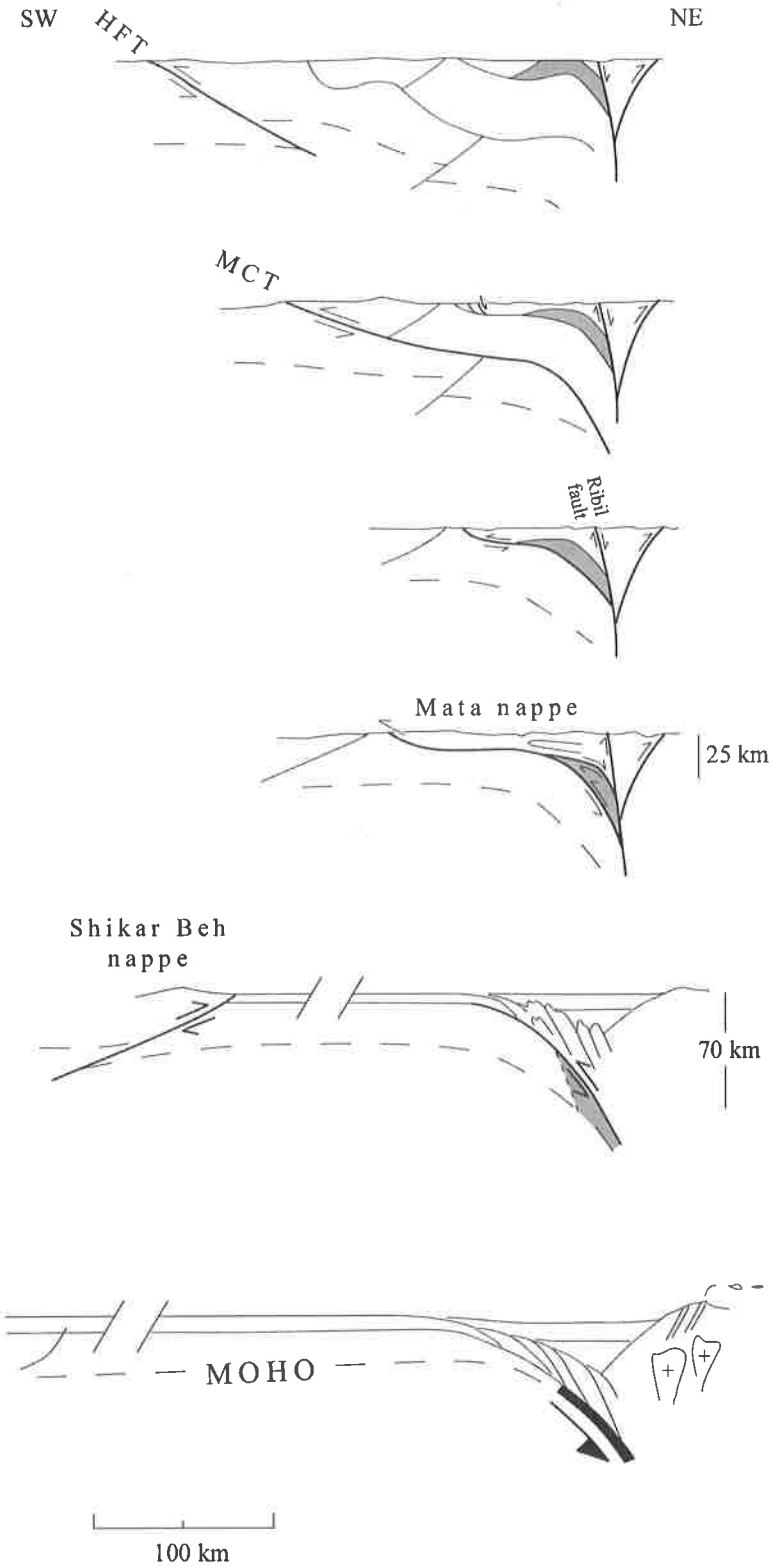

Present
Thrusting along the Himalayan Frontal Thrust (HFT).
Dome and bassin folding and dextral transpression.

20 Ma
Extrusion of the crystalline nappes along the Main Central Thrust (MCT).
Extension in front of the Mata nappe.

30 Ma
Exrusion of Tso Morari + Mata nappes.
Greenschist facies retrogressive metamorphism.

47 Ma
Extrusion of the Tso Morari nappe.
End of Mata nappe emplacement.
Amphibolite facies conditions in the Tso Morari and Mata nappes.

55 Ma
HP-LT eclogite facies condition in the Tso Morari slab.
Shikar Beh nappe emplacement.
Beginning of Mata nappe emplacement.

> 55 Ma
End of oceanic subduction
End of Ladakh magmatism

Fig. 6.1: Tectonic model for the evolution of the Rupshu area. Active structures are in bold. The Tso Morari nappe is represented in grey. Radiometric ages (de Sigoyer et al., 2000; Hubbard and Harrison, 1989). Burial depth for the Tso Morari eclogites (de Sigoyer et al., 1997).

Bibliography

Andrew, J. M., W. B. Douglas, and A. B. Richard, (1995): *Middle-Late Miocene (>10 Ma) formation of the Main Boundary thrust in western Himalaya*: Geology, v. 23, p. 423-426.

Argles, T., C. I. Prince, G. L. Foster, and D. Vance, (1999): *New garnets for old? Cautionary tales from young mountain belts*: Earth Planetary Sc. Letters, v. 172, p. 301-309.

Arkell, W. J., (1956): *The ranges of southeast Asia-Spiti and Niti*, Jurassic geology of the world, Edinburgh, Oliver & Boyd, p. 406-409.

Auden, J. B., (1937): *Traverses in the Himalaya*: Rec. Geol. Survey India, v. 69, p. 123-167.

Bassoullet, J. P., M. Colchen, T. Juteau, J. Marcoux, and G. Mascle, (1980): *L'édifice de nappes du Zanskar (Ladakh, Himalaya)*: C.R. Acad. Sc. Paris, v. 290, p. 389-392.

Baud, A., M. Gaetani, E. Garzanti, E. E. Fois, A. Nicora, and A. Tintori, (1984): *Geological observation in southeastern Zansakar and adjacent Lahul area (Northwestern Himalaya)*: Eclogae Geol. Helv., v. 77, p. 171-197.

Berman, R., (1988): *Internally consistant thermodynamic data for minerals in the system Na2O-K2O-CaO-MgO-FeO-Fe2O3-Al2O3-SiO2-TiO2-H2O-CO2*: J. Petrology, v. 29, p. 445-522.

Berthelsen, A., (1953): *On the Geology of the Rupshu District, NW Himalaya*: Bulletin of the Geological Society of Denmark, v. 12, p. 350-414.

Berthelson, A., (1951): *Geological Section through the Himalaya.*: Medd. fra Dansk Geol. Forening. Kobenhavn.

Besse, J., and V. Courtillot, (1988): *Paleogeographic maps of the continents bordering the Indian Ocean since the Early Jurassic.*, *in* S. Banerjee, and K. Hoffman, eds., Special section; tribute to Allan Cox: Journal of Geophysical Research, B, Solid Earth and Planets, v. 93, p. 11,791-11,808.

Bhargava, O. N., (1987): *Stratigraphy, microfacies and paleoenvironment of the Lilang group (Scythian-Dogger), Spiti valley, Himachal Himalaya, India*: Journal Paleont. Soc. India, v. 32, p. 92-107.

Bonin, B., A. Azzouni-Sekkal, F. Bussy, and S. Ferrag, (1998): *Alkali-calcic to alkaline post-collision granite magmatism: petrologic constraints and geodynamic settings*: Lithos, v. 45, p. 45-70.

Brookfield, M. E., (1993): *The Himalayan passive margin from Precambrian to Cretaceous times*: Sedimentary Geology, v. 84, p. 1-35.

Burchfiel, B. C., Z. Chen, K. V. Hodges, Y. Liu, L. H. Royden, and C. Deng, (1992): *The South Tibetan Detachment System, Himalayan orogen: extension contemporaneous*

with and parallel to shortening in a collisional mountain belt: Geol. Soc. America Spec. Paper, v. 269, p. 41.

Burchfiel, B. C., Q. Deng, P. Molnar, L. Royden, Y. Wang, P. Zhang, and W. Zhang, (1989): *Intracrustal detachment within zones of continental deformation*: Geology (Boulder), v. 17, p. 748-752.

Burrard, and H. H. Hayden, (1908): *A sketch of the geography and geology of the Himalaya*: Delhi.

Bussy, F., and P. Cadoppi, (1996): *U-Pb zircon dating of granitoids from the Dora-Maira massif (western Italian Alps)*: Schweiz. Mineral. Petrogr. Mitt., v. 76.

Catlos, E., T. Harrison, M. Searl, and M. Hubbard, (1999): *Evidence for Late Miocene reactivation of the Main Central Thrust: From Garwhal to the Nepali Himalaya*: 14th HKT workshop, Terra Nostra, v. 99, p. 20.

Coleman, M. E., (1996): *Orogen-parallel and orogen-perpendicular extension in the Central Nepalese Himalayas*: Geological Society of America Bulletin, v. 108, p. 1594-1607.

Colombi, A., (1989): *Métamorphisme et géochimie des roches mafiques des Alpes ouest-centrales (géoprofil Viège-Domodossola-Locarno)*: PhD thesis, Université de Lausanne, Lausanne, 216 p.

Crespo-Blanc, A., H. Masson, Z. Sharp, M. Cosca, and J. Hunziker, (1995): *A stable and Ar/Ar isotope study of a major thrust in the Helvetic nappes (Swiss Alps): Evidence for fluid flow and constraints on nappe kinematics*: GSA Bull., v. 107, p. 1129-1144.

Dalziel, I. W. D., (1991): *Pacific margins of Laurentia and East Antarctica-Australia as a conjugate rift pair; evidence and implications for an Eocambrian supercontinent*: Geology (Boulder), v. 19, p. 598-601.

De Sigoyer, J., (1995): *Evolution tectonometamorphique des roches de Haute Pression du Dôme du Tso Morari: conséquences sur l'évolution géodynamique de la marge continentale N-indienne au cours de l'orogenèse himalayenne*: DEA thesis, Université Claude Bernard, Lyon, 41 p.

De Sigoyer, J., (1998): *Mécanismes d'exhumation des roches de haute pression basse température en contexte de convergence continentale (Tso Morari, NO Himalaya)*: PhD thesis, Lyon, 236 p.

De Sigoyer, J., V. Chavagnac, J. Blichert-Toft, I. Villa, B. Luais, S. Guillot, M. Cosca, and G. Mascles, (2000): *Dating the Indian continental subduction and collisional thickening in the northwest Himalaya: Multichronology of the Tso Morari eclogites*: Geology, v. 28, p. 487-490.

De Sigoyer, J., S. Guillot, J. M. Lardeaux, and G. Mascles, (1997): *Glaucophane bearing eclogites in the Tso Morari dome (Eastern Ladakh, NW Himalaya).*: European J. Mineralogy, v. 9, p. 1073-1083.

De Sigoyer, J., I. Villa, V. Chavagnac, S. Guillot, and G. Mascles, (1998): *Multichronometry of Tso Morari eclogites: Ordovician plutonism, Tertiary eclogitization and inheritance*: 13th Himalay Karakorum Tibet Workshop, p. 185-186.

Dèzes, P., (1999): *Tectonic and metamorphic evolution of the Central Himalayan Domain in southeast Zanskar (Kashmir, India)*, Mémoires de Géologie (Lausanne), v. 32, 145 p.

Dèzes, P., J. C. Vannay, A. Steck, F. Bussy, and M. Cosca, (1999): *Synorogenic extension: Quantitative constraints on the age and displacement of the Zanskar Shear Zone (NW Himalaya)*: Geol. Soc. America Bull., v. 111, p. 364-374.

Diener, C., (1908): *Ladinic, Carnic and Noric faunae of Spiti*: Paleont. Indica, v. 5, Mem 3: Calcutta, 157 p.

Ferrara, G., B. Lombardo, and S. Tonarini, (1983): *Rb/Sr geochronology of granites and gneisses from the Mount Everest region, Nepal Himalaya*: Geologische Rundschau., v. 72/1, p. 119-136.

Fontan, D., (in prep.): *Regional geological mapping, metamorphic P-T-t paths evaluations and ore potential assessment in Neelum Valley, Azad Kashmir, NE Pakistan*: PhD thesis, Université catholique de Louvain.

Fontan, D., and M. Schouppe, (1994): *Contribution to the geology of Azad Kashmir (NE Pakistan); mapping of the Neelum Valley, recent geological results*: 9th HKT workshop, J. Nepal Geological Society, Special issue, v. 10, p. 42-44.

Frank, W., B. Graseman, P. Guntli, and C. Miller, (1995): *Geological map of the Kishtwar-Chamba-Kulu region (NW Himalaya, India)*: Jahrbuch Geologischen Bundesanstalt, v. 138, p. 299-308.

Frank, W., G. Hoinkes, C. Miller, F. Purtscheller, W. Richter, and M. Thöni, (1973): *Relations between metamorphism and orogeny in a typical section of the Indian Himalayas*: Tschermaks Mineralogische Petrographische Mitteil., v. 20, p. 303-332.

Frank, W., M. Thöni, and F. Purtscheller, (1977): *Geology and petrology of Kullu-south Lahul area*: Colloq. int. CNRS, v. 268, p. 147-172.

Fuchs, G., (1982): *The geology of the Pin valley in Spiti, HP, India*: Jb. Geol. Bundesanst. (Wien), v. 124, p. 325-359.

Fuchs, G., and M. Linner, (1995): *Geological traverse across the W Himalaya. A contribution to the geology of eastern Ladakh, Lahul and Chamba.*: Jb. Geol. Bundesanst. (Wien), v. 138, p. 655-685.

Fuchs, G., and M. Linner, (1996): *On the Geology of the suture zone and Tso Morari Dome in Eastern Ladakh (Himalaya)*: Jb. Geol. Bundesanst. (Wien), v. 139, p. 191-207.

Fuchs, G., and H. Willems, (1990): *The Final Stages of sedimentation in the Tethyan Zone of Zanskar and their Geodynamic Significance (Ladakh-Himalaya).*: Jb. Geol. Bundesanst. (Wien), v. 133, p. 259-273.

Gaetani, M., R. Casnedi, E. Fois, E. Garzanti, F. Jadoul, A. Nicora, and A. Tintori, (1986): *Stratigraphy on the Tethys Himalaya in Zanskar, Ladakh: initial report*: Riv. It. Paleont. Strat., v. 91, p. 443-478.

Gaetani, M., E. Garzanti, and A. Tintori, (1990): *Permo-Carboniferous stratigraphy in SE Zanskar and NW Lahul (NW Himalaya, India).*: Eclo. Geol. Helv., v. 83/1, p. 143-161.

Gansser, A., (1964): *Geology of the Himalayas*: London, John Wiley & Sons, 289 p.

Gansser, A., (1980): *The significance of the Himalayan suture zone*: Tectonophysics, v. 62, p. 37-52.

Gansser, A., (1991): *Facts and theories on the Himalayas*: Eclog. Geol. Helv., v. 84, p. 33-59.

Garzanti, E., L. Angiolini, and D. Sciunnach, (1996a): *The Mid-Carboniferous to Lowermost Permian sucession of Spiti (Po Group and Ganmachidam Formation; Tethys Himalaya, Northern India): Gondwana glaciation and rifting of Neo-Tethys*: Geodinamica Acta, v. 9, p. 78-100.

Garzanti, E., L. Angiolini, and D. Sciunnach, (1996b): *The Permian Kuling group (Spiti, Lahul and Zanskar; NW Himalaya): sedimentary evolution during rift/drift transition and initial opening of Neo-Tethys*: Riv. It. Paleonto. Stratigraphia, v. 102, p. 175-200.

Garzanti, E., R. Casnedi, and F. Jadoul, (1986): *Sedimentary evidence of a Cambro-Ordovician orogenic event in the northwestern Himalaya*: Sedimentary Geology, v. 48, p. 237-265.

Garzanti, E., F. Jadoul, A. Nicora, and F. Berra, (1995): *Triassic of Spiti (Thetys Himalaya, N India)*: Riv. It. Paleonto. Stratigraphia, v. 101/3, p. 267-300.

Garzanti, E., and T. Van Haver, (1988): *The Indus clastics: Forearc bassin sedimentation in the Ladakh Himalaya (India)*: Sedimentary Geology, v. 59, p. 237-249.

Girard, M., and F. Bussy, (1999): *Late Pan-African magmatism in the Himalaya: new geochronological and geochemical data from the Ordovician Tso Morari metagranites (Ladakh, NW India)*: Schweiz. Mineral. Petrogr. Mitt., v. 79, p. 399-417.

Girard, M., A. Steck, and P. Thélin, (1999): *The Dutung-Thaktote extensional fault zone and nappe structures documented by illite crystallinity and clay-mineral paragenesis in the Tethys Himalaya between Spiti river and Tso Morari, NW India*: Schweiz. Mineral. Petrogr. Mitt., v. 79, p. 419-430.

Girard, M., P. Thélin, and A. Steck, (in press): *Synorogenic extension in the Tethyan Himalaya documented by tectonics and the Kübler index, Lachung La area, NW India.*: Clay Minerals.

Greco, A., G. Martinotti, K. Papritz, J.-G. Ramsay, and R. Rey, (1989): *The crystalline rocks of the Kaghan Valley (NE Pakistan).*: Eclogae Geol. Helv., v. 82, p. 629-653.

Griesbach, C. L., (1891): *Geology of the Central Himalayas*: Mem. Geol. Surv. India, v. 23, p. 232 p.

Guillot, S., J. De Sigoyer, J. M. Lardeaux, and G. Mascle, (1997): *Eclogitic metasediments from the Tso Morari area (Ladakh, Himalaya): evidence for continental subduction during India-Asia convergence*: Contrib. Mineral. Petrol., v. 128, p. 197-212.

Guillot, S., K. V. Hodges, P. LeFort, and A. Pêcher, (1994): *New constraints on the age of the Manaslu leucogranite: Evidence for episodic tectonic denudation in the Central Himalayas*: Geology, v. 22, p. 559-562.

Gupta, V. J., G. Mahanj, S. Kumar, D. K. Chadha, P. C. Bisaria, N. S. Virdi, N. Kochar, and S. R. Kashyap, (1970): *Stratigraphy along the Manali-Leh road*: Pub. CAS Geol., v. 7, p. 77-84.

Harrison, T. M., K. D. McKeegan, and P. Le Fort, (1995): *Detection of inherited monazite in the Manaslu leucogranite by Pb/Th ion microprobe dating: Crystallisation age and tectonic implications*: Earth Planetary Science Letters, v. 133, p. 271-282.

Hayden, H. H., (1904): *Geology of Spiti, with parts of Bashahr and Rupshu*, Geological Survey of India, Calcutta, p. 127.

Hayden, H. H., (1908): *Geography, geology of the Himalaya (part 4)*: Geol. Survey India, p. 233-236.

Heim, A., and A. Gansser, (1939): *Central Himalaya, geological observations of the Swiss expedition 1936*: Mem. Soc. Helv. Sci. Nat., v. 73, p. 1-245.

Herren, E., (1987): *Zanskar shear zone; northeast-southwest extension within the Higher Himalayas (Ladakh, India)*: Geology, v. 15, p. 409-413.

Hodges, K., (2000): *Tectonics of the Himalaya and southern Tibet from two perspectives*: GSA bulletin, v. 112, p. 324-350.

Hodges, K. V., R. R. Parrish, T. B. Housh, D. R. Lux, B. C. Burchfiel, and L. H. Royden, (1992): *Simultaneous Miocene extension and shortening in the Himalayan orogen*: Science, v. 258, p. 1466-1470.

Hodges, K. V., R. R. Parrish, and M. P. Searl, (1996): *Tectonic evolution of the central Annapurna Range, Nepalese Himalayas*: Tectonics, v. 15, p. 1264-1291.

Holland, T., and R. Powell, (1998): *An internally consistent thermodynamic data set for phases of petrological interest*: J. Metam. Geol., v. 16, p. 309-343.

Honegger, K., V. Dietrich, W. Frank, A. Gansser, M. Thöni, and V. Trommsdorff, (1982): *Magmatism and metamorphism in the Ladakh Himalayas (the Indus-Tsangpo suture zone).*: Earth and Planetary Science Letters, v. 60, p. 253-292.

Hubbard, M. S., and T. M. Harrison, (1989): *40Ar/39Ar age constraints on deformation and metamorphism in the Main Central Thrust zone and Tibetan Slab, eastern Nepal Himalaya*: Tectonics, v. 8, p. 865-880.

Huges, N. C., and P. A. Jell, (1999): *Biostratigraphy and biogeography of Himalayan Cambrian trilobites*: Geological Soc. America, Spec. Paper, v. 328, p. 109-116.

Jadoul, F., E. Garzanti, and E. Fois, (1990): *Upper Triasic-lower Jurassic stratigraphy and paleogeographic evolution of the Zanskar Tethys Himalaya (Zangla Unit).*: Rivista Italiana Paleontologia Stratigrafia., v. 95, p. 351-396.

Kumar, G., B. K. Raina, O. N. Bhargava, P. K. Maithy, and R. Babu, (1984): *The Precambrian-Cambrian boundary problem and its prosepects, Northwest Himalaya, India.*: Geological Magazine, v. 121, p. 211-219.

Le Fort, P., F. Debon, A. Pêcher, J. Sonet, and P. Vidal, (1986): *The 500 Ma magmatic event in Alpine Southern Asia, a thermal episode at Gondwana scale*: Mémoire des Sciences de la Terre (Nancy), v. 47, p. 191-209.

Le Fort, P., S. Guillot, and A. Pêcher, (1997): *HP metamorphic belt along the Indus suture zone of NW Himalaya: new discoveries and significance*: C. R. Acad. Sci. Paris, v. 325, p. 773-778.

Leak, E., A. Wooley, C. Arps, W. Birch, M. Gilbert, J. Grice, F. Hawthorn, A. Kato, H. Kisch, V. Krivovichev, K. Linthout, J. Laird, W. Maresch, E. Nickel, N. Rock, J. Shumacher, D. Smith, N. Stephenson, L. Ungareti, E. Whittaker, and G. Youzhi, (1997): *Nomenclature of amphiboles report of the subcommittee on amphiboles of the international mineralogical association commission on new minerals and minerals names*: Eur. J. Mineral., v. 9, p. 623-651.

Linner, M., G. Fuchs, and F. Koller, (1997): *Permian Rifting and the eclogites of the Tso Morari dome*: 12th Himalaya Karakorum Tibet Workshop, p. 175-176.

Mahéo, G., S. Bertrand, S. Guillot, G. Mascle, A. Pêcher, C. Picard, and J. De Sigoyer, (2000): *Témoins d'un arc immature téthysien dans les ophiolites du Sud Ladakh (NW Himalaya, Inde)*: C.R. Acad. Sc. Paris, v. 330, p. 289-295.

Mascle, G., G. Hérail, T. Van Haver, and B. Delcaillau, (1986): *Structure et évolution des bassins d'épisuture et de périsuture liés à la chaîne Himalayenne*: Bull. Centre Rech. Explo.-Prod. Elf-Aquitaine, v. 10, p. 181-203.

Mc Kenna, L., and K. Hodges, (1988): *Accuracy versus precision in locating reaction boundaries: Implications for the garnet-plagioclase-aluminum silicate-quartz geobarometer*: American Mineralogist, v. 73, p. 1205-1208.

McElroy, R., J. Cater, I. Roberts, A. Peckham, and M. Bond, (1990): *The structure and stratigraphy of SE Zanskar, Ladakh Himalaya.*: J. Geol. Soc. London, v. 147, p. 989-997.

Middelmiss, C. S., (1910): *A revision in the Silurian-Trias sequence in Kashmir*: Rec. Geol. Surv. India, v. 40, p. 206-260.

Molnar, P., and P. Tapponier, (1975): *Cenozoic tectonics of Asia; effects of a continental collision*: Science, v. 189, p. 419-426.

Nanda, M. M., and M. P. Singh, (1976): *Stratigraphy and sedimentation of the Zaskar area, Ladakh and adjoining parts of the Lahul region of Himachal Pradesh*: Himalayan Geology, p. 365-388.

Oldham, R. D., (1888): *Some notes on the geology of the NW Himalayas*: Rec. Geol. Surv. India, v. 21, 149 p.

Patriat, P., and J. Achache, (1984): *India-Eurasion collision chronology has implication for crustal shortening and driving mechanism of plates*: Nature, v. 311, p. 615-621.

Pêcher, A., (1991): *The contact between the HHC and the Tibetan sedimentary series: Miocene large-scale dextral shearing.*: Tectonics, v. 10/3, p. 587-598.

Pognante, U., and B. Lombardo, (1989): *Metamorphic evolution of the High Himalayan Crystallines in SE Zanskar, India.*: Journal of metamorphic geology, v. 7, p. 9-17.

Pognante, U., and D. A. Spencer, (1991): *First report of eclogites from the Himalayan belt, Kaghan valley (northern Pakistan).*: Eur. J. Mineral., v. 3, p. 613-618.

Powell, R., and T. Holland, (1988): *An internally consistant dataset with uncertainties and correlations: 3. Applications to geobarometry, worked examples and a computer program*: J. Metamorphic Geol., v. 6, p. 173-204.

Powell, R., and T. Holland, (1994): *Optimal geothermometry and geobarometry*: American Mineralogist, v. 79, p. 120-133.

Raina, V. K., and D. P. Bhattacharyya, (1974): *The geology of a part of the Chharap and Sarchu valleys, Lahul and Spiti District, Himachal Pradesh.*

Robertson, A., and P. Degnan, (1994): *The Dras arc Complex: lithofacies and reconstruction of a late Cretaceous oceanic volcanic arc in the Indus Suture Zone, Ladakh Himalaya*: Sedimentary Geology, v. 92, p. 117-145.

Sacks, P. E., C. G. Nambiar, and L. J. Walters, (1997): *Dextral Pan-African Shear along the Southwestern Edge of the Achenkovil Shear Belt, South India: Constraints on Gondwana Reconstructions*: The Journal of Geology, v. 105, p. 275-284.

Schaltegger, U., and F. Corfu, (1995): *late Variscan "Basin and Range" magmatism and tectonics in the central Alps: evidence from U-Pb geochronology*: Geodinamica Acta, v. 8, p. 82-98.

Schärer, U., J. Hamet, and C. J. Allègre, (1984): *The Trans-Himalayan (Gangdese) plutonism in the Ladakh region: U-Pb and Rb-Sr study*: Earth Planet. Sc. Lett, v. 67, p. 327-339.

Sharma, K. K., and S. Kumar, (1978): *Contribution to the Geology of Ladakh, NW Himalaya*: Himalayan Geology, v. 8, p. 252-287.

Sharp, Z., (1995): *Oxygen isotope geochemistry of the Al2SiO5 polymorphs*: American J. Sci., v. 295, p. 1058-1076.

Sharp, Z. D., (1990): *A laser based microanalytical method for the in situ determination of oxygen isotope ratios of silicate and oxides.* Geoch. Cosmo. Acta, v. 54, p. 1353-1357.

Sharp, Z. D., and D. L. Kirschner, (1994): *Quartz-Calcite oxygen isotope thermometry: A calibration based on natural isotopic variations.*: Geoch. Cosmo. Acta, v. 58, p. 4491-4501.

Smith, A. G., A. M. Hurley, and J. C. Briden, (1981): *Phanerozoic paleocontinental world maps*: Cambridge, Cambridge University Press, 102 p.

Spear, F., and J. Selverstone, (1983): *Quantitative P-T Paths from zoned minerals: Theory and tectonic applications*: Contrib Mineral Petrol, v. 83, p. 348-357.

Spencer, D. A., (1993): *Tectonics of the Higher- and Tethyan Himalaya, Upper Kaghan Valley, NW Himalaya, Pakistan: Implications of an early collisional, high pressure (eclogite facies) metamorphism to the Himalayan belt.*: PhD thesis, ETHZ, Zurich.

Spring, L., (1993): *Structure gondwaniennes et himalayennes dans la zone tibétaine du Haut Lahul-Zanskar oriental (Himalaya Indien)*, Mémoire de Géologie (Lausanne), v. 14, 147 p.

Srikantia, S. V., (1981): *The lithostratigraphy, sedimentation and structure of Proterozoic-phanerozoic formations of Spiti basin in the High Himalaya of Himachal Pradesh, India.*, *in* A. K. Sinha, ed., Contemporary geoscientific researches in Himalaya, v. 1, p. 31-48.

Srikantia, S. V., and O. N. Bhargava, (1983): *Geology of the Palaeozoic sequence of the Kashmir Tethys Himalayan bassin in the Lidder valley, Jammu and Kashmir*: J. Geol. Soc. India, v. 24, p. 363-377.

Srikantia, S. V., T. M. Ganesan, P. N. Rao, P. K. Sinha, and B. Tirkey, (1980): *Geology of Zanskar area, Ladakh Himalaya*: Himalayan Geology, v. 2, p. 1009-1033.

Steck, A., J. L. Epard, J. C. Vannay, J. Hunziker, M. Girard, A. Morard, and M. Robyr, (1998): *Geological transect across the Tso Morari and Spiti areas: The nappe structures of the Tethys Himalaya*: Eclogae Geol. Helv., v. 91, p. 103-121.

Steck, A., L. Spring, J. C. Vannay, H. Masson, E. Stutz, H. Bucher, R. Marchant, and J. C. Tieche, (1993): *Geological transect across the northwestern Himalaya in eastern Ladakh and Lahul (a model for the continental collision of India and Asia)*: Eclogae Geol. Helv., v. 86, p. 219-263.

Stoliczka, F., (1866a): *Geological Sections across the Himalayan Mountains from Wangtu Bridge on the River Sutlej tu Sungdo on the Indus, with an account of the formations in spiti, accomanied by a revision of all known fossils from that district*: Geol. Survey India, memoirs, v. 5, p. 1-153.

Stoliczka, F., (1866b): *Summary of geological Observations during a visit to the Provinces - Rupshu, Karnag, S Ladakh, Zanskar, Suro and Dras - of western Tibet*: Memoirs of the Geological Survey of India, v. 5, p. 337-355.

Stutz, E., (1988): *Géologie de la chaine du Nyimaling aux confins du Ladakh et du Rupshu (NW Himalaya, Inde); évolution paléogéographique et tectonique d'un ségment de la marge nord indienne*, Mémoires de géologie (Lausanne), v. 3, 149 p.

Stutz, E., and A. Steck, (1986): *La terminaison occidentale du Cristallin du Tso Morari (Haut Himalaya; Ladakh meridional, Inde): Subdivision et tectonique de nappe*: Eclogae Geologicae Helvetiae, v. 79, p. 253-269.

Stutz, E., and M. Thöni, (1987): *The lower paleozoïc Nyimaling granite in the Indian Himalaya (Ladakh): New Rb-Sr data versus zircon typology*: Geologische Rundschau, v. 76, p. 307-315.

Thakur, V. C., (1983): *Deformation and metamorphism of the Tso Morari crystalline complex, in* V. C. Thakur, and K. K. Sharma, eds., Geology of Indus Suture Zone of Ladakh, Dehra Dun, Wadia Institut of Himalayan Geology.

Thakur, V. C., and N. S. Virdi, (1979): *Lithostratigraphy, structural framework, deformation and metamorphism of the SE region of Ladakh, Kashmir Himalaya, India*: Himalayan Geology, v. 9, p. 63-78.

Tonarini, S., I. M. Villa, F. Oberli, M. Meier, D. A. Spencer, U. Pognante, and J. Ramsay, (1993): *Eocene age of eclogite metamorphism in Pakistan Himalaya: Implication for India-Eurasia collision*: Terra Nova, v. 5, p. 13-20.

Treolar, P., and C. Izatt, (1993): *Tectonics of the Himalayan collision between the Indian plate and the Afghan block: A synthesis.*: Geol. Soc.London Spec. Pub., v. 74, 69-87.

Trivedi, J. R., K. S. Kewal, and K. Gopalan, (1986): *Widespread caledonian magmatism in Himalaya and its tectonic significance*: Terra Cognita, v. 6, p. 144.

Valdiya, K., (1995): *Proterozoic sedimentation of Pan-African geodynamic development in the Himalaya*: Precambrian Research, v. 74, p. 35-55.

Vannay, J., Z. Sharp, and B. Grasemann, (1999): *Himalayan inverted metamorphism constrained by oxygen isotope thermometry*: Contrib Mineral Petrol, v. 137, p. 90-101.

Vannay, J. C., (1993): *Géologie des chaînes du Haut Himalaya et du Pir Panjal au Haut-Lahul (NW Himalaya, Inde)*, Mémoires de géologie (Lausanne), v. 16, 148 p.

Vannay, J. C., and B. Grasemann, (1998): *Inverted metamorphism in the High Himalaya of Himachal Pradesh (NW India): phase equilibria versus thermobarometry*: Schweiz. Mineral. Petrogr. Mitt., v. 78, p. 107-132.

Vannay, J. C., and A. Steck, (1995): *Tectonic evolution of the High Himalaya in Upper Lahul (NW Himalaya, India)*: Tectonics, v. 14, p. 253-263.

Virdi, N. S., V. C. Thakur, and R. J. Azmi, (1978): *Discovery and Significence of Permian Microfossils in the Tso Morari Cristallines of Ladakh, J & K, India*: Him. Geol., v. 8, p. 993-1000.

Windley, B. F., M. J. Whitehouse, and M. A. O. Ba-Bttat, (1996): *Early Precambrian gneiss terranes and Pan-African island arcs in Yemen: Crustal accretion of the eastern Arabian Shield*: Geology (Boulder), v. 24, p. 131-134.

Wyss, M., (1999): *Structural geology and metamorphism of the Spiti valley-eastern Lahul-Parvati valley area, Himachal Himalaya (India)*: PhD thesis, Lausanne Uni., 183 p.

Wyss, M., and J. Hermann, (submitted): *Himalayan olivine gabbros : Evidence for extension-related magmatism and early granulite facies metamorphism.*: Tectonics.

Wyss, M., J. Hermann, and A. Steck, (1999): *Structural and metamorphic evolution of the northern Himachal Himalaya, NW India*: Eclogae, Geol. Helv., v. 92, p. 3-44.

Wyss, M. (2000): *Metamorphic evolution of the northern Himachal Himalaya: phase equilibria constraints and thermobarometry:* Schweiz. Mineral. Petrogr. Mitt., v. 80, p. 317-350

No. 28 HÜRLIMANN A., BESSON-HURLIMANN A and MASSON H. 1995. Stratigraphie et tectonique de la partie orientale de l'écaille de la Gummfluh (Domaine Briançonnais des Préalpes). 132 pp. 62 text-figs., 39 pl.., 6 maps.

No. 29 DOBMEIER C. 1996. Die variskische Entwicklung des südwestlichen Aiguilles Rouges Massives (Westalpen, Frankreich). 191 pp. 70 text-figs., 18 tables., 1 map.

No. 30 BAUD A., POPOVA I., DICKINS J.M., LUCAS S. and ZAKHAROV Y. 1997. Late Paleozoic and early Mesozoic circum-Pacific events : biostratigraphy, tectonic and ore deposits of Primoryie (far East Russia). IGCP Project 272. 202 pp., 71 text-figs., 48 pls.

No. 31 ARMANDO G. 1999. Intracontinental alkaline magmatism : geology, petrography, mineralogy and geochemistry of the Jebel Hayim Massif (Central High Atlas, Morocco). 106 pp. 51 text-figs., 23 tab., 1 map.

No. 32 DEZES P. 1999. Tectonic and metamorphic evolution of the Centrtal Himalayan Domain in Southeast Zanskar (Kashimr, India). 145 pp., 89 text-figs., 1 map.

No. 33 AMODEO F. 1999. Il Triassico terminale- Giurassico del Bacino Lagonegrese. Studi stratigrafici sugli Scisti Silicei della Basilicata (Italia meridionale). 160 pp., 50 text-figs., 10 pl.

No. 34 SAVARY J. and GUEX J. 1999. Discrete biochronological scales and Unitary Associations: Description of the BioGraph computer program. 282 pp. 21 text-figs.

No. 35 GIRARD M. 2001 : Metamorphism and tectonics of the transition between non metamorphic Tethyan Himalaya sediments and the North Himalayan Crystalline Zone (Rupshu area, Ladakh, NW India). 96 pp., 7 pl.

No. 36 STAMPFLI G.M. 2001 (ed.) : Geology of the western Swiss Alps – a guide-book . 195 pp., 67 text-figs., 7 pl.

Geography of the Rupshu area, Ladakh, NW India

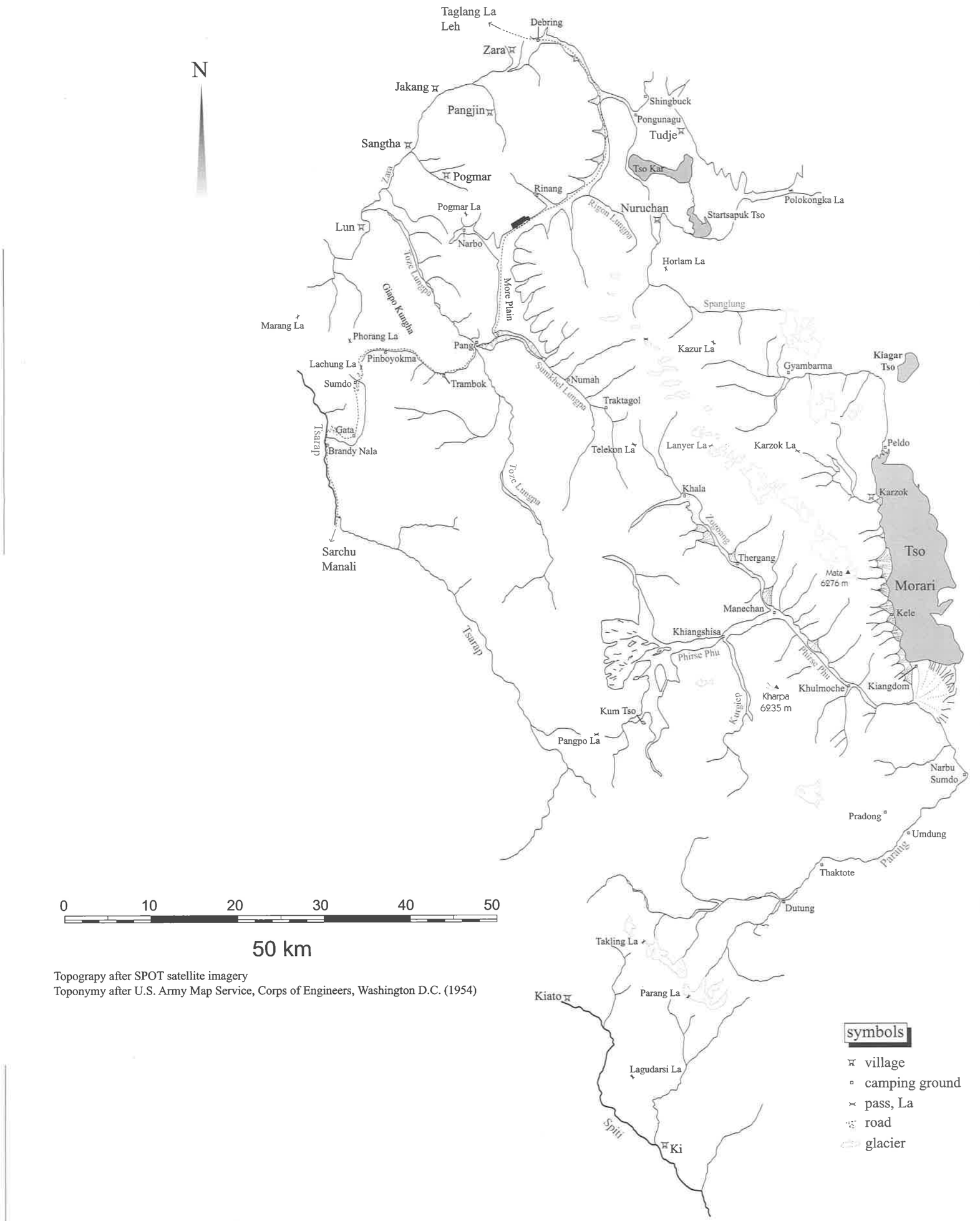

Topograpy after SPOT satellite imagery
Toponymy after U.S. Army Map Service, Corps of Engineers, Washington D.C. (1954)

Plate 1.1: Geography of Rupshu. Most names are taken from the U.S. Army maps, except some names given by locals.

Geological map of the Rupshu area, Ladakh, NW India

Matthieu Girard, 2001

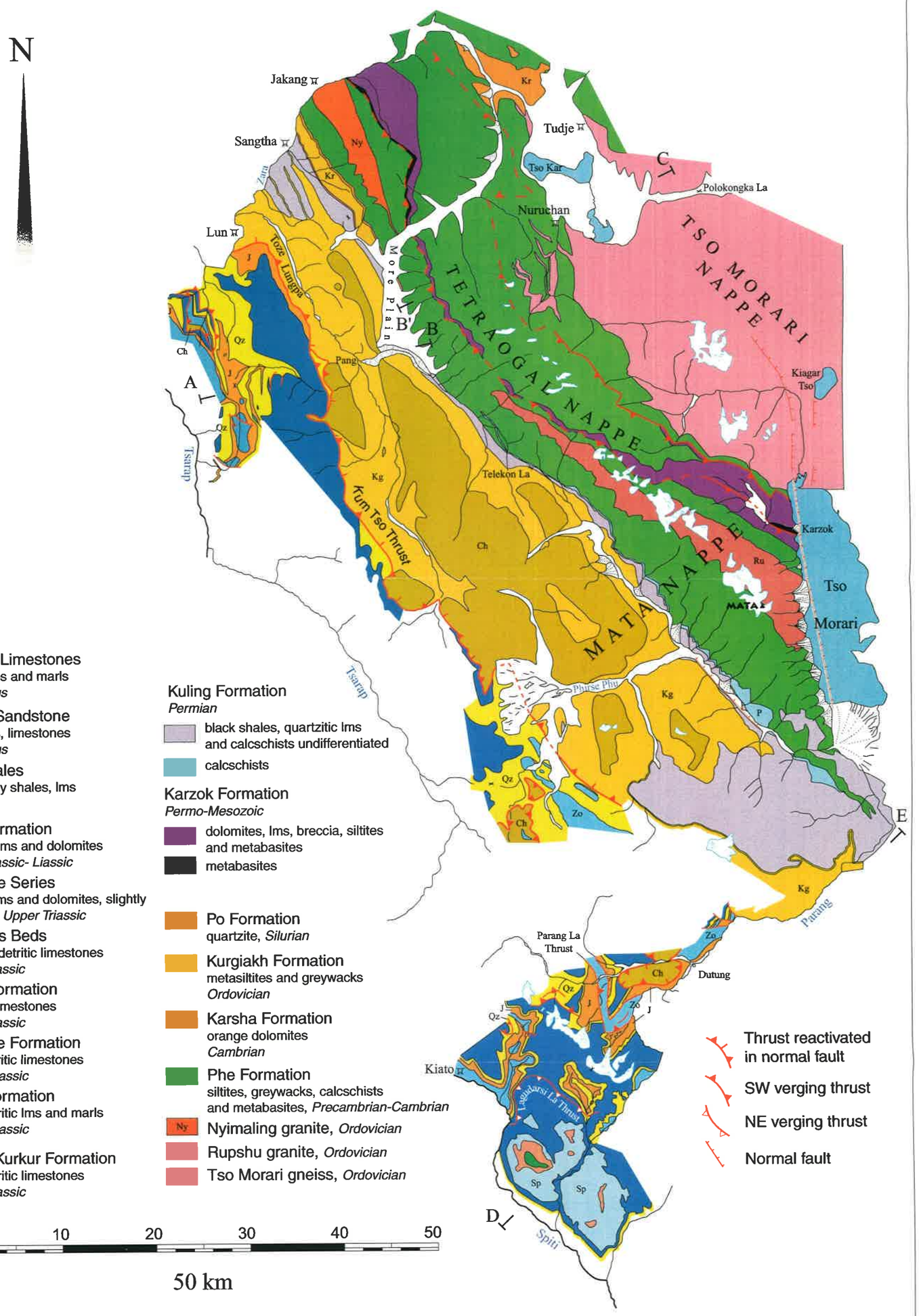

Plate 1.2: Geological map of Rupshu based on a 1:50'000 mapping. Lms = limestones.

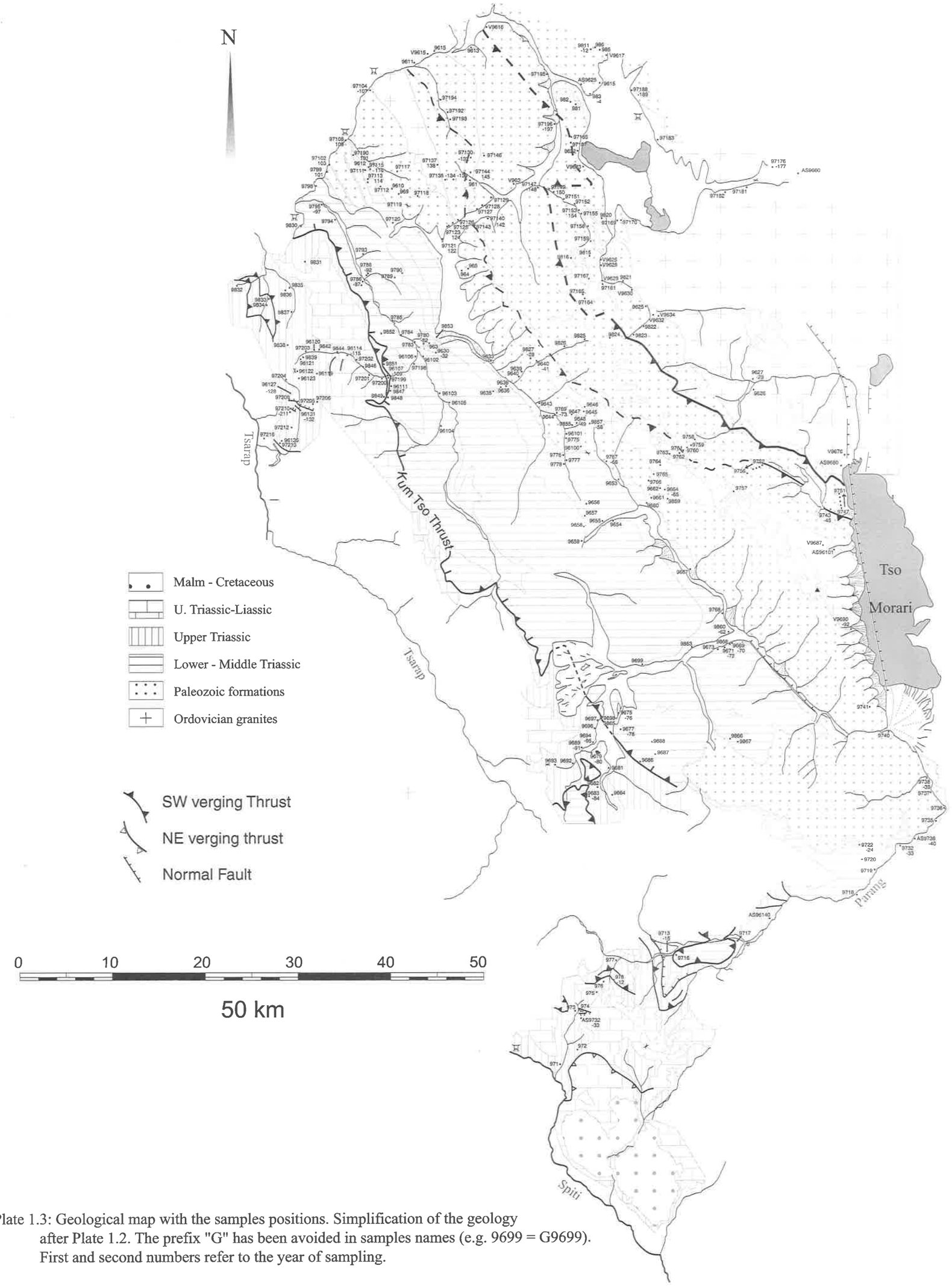

Plate 1.3: Geological map with the samples positions. Simplification of the geology after Plate 1.2. The prefix "G" has been avoided in samples names (e.g. 9699 = G9699). First and second numbers refer to the year of sampling.

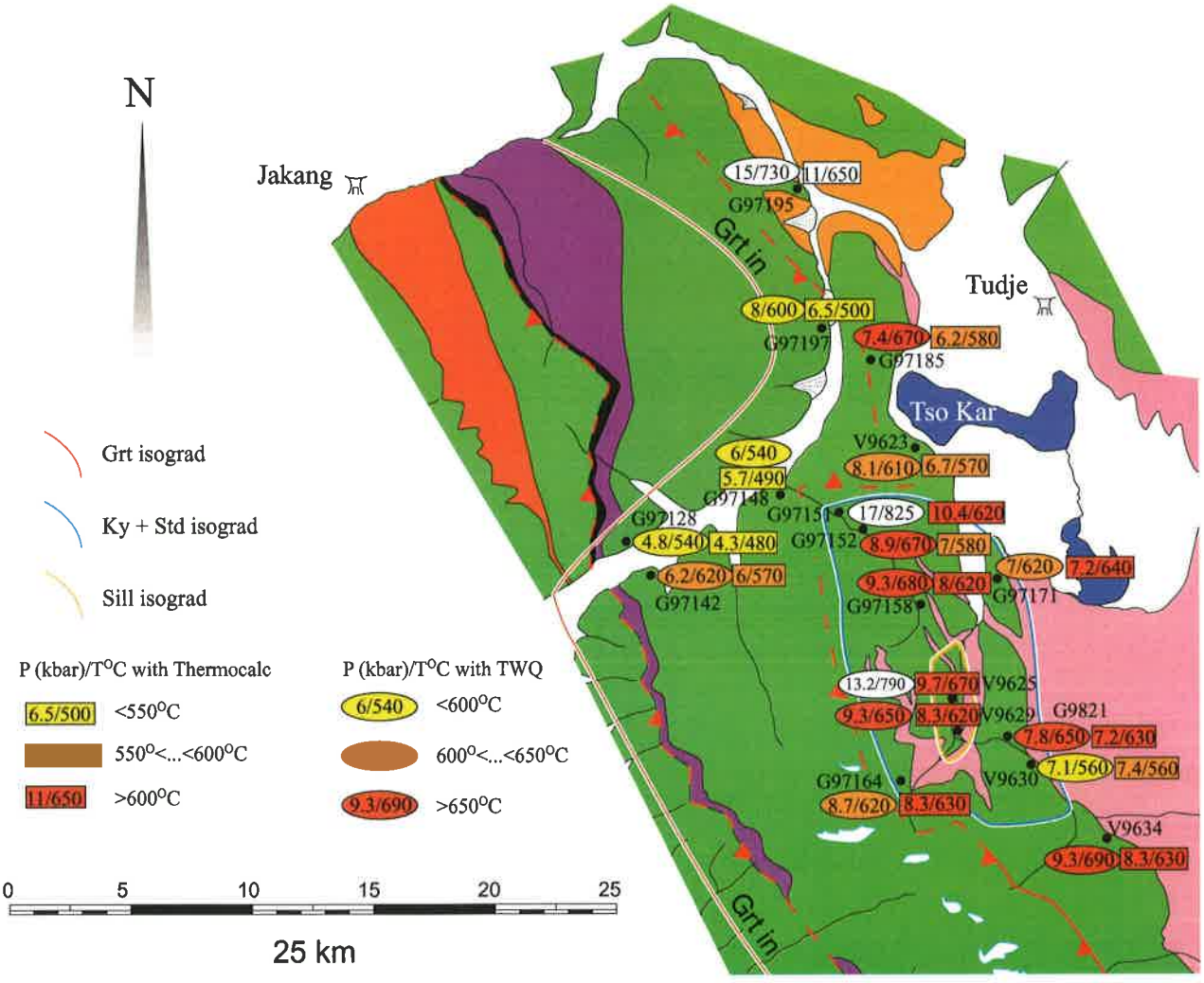

Plate 5.1: Geological map showing the P/T results in °C/Kbar, obtained with Thermocalc (boxes) and TWQ (ellipses) calculations on metapelites. Uncoloured boxes are samples with doubtful results. Samples names are indicated (e.g. G97128). See plate 1.2 for lithologies index.

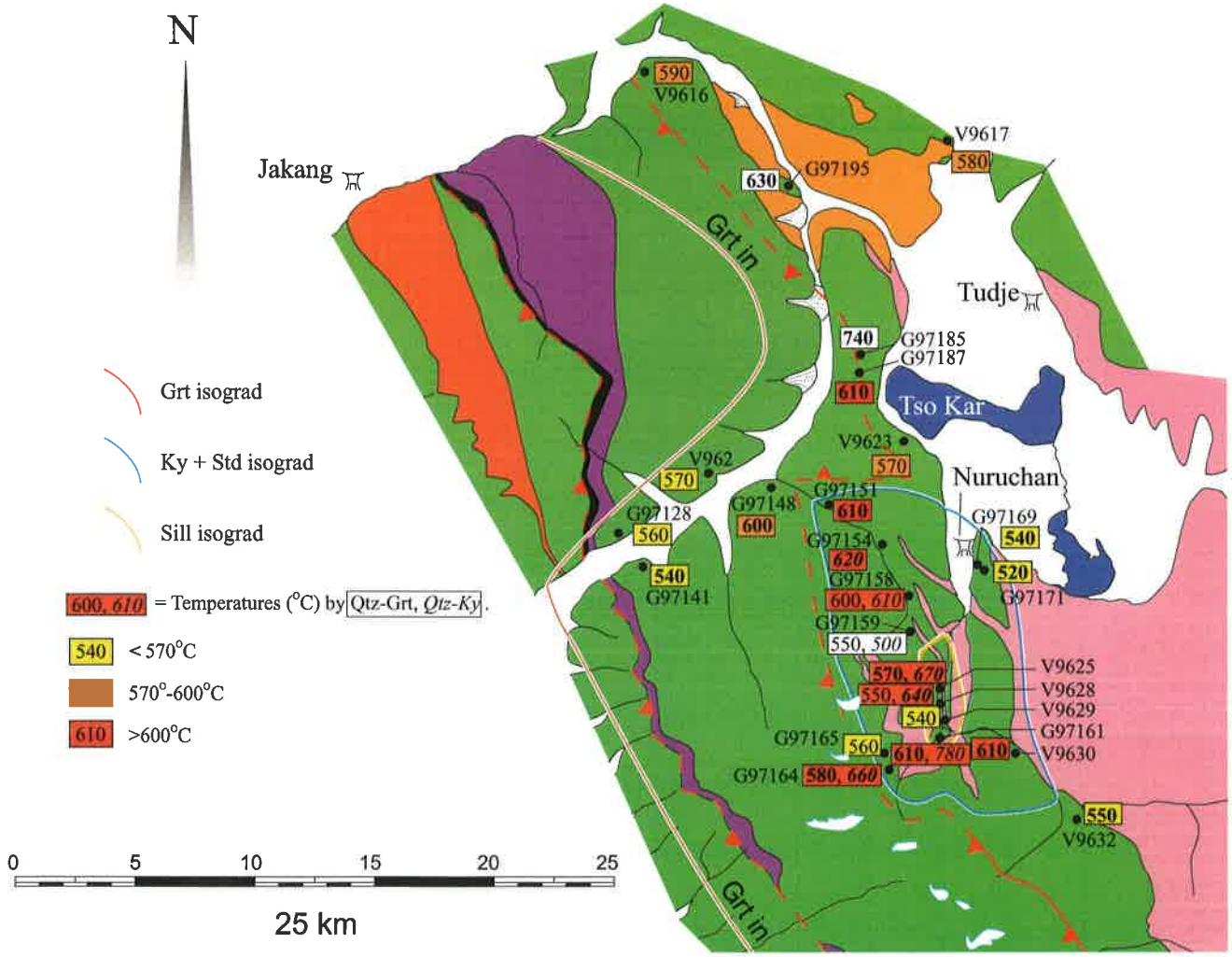

Plate 5.2: Geological map showing the temperatures results in °C, obtained with quartz-garnet and quartz-kyanite (italic) isotopic thermometers on metapelites. Uncoloured boxes are samples with doubtful results, and bold numbers are better constrained results. Samples names are indicated (e.g. G97128). See plate 1.2 fore litologies index.

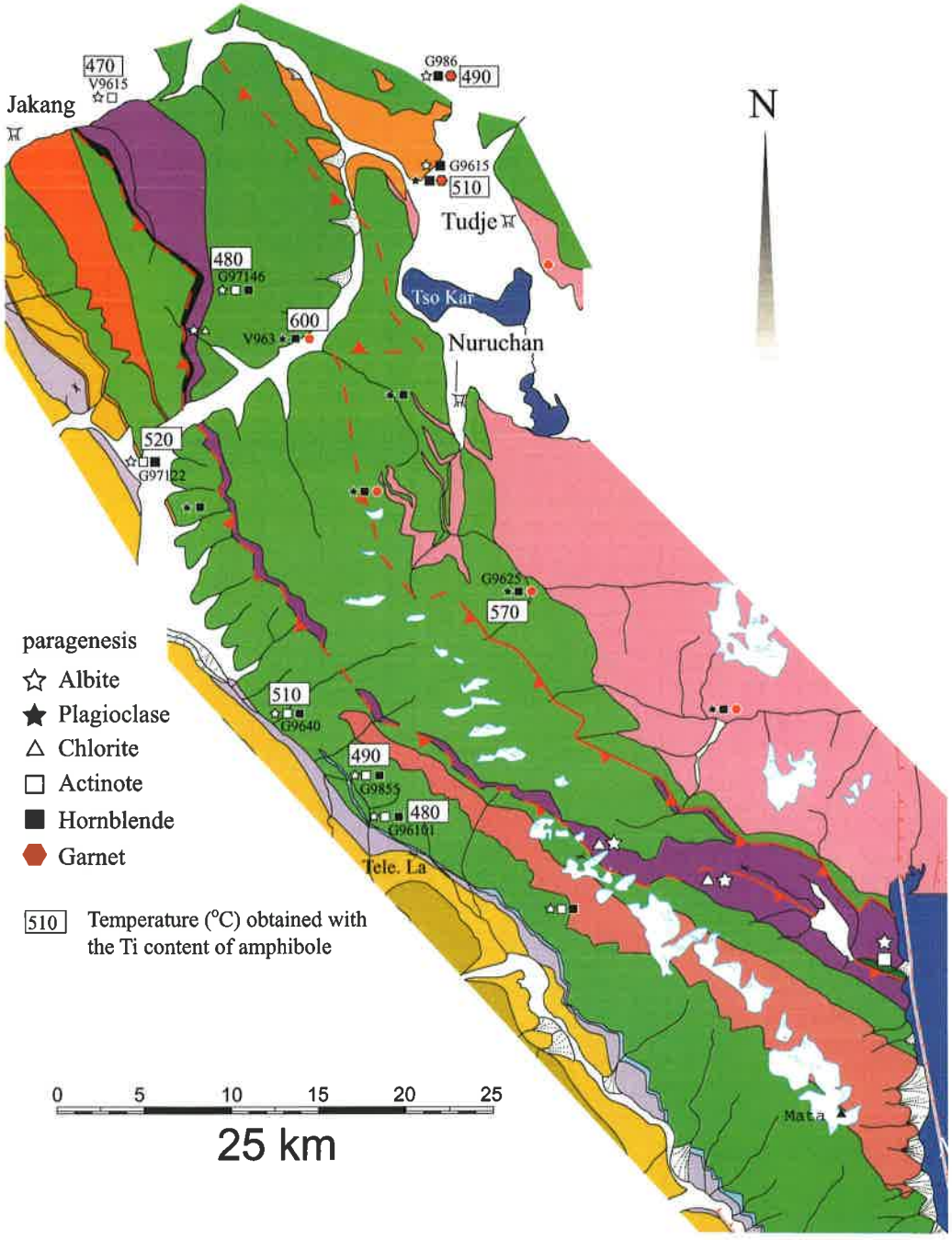

Plate 5.3: Geological map of Rupshu showing the mineral assemblages of the regional metamorphism in metabasic rocks, and the temperatures obtained with the empirical thermometer based on the Ti content of amphiboles (Colombi, 1989). Sample names are indicated when microprobe analyses have been done (Tab. 5.4). Other mineral determinations have been done with optical microscopy.

Metamorphic map of the Rupshu area, Ladakh, NW India

Matthieu Girard, 2001

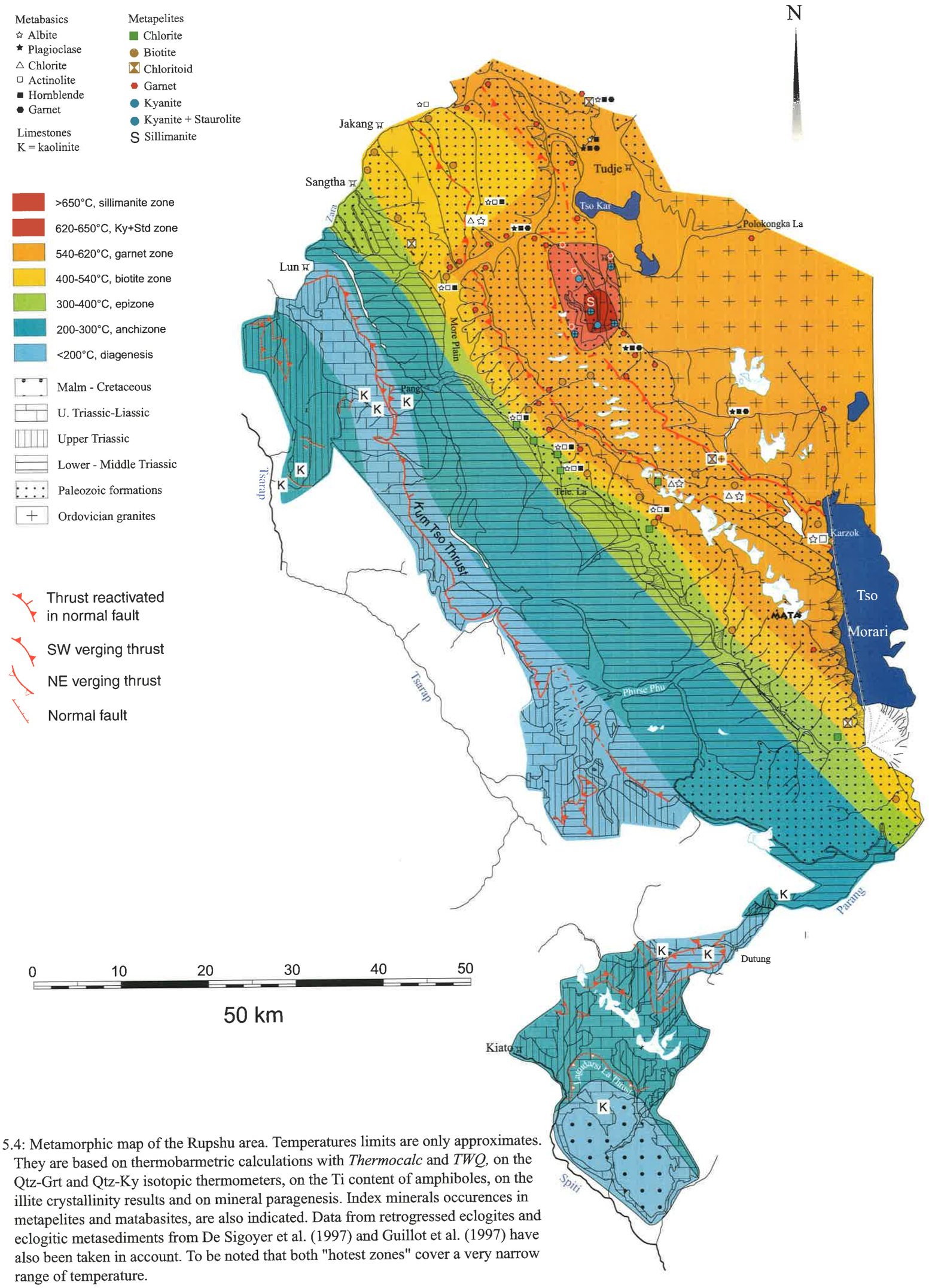

Plate 5.4: Metamorphic map of the Rupshu area. Temperatures limits are only approximates. They are based on thermobarmetric calculations with *Thermocalc* and *TWQ,* on the Qtz-Grt and Qtz-Ky isotopic thermometers, on the Ti content of amphiboles, on the illite crystallinity results and on mineral paragenesis. Index minerals occurences in metapelites and matabasites, are also indicated. Data from retrogressed eclogites and eclogitic metasediments from De Sigoyer et al. (1997) and Guillot et al. (1997) have also been taken in account. To be noted that both "hotest zones" cover a very narrow range of temperature.

Mémoires de Géologie (Lausanne)

No. 1* BAUD A. 1987. Stratigraphie et sédimentologie des calcaires de Saint-Triphon (Trias, Préalpes, Suisse et France). 202 pp., 53 text-figs., 29 pls.

No. 2 ESCHER A., MASSON H. and STECK A. 1988. Coupes géologiques des Alpes occidentales suisses. 11 pp., 1 text-figs., 1 map.

No. 3* STUTZ E. 1988. Géologie de la chaîne Nyimaling aux confins du Ladakh et du Rupshu (NW-Himalaya, Inde). Evolution paléogéographique et tectonique d'un segment de la marge nord-indienne. 149 pp., 42 text-figs., 11 pls. 1 map.

No. 4 COLOMBI A. 1989. Métamorphisme et géochimie des roches mafiques des Alpes ouest-centrales (géoprofil Viège-Domodossola-Locarno). 216 pp., 147 text-figs., 2 pls.

No. 5 STECK A., EPARD J.-L., ESCHER A., MARCHANT R., MASSON H. and SPRING L. 1989 Coupe tectonique horizontale des Alpes centrales. 8 pp., 1 map.

No. 6 SARTORI M. 1990. L'unité du Barrhorn (Zone pennique, Valais, Suisse). 140 pp., 56 text-figs., 3 pls.

No. 7 BUSSY F. 1990. Pétrogenèse des enclaves microgrenues associées aux granitoïdes calco-alcalins: exemple des massifs varisque du Mont-Blanc (Alpes occidentales) et miocène du Monte Capanne (Ile d'Elbe, Italie). 309 pp., 177 text-figs.

No. 8* EPARD J.-L. 1990. La nappe de Morcles au sud-ouest du Mont-Blanc. 165 pp., 59 text-figs.

No. 9 PILLOUD C. 1991. Structures de déformation alpines dans le synclinal de Permo-Carbonifère de Salvan-Dorénaz (massif des Aiguilles Rouges, Valais). 98 pp., 59 text-figs.

No. 10* BAUD A., THELIN P. and STAMPFLI G. 1991. (Eds.). Paleozoic geodynamic domains and their alpidic evolution in the Tethys. IGCP Project No. 276. Newsletter No. 2. 155 pp.

No. 11 CARTER E.S. 1993 Biochronology and Paleontology of uppermost Triassic (Rhaetian) radiolarians, Queen Charlotte Islands, British Columbia, Canada. 132 pp., 15 text-figs., 21 pls.

No. 12* GOUFFON Y. 1993. Géologie de la "nappe" du Grand St-Bernard entre la Doire Baltée et la frontière suisse (Vallée d'Aoste -Italie). 147 pp., 71 text-figs., 2 pls.

No. 13 HUNZIKER J.C., DESMONS J., and HURFORD AJ. 1992. Thirty-two years of geochronological work in the Central and Western Alps: a review on seven maps. 59 pp., 18 text-figs., 7 maps.

No. 14 SPRING L. 1993. Structures gondwaniennes et himalayennes dans la zone tibétaine du Haut Lahul-Zanskar oriental (Himalaya indien). 148 pp., 66 text-figs, 1 map.

No. 15 MARCHANT R. 1993. The Underground of the Western Alps. 137 pp., 104 text-figs.

No. 16 VANNAY J.-C. 1993. Géologie des chaînes du Haut-Himalaya et du Pir Panjal au Haut-Lahul (NW-Himalaya, Inde). Paléogéographie et tectonique. 148 pp., 44 text-figs., 6 pls.

No. 17* PILLEVUIT A. 1993. Les blocs exotiques du Sultanat d'Oman. Evolution paléogéographique d'une marge passive flexurale. 249 pp., 138 text-figs., 7 pls.

No. 18 GORICAN S. 1994. Jurassic and Cretaceous radiolarian biostratigraphy and sedimentary evolution of the Budva Zone (Dinarides, Montenegro). 120 pp., 20 text-figs., 28 pls.

No. 19 JUD R. 1994. Biochronology and systematics of Early Cretaceous Radiolaria of the Western Tethys. 147 pp., 29 text-figs., 24 pls.

No. 20 DI MARCO G. 1994. Les terrains accrétés du sud du Costa Rica. Evolution tectonostratigraphique de la marge occidentale de la plaque Caraïbe. 166 pp., 89 text-figs., 6 pls.

No. 21* O'DOGHERTY L. 1994. Biochronology and paleontology of Mid-Cretaceous radiolarians from Northern Apennines (Italy) and Betic Cordillera (Spain). 415 pp., 35 text-figs., 73 pls.

No. 22 GUEX J. and BAUD A. (Eds.). 1994. Recent Developments on Triassic Stratigraphy. 184 pp.

No. 23 BAUMGARTNER P.O., O'DOGHERTY L., GORICAN S., URQUHART E., PILLEVUIT A. and DE WEVER P. (Eds.). 1995. Middle Jurassic to Lower Cretaceous Radiolaria of Tethys: Occurrences, Systematics, Biochronolgy. 1162 p.

No. 24 REYMOND B. 1994. Three-dimensional sequence stratigraphy offshore Louisiana, Gulf of Mexico (West Cameron 3D seismic data). 215 pp., 169 text-figs., 49 pls.

No. 25 VENTURINI G. 1995. Geology, Geochronology and Geochemistry of the Inner Central Sezia Zone. (Western Alps - Italy). 183 pp. 57 text-figs, 12 pls.

No. 26 SEPTFONTAINE M., BERGER J.P., GEYER M., HEUMANN C., PERRET-GENTIL G. and SAVARY, J. 1995. Catalogue des types paléontologiques déposés au Musée Cantonal de Géologie, Lausanne. 76 pp.

No. 27 GUEX, J. 1995. Ammonites hettangiennes de la Gabbs Valley Range (Nevada, USA). 130 pp., 22 figs., 32 pl.

*: out of print (continued inside)

Order from **Institut de Géologie et Paléontologie,**
Université de Lausanne. BFSH-2. CH-1015, SWITZERLAND.
http://www-sst.unil.ch/publications/memoires.htm Fax: (41) 21-692.43.05
Bank Transfer: Banque Cantonale Vaudoise 1002 Lausanne
Account Number: **C.323.52.56** Institut de Géologie, rubrique: Mémoires
Price CHF 30 per volume except volume 23 (CHF 100). The price doesn't include postage and handling.
- Please do not send check -